SYNTHESIS, SPECTRAL AND ELECTROCHEMICAL STUDIES OF HETEROBIMETALLIC COMPLEXES CONTAINING MOLYBDENUM (V) LINKED TO NICKEL AND COBALT SCHIFF BASE COMPLEXES

BY

GICHUKI JOHN GITHAIGA

THESIS SUBMITTED TO THE SCHOOL OF SCIENCE IN PARTIAL FULFILMENT OF THE REQUIREMENTS FOR THE AWARD OF A DEGREE OF MASTERS OF SCIENCE IN CHEMISTRY.

UNIVERSITY OF ELDORET.

2013

DECLARATION

Declaration by the student

This thesis is my original work and has not been presented for a degree in any other University. No part of this thesis may be reproduced without the prior written permission of the author and/or University of Eldoret.

Gichuki John G.

Signature…….. Date……..…

Reg. No. SC/PGC/22/04

Declaration by the supervisors

This thesis has been submitted with our approval as University supervisors.

Signature…… Date……..

Prof. S.M. Kagwanja,

Chuka University, Chuka, Kenya

Signature…… Date……..

Prof. Lusweti Kituyi,

University of Eldoret, Eldoret, Kenya

DEDICATION

To my parents (Peter Gichuki and Maggie Njeri), brothers and sisters.

ABSTRACT

In this thesis, the synthesis, characterization and electrochemical studies of monometallic and bimetallic complexes of schiff base ligands have been undertaken. Synthesis of bimetallic complexes initially involved preparation of appropriate tetradentate schiff base ligands, *meta* and *para* (TS1-TS4 and TS5-TS8) capable of accommodating two metal centres. This involved condensation of diamines with salicylaldehyde and 2,4- and 2,5-dihydroxybenzaldehyde that produced yellow solids, which were characterized using I.R and U.V analysis. Their formation was monitored by the $\upsilon_{C=N}$ bond occurring in the range of 1616 to 1636cm^{-1} and 1632 to 1654cm^{-1} for meta and para respectively. The preformed schiff base ligands were reacted with nickel chloride and cobalt acetate to afford monometallic complexes (TS9-TS24). They were characterized using F.T.I.R, U.V and cyclic voltammetric studies. The spectroscopic handle to monitor their formation was the shift of $\upsilon_{C=N}$ bond to lower frequencies in the range of 1612 to 1627cm^{-1} and 1608 to 1622cm^{-1} for nickel and cobalt meta complexes, respectively. For para substituted monometallic complexes, the shift was observed in the range of 1622 to 1629cm^{-1} and 1600 to 1612cm^{-1} for nickel and cobalt, respectively. This indicates a decrease in bond order as compared to the schiff bases due to the attachment of the metals at the tetradentate cavity of the schiff base. They all contain a broad absorption in the visible region, which can be assigned to a metal-to-ligand charge transfer (M.L.C.T) process due to the fact that there is a wide variation in λmax with the nature of linking group between the aromatic rings. This suggests the involvement of the polyethylene ligand in the transitions. Synthesis of bimetallic complexes (TS25-TS40) involved the addition of the appropriate monometallic complex to precursor molecule, Mo(O)Tp*Cl_2, in a 1:1 molar ratio in presence of an excess triethylamine. They were characterized using F.T.I.R, U.V and Cyclic voltammetry studies. F.T.I.R studies indicated that the characteristic $\nu_{C=N}$ bond in all complexes underwent a hypsochromic (red shift) to higher frequencies. The $\upsilon_{Mo=O}$ bond which was observed at the frequency of 960 cm^{-1} and 948 to 981cm^{-1} for nickel and cobalt meta, respectively acted as the spectroscopic handle to monitor the coordination of Mo(O)Tp* in the complex formation. For para bimetallic complexes, this bond was observed at 960cm^{-1} for nickel and 933 to 962cm^{-1} for cobalt. he electrochemical behaviour for all bimetallic complexes indicated that Mo(V) undergoes a one electron reduction reaction to Mo(IV) and a one electron oxidation to Mo(VI). The reduction potentials increased cathodically as the length of the polymethylene chain increases. In ACN, nickel and cobalt bimetallic complexes of type B reduced irreversibly at potentials between –0.572to –0.589V and –0.531 to –0.548V respectively while in DCM, the reduction was observed within –0.541 to –0.547V and –0.531 to –0.542V for nickel and cobalt respectively. Respective potential values for type A bimetallic nickel and cobalt complexes in ACN also reduced irreversibly within the ranges –0.561 to –0.590V and –0.551 to –0.559V while in DCM were –0.520 to –0.543V and –0.563 to –0.571V. This indicates that the electrochemical studies of bimetallic complexes are solvent dependent.

TABLE OF CONTENTS

LIST OF TABLES

LIST OF FIGURES

LIST OF SCHEMES

LIST OF ABBREVIATIONS

ACN	Acetonitrile
Ag/AgCl	Silver/silver chloride electrode
A.R	Analytical Reagent
B	Schiff base backbone
BM	Bohr magneton
BPA	1, 2-bis(4-pyridyl) ethane
BPE	trans-1, 2-bis(4-pyridyl) ethane
BPM	1, 2-bis(4-pyridyl) methane
Bpy	2,2-bipyridine
cm^{-1}	wave number: frequency in reciprocal cm, or $1/\lambda$
C.F.S.E	Crystal Field Stabilization Energy
CV	Cyclic voltammetry
DCM	Dichloromethane
Dm	decimeter
DMF	Dimethyl Formamide
DMSO	Dimethyl Sulphoxide
DPMz	3,5-dimethyl pyrazolyl
DPV	Differential Pulse Voltammetry
E	Molar extinction coefficient
EPR	Electron Paramagnetic Resonance
En	Ethylene
E_p	Peak potential

$E_{1/2}$	Half-wave potential
ΔE	Separation between anodic and cathodic wave potentials
Fc/Fc^{+}	Ferrocene/ferrocenium
F.T.I.R	Fourier Transform Infrared
HOMO	Highest occupied molecular orbital
i.r	Infrared
I.V.C.T	Intervalence Charge Transfer
LUMO	Lowest unoccupied molecular orbital
m	*meta*
nm	nanometer, same as millimicron (mμ), 10^{-9}m
p	*para*
Pz	Pyrazole
Salen	N,N'-bis salicylaldene imine
THF	Tetrahydrofuran
Tp*	Tris(3,5-dimethylpyrazolyl) borato anion
U.V	Ultra Violet
λ	Wavelength
υ	frequency in Hz (cycles per second)
W.E	working electrode

ACKNOWLEDGEMENT

The enormous work of carrying out this research project has not been an easy one. I could not have made it were it not for the unreserved support I received from various people and institutions. I am deeply indebted to thank my supervisors Prof. S.M. Kagwanja, Chuka University and Prof. Lusweti Kituyi for their guidance. I appreciate Esther whose moral and spiritual support has seen me this far. Her inspirations will never be forgotten. Special thanks to Mr. Joel Mwangi who has been my close friend and course mate all through. I will also not like to forget the laboratory technicians of the University of Eldoret, Department of Chemistry and Biochemistry especially Mr. Karanja, Mr. Opanga, Mr. King'ang'i, Mr. Abdalla and Mr. Ekeya for their assistance. My thanks go to laboratory technicians of Egerton, JKUAT, Nairobi and Kenyatta University for allowing me to use their laboratory and equipments.

Since it is not possible to write down all those in one-way or another who made this project a success, I convey my gratitude to them all. Finally, to my God who saw me through every challenge that came my way and provided a way out, I say "Surely you are my Ebenezer."

CHAPTER ONE

INTRODUCTION

1.1 Background Information

There has been an increase in the awareness of the potential importance of the binuclear metal complexes, which contain redox active sites adjacent to each other and those separated by a spacer in which the redox sites are remote to each other (Lutta, 1996). The multi-metallic complexes are crucial in nature as active sites in many metalloenzymes and play a significant role in catalysis. Such systems have distinctive chemical and physical properties, which may be altered systematically through chemical synthesis. There is also a possibility of co-operative chemical and electronic interactions between the chemically linked metal centres. This has led to chemistry that is different from that displayed by single metal counterpart (Meyer, 1989). Such metal complexes also present some particular mechanistic aspects; an example being the possibility of having sequential electron transfer steps leading to charge separation over non-adjacent components (Balzani and Scandola, 1991).

The ability to control electronic and magnetic interactions between metal centres across a bridging ligand is of fundamental importance in inorganic and materials chemistry. An electronic interaction between two (usually chemically equivalent) metal centres is manifested by a separation between their redox potentials, such that the intermediate potential domain of the complex exists in a mixed valence state and can undergo optically induced intervalence electron transfer. The significance of this is two fold. First, the most fundamental process in chemistry, electron transfer may be studied under controlled

intramolecular conditions: across a fixed distance, between fragments of known properties and through a conduit whose conformation and electronic characteristics are well defined. This contrasts with the situation for the intermolecular electron transfer, where the separation, conformation and relative orientation of the interacting complexes at the moment of collision are difficult to know accurately. Second, the ability of long, conjugated bridging ligands to act as "molecular wires" for possible use in molecular electronic devices may be evaluated, because the ability of a bridging ligand to mediate a transfer of one electron across it within a molecule may be a reasonable guide to its ability to permit transport of electrons across it in a nanoscopic circuit (McCleverty *et al.,* 1998).

Recent years have witnessed research into binuclear and polynuclear metal complexes which are redox-active. These complexes represent a class of materials with distinctive chemical and physical properties that can be varied at will through chemical synthesis. In binuclear complexes, which contain reducible and/or oxidizable peripheral fragments connected by a multi-atom bridge, the redox properties of one centre can efficiently be communicated through the bridging ligand to the neighboring redox centres. This is particularly so in compounds containing bipyridyls or quinines, where the ligands themselves are capable of redox activity.

Several factors related to the possible general applications of these systems in biomimetic, molecular electronics, and environmental pollution control has triggered the interest of this work. These complexes are also capable of acting as potential electro-catalysts or as simple synthetic redox active model compounds which may mimic biological systems such as

proteins and enzymes in which two or more metal ions are required in their activity (Elder *et al*., 1983). They may be designed for study of intramolecular electron transfer process between electron deficient and electron rich metal centres linked by a variety of bridging ligands (Balzan and Scandola., 1991). The basic idea in the field of molecular electronics is intramolecular electron transfer, where currently synthetic chemists have been studying possibility of producing elongated molecules which contain a donor site and an acceptor site linked by a conjugated pathway capable to assist movement of electrons from donor site to electron deficient site (Mark *et al*., 1997). The conjugated pathway is usually an organic bridging ligand. The whole system then would be considered to act as a molecular wire. Production of these types of materials requires skillful design of the bridging ligand. Unsaturated ligands have been found to give the best conduction of charge from donor to acceptor site because their delocalized pi electrons are far more mobile than those of simple sigma framework of saturated ligands (Barigelleti and Flamigni, 2000). Polynuclear systems can be designed so as to contain a redox active centre capable of changing its spectroscopic, magnetic or electrochemical properties in response to the binding of a cation at the receptor site, which raises their potential use as chemical sensors. For instance, redox active ligands whose redox potentials change on encapsulating foreign metal ions have been synthesized (Akabori *et al*., 1985).

Generation of such oxidizable and / or reducible elongated molecules may initially involve synthesis of simple prototype binuclear complexes that can serve as basic units for constructing larger molecules. Tris (3,5-dimethyl pyrazolyl borato) Oxo Mo(V) complex ($MoTP^{*}(O)Cl_2$) have been well characterized and readily synthesized. It affords a

particular convenient vehicle for generating bimetallic species exhibiting interesting redox, photochemical and optical properties (Van *et al*., 1977). This is particularly so in compounds containing $(OC_6H_6O)^{2-}$ and $(NH_6H_4NH)^{2-}$ bridging ligands where larger electronic interactions between two molybdenum redox centres have been detected. However, the extent of metal-metal interactions dwindles substantially on lengthening the bridging ligand (Charsely *et al*., 1988).

Construction and characterization of electrochemical studies of complexes containing copper (II), Nickel (II) and Palladium (II) centres attached to two molybdenum nitrosyl centres have been reported (Kagwanja *et al*., 1994). In these studies, it was found that the Copper, Nickel and Palladium atoms had small but detectable influence on the redox behaviour of molybdenum centres, which themselves were only weakly interacting electrochemically. Construction of these complexes was based on robust schiff base ligands derived from 2,4-dihydroxybenzaldehyde, 2,5-dihydroxybenzaldehyde and α, ω-diamines. The interest was to investigate the redox behaviour of the central metal atom under the influence of one oxo molybdenum redox centre and vice versa. Of particular interest was to discover whether it was possible to enhance electronic interaction between the central metal atoms implanted in the Schiff base bridging ligand and the peripheral oxo molybdenum centre.

The main concern here on redox active polynuclear systems is due to the fact that as advancement in the electronic era continues, there is a possibility of these systems to form basic systems of “molecular wires”, “switches” as well as “information storage chips”

(Day *et al*., 1990). Information storage chips formed by molecules are capable of storing 256 million bytes of information per chip of area $1cm^2$ in comparison to only 16 million bytes for the commonly used silicon chips. Moreover, polymetallic systems have been found to have potential use in other fields ranging from medicine (Lippard and Sussana, 1997) to corrosion inhibitors, lubricants, antiwear additives (Syamal and Mauryo, 1989) as well as being used as molecular sieves (Riederer and Sawdny, 1978).

The compounds investigated in this study were of types **A** and **B** (shown below) where type A refers to the *para* compounds while type B refers to the *meta* compounds.

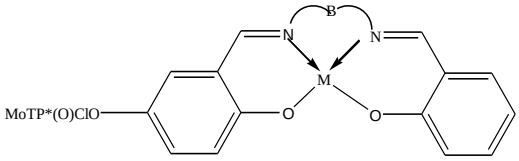

A

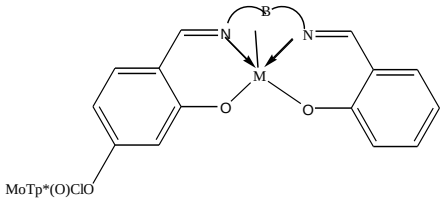

B

Figure 1: Bimetallic complexes

Where M= Ni or Co in this case, B= C_6H_4, $(CH_2)_n$; n=2- 4

Production of such compounds requires skillful design of the ligands. The complexes are redox-active and their reduction potentials may be influenced by the metal implanted in the

central cavity of the tetradentate schiff base ligand and possibly by the distortion of the geometry of the central chelate complex occasioned by varying the polymethylene carbon skeleton of the schiff base ligand.

1.2 Statement of the Problem

Studies of redox responsive metal complexes with emphasis on investigation of the mechanism of transmission of interelectronic effects from one redox metal centre to another have grown considerably. Their interest in the coordination chemistry of metallated ligands has rapidly expanded because of their technological applications (Tabassum *et al*., 2001). A series of complexes have been prepared in which a precursor having oxo-molybdenum centre have been coordinated with ligands containing binding sites. In these complexes, the metal centres may exhibit their characteristic redox and spectroscopic behaviour or they may influence each other weakly, moderately or strongly, depending on the ability of the bridging ligand to transfer electrons from one metal centre to the other. The bridging ligands are therefore a critical element in the successful design of these compounds. The electronic effects of one metal centre upon the other can thus be studied across a range of bridging ligands which are designed to allow the study of the effects of their nature and length (Obaidi et al., 1986, Charsley et al., 1988). The anticipation that reduction of copper, nickel and palladium centres in the trimetallic complexes would probably occur at potentials more cathodic than the peripheral molybdenum centres was apparent that no detectable reductions or oxidation waves associated with these central metal atoms were observed over a wide voltage range. There was no possible explanation for this behaviour and although it was suggested that

reductions of the central metal atoms were masked by the solvent decomposition processes, this was not empirically ascertained (Kagwanja *et al*., 1994). All this have been done using molybdenum nitrosyl centres. The work described in this thesis deals with oxo-molybdenum complexes of Tris(3,5-Dimethyl-1-pyrazolyl) Borato anion. This is in order to investigate whether there is any significant difference when precursor centre is changed.

1.3 Objectives

1.3.1 General Objective

To synthesize monometallic and bimetallic complexes of Schiff base ligands, characterize them and explore their redox potentials.

1.3.2 Specific Objectives

1. To design, synthesize and characterize schiff base ligands capable of securing two potential redox metal centres.
2. To synthesize and characterize Nickel (II) and Cobalt (II) Schiff base complexes and their monometallic derivatives.
3. Synthesize and characterize Nickel (II) and Cobalt (II) bimetallic Schiff base complexes.
4. To investigate how bridging ligand structure controls the magnitude of transmission of electronic effects from one redox metal centre to another in these monometallic and bimetallic complexes.

CHAPTER TWO

LITERATURE REVIEW

2.1 Schiff Bases: Definition and Formation

Schiff bases are compounds containing the azomethine group, RR'C=N- where R' is hydrogen and R is alkyl or aryl substituents (Layer, 1962). Metal complexes derived from schiff base ligands have been known for over one hundred and fifty years and they were discovered by Schiff in 1869. Hugo Schiff described the condensation between aldehyde and amine leading to schiff base in 1864. Schiff base ligands are able to coordinate metals through imine nitrogen and another group, usually linked to the aldehyde. Modern chemists still prepare schiff bases, and nowadays active and well-designed schiff base ligands are considered privileged ligands. They are able to stabilize many different metals in various oxidation states, hence, controlling the performance of metals in a large variety of useful catalytic transformations. They are also able to transmit chiral information to produce non-racemic products through a catalytic process; chiral aldehydes or chiral amines can be used. Generally, active catalytic schiff base metal complexes are obtained in situ, and are not well characterized. However, the appropriate choice of metal precursor and the reaction conditions are crucial for catalytic properties. The so called salen ligands, with four coordinating sites and two axial sites open to ancillary ligands, are very much like porphyrins, but more easily prepared. The term salen was used originally only to describe the tetradentate schiff bases derived from ethylenediamine; the more general term salen-type is used in the literature to describe the class of [O,N,O] tetradentate bis-schiff base ligands (Pier, 2004).

Schiff bases may act as multidentate chelating ligands and form complexes with special and manipulable properties. Because of the facile synthetic flexibility of schiff bases, many ligands of diverse structural types can be synthesized. They are easy to prepare by condensation of primary amines with an active carbonyl compound as shown in Scheme 1 (Speck *et al*., 1963). The mechanism of schiff base formation is via an intermediate carbinolamine, which rapidly eliminates water after production to give the schiff base as illustrated in Scheme 1.

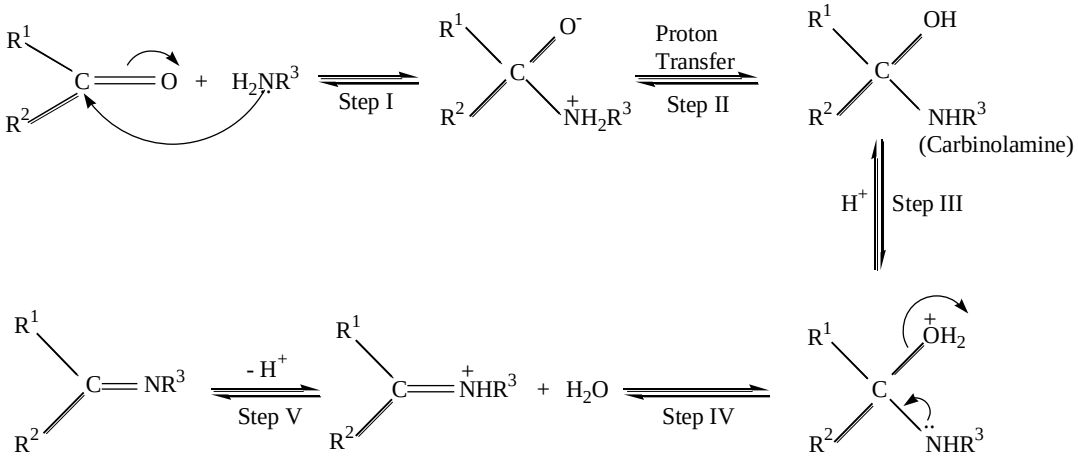

Scheme 1: Formation of Schiff base via carbinolamine intermediate.

Sometimes, the reaction for the formation of the Schiff bases can be acid-catalyzed. Hammet (1940) proposed that the acid protonates the carbonyl to give a carbonium ion which adds to the amine in a very fast reaction to form a carbinolamine which on deprotonation gives water and an imine. This is illustrated in scheme 2 below.

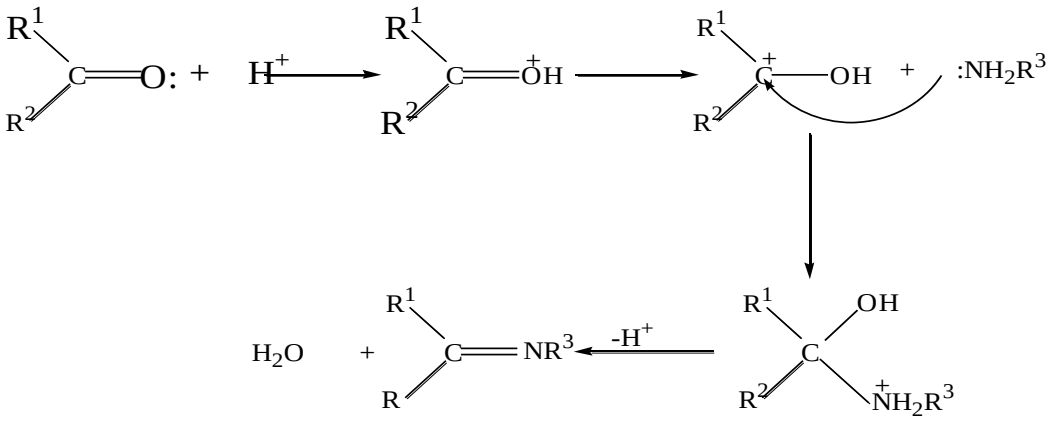

Scheme 2: Acid catalysis for the formation of schiff bases.

Schiff bases form multidentate chelating ligands which are polyfunctional and capable to bind to a single atom by three or more donor atoms. They have played a central role as chelating ligands because they are able to form complexes with most of the transition metals (Holm *et al*., 1966).

Although the complexes are quite stable, care needs to be taken in their synthesis. With achiral schiff bases, harsh conditions such as refluxing in high boiling solvents, causes alkylation in the imine of the schiff bases. In the synthesis of the metallic complexes, oxygen-containing solvents are normally avoided. The schiff base metal complex is insoluble, and is recovered by filtration. The greater the flexibility of the backbone (bifunctional schiff base ligands), the frequently trigonal bipyramidal geometry is obtained. An important aspect of the coordination chemistry of schiff bases is how the metal is displaced out of the plane of the ligand core. This distance is important in the

catalysis as it allows the transmission of chiral information and is crucial to the catalytic step (Pier., 2004). As in nature, schiff base metal complexes were designed to include a cavity, in order to accommodate dioxygen or some small ligands (Bushby and Pallaud, 1995). They have an important role to perform as polymerization catalysts and are able to stabilize a reactive cationic metal complex. They are able to act as a metallo crown and an interesting structure containing different metals can result (DiMaurio *et al*., 2002).

2.2 Preparation of Schiff Bases

Condensation between the aldehydes and amines is realized in different reaction conditions and in different solvents. The presence of dehydrating agents normally favours the formation of schiff bases. $MgSO_4$ is commonly employed as a dehydrating agent. The water produced in the reaction can also be removed from the equilibrium using a dean-stark apparatus, when conducting in toluene or benzene. Finally, ethanol, at room temperature or in refluxing conditions, is also a valuable solvent for the preparation of schiff bases.

Problems encountered

1. Degradation can occur during the purification step.
2. Chromatography of schiff bases are on silica gel and can cause some degree of decomposition of the schiff bases, through hydrolysis.

Corrections

1. Purifying the schiff base by crystallization.
2. If the schiff bases are insoluble in hexane or cyclohexane, they can be purified by stirring the crude reaction mixture in these solvents, sometimes adding a small

portion of a more polar portion (Et_2O, CH_2Cl_2), in order to eliminate impurities. Condensation of salicylaldehyde or salicylaldehyde derivatives with 1,2-diamines leads to the formation of one extremely important class of ligands, "salen".

2.3 Salicylaldimine Complexes

The schiff base ligands reported in this work are derived from condensation of salicylaldehyde and substituted salicylaldehyde with primary amines. It is therefore necessary to review some of the major factors relevant to the formation of salicylaldimine metal complexes. A variety of physico-chemical investigations of salicylaldimine complexes have served to provide a fairly clear understanding of their stereochemical and electronic properties.

The basic salicylaldimine ligand offers an advantage in having a flexible synthetic procedure, which has allowed preparation of a wide variety of complexes with a given metal whose properties are often strongly dependent on the detailed ligand structure. On this basis, it has been possible to effect certain stereochemical and electronic changes which can be examined in a graded homologous series of complexes (Holm *et al*., 1966).

Salicylaldimine has been shown to form stable complexes with all transition metals except Tc, Re, Ru, Os, Ir, Ag, Au, the lanthanides and actinides excluding Th and U (Holm *et al*., 1966). The only steric constraint to the formation of complexes by these ligands might occur for example when B is a two-carbon bridge such as ethylene or phenyl. The size of the metal ion accommodated in the stable complexes is not critical if the ionic radius is in

the range of 0.53A – 0.97A that permits chelation of tri- and tetravalent ions of the lower transition series (Holm *et al*., 1966). There is some evidence that an ion as larger as Ba^{2+} (ionic size 1.35A) can be introduced in 3 with B= ethylene forming salen (where salen = N,N'-bis salicylaldene imine). However, this compound has not been definitely characterized and its stability assessed.

Currently, the most significant complexes of salicylaldimine are those of the structural types (**c**) and (**d**), in which R, X and B´ are generalized nitrogen, ring and bridging group substituents respectively.

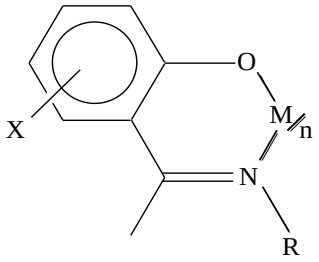

C

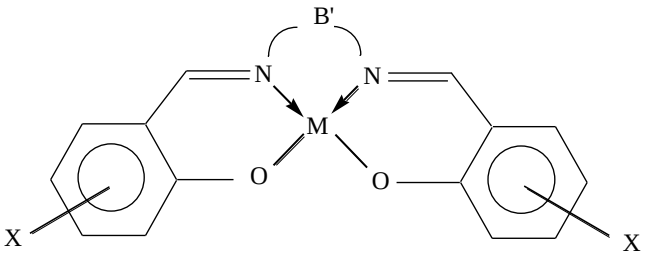

d

2.4 Geometry of the Schiff Base

Schiff base complexes have been observed to have variety of structures with tetrahedral and/or square planar and octahedral geometries, respectively. The complexes adopt geometry around the central metal, which maximizes the crystal field stabilization energy (C.F.S.E). However, the geometrical properties are often strongly dependent on the detailed ligand structure and on this basis; it has been possible to effect certain stereochemical changes in a graded homologous series of the complexes by systematically varying the ligand structure. For example, the metal complexes below containing a tetradentate ligand offer the possibility of existing in square planar or tetrahedral forms depending on the number of the methylene groups in the central chelate ring and nature of R.

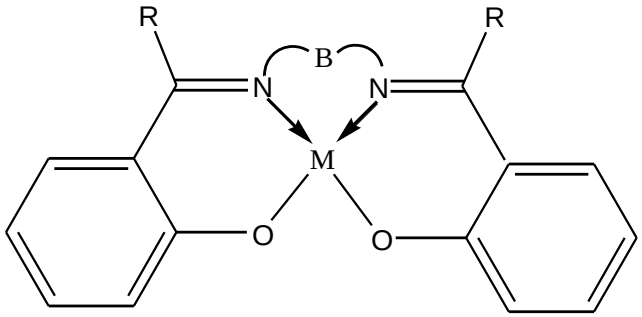

Figure 2: N,N'-bis (salicylidene) polymethylene diamine

Several reports revealed that the metal chelates of N, N'-bis (salicylidene) polymethylene diamine above changes their stereochemistry with the expansion of central chelate ring (Holm, 1960; Hariharan and Urbach, 1971). It has been observed that N,N'- bis (salicylidene) trimethylene diamine forms a high spin Co (II) chelate with a very flattened tetrahedral structure (Hariharan and Urbach, 1971) and in their planar Cu(II) and Ni (II)

chelates, a significant decrease of apparent ligand field strength is observed relative to the corresponding dimethylene chelates (Holm, 1960). This failure of the Co (II) chelate to adopt a well known pseudo tetrahedral geometry preferred by Co (II) ion was explained in terms of insufficient flexibility of the six membered ring containing $(CH_2)_3$ chain to allow the donor atoms to occupy essentially tetrahedral coordination positions when coordinated to Co (II). It can be logically argued that as the polymethylene carbon chain lengthens the flexibility of the ligand is increased and this allows the donor atoms to move out of a planar coordination, particularly when the metal does not impose a strong preference for this geometry.

The nature of the substituents group R also plays a role in determining the geometry of the schiff base complexes. For instance, if $M=Ni^{2+}$ and R is hydrogen in the above structure, a planar geometry, which maximizes the C.F.S.E is preferred. However, when R=aryl or alkyl substituents, the complex assumes tetrahedral geometry due to the greater steric interactions between the bulkier alkyl groups and thus the stability of the planar form is dependent on the steric requirements of the R group.

In the work described in this thesis, a variety of schiff base ligands were synthesized. The length of the polymethylene carbon backbone of the schiff base moiety has been systematically varied to effect certain stereochemical and electronic changes in a graded homologous series of the complexes under study.

2.5 Substitution and Conformational Effects in Schiff Bases

Coordination of the metal in bi- or tridentate schiff bases can produce dimeric, or saturated metal complex. Particularly with early transition metals, which have a tendency to coordinate ligands in an octahedral manner, the complexation step realized in situ can produce a saturated octahedral complex. When chiral schiff bases are used in the catalytic process, the formation of a saturated inactive complex is detrimental to catalysis. Metals coordinated to schiff bases can transmit chiral information via the coordination of the electrophile to the Lewis acidic centre, or via an activation of the nucleophile. Although stereogenic centres are normally placed in the diamine moiety, subtle conformational effects transfer the chiral information. When different elements of chirality are present in the same ligand, the conformational effects are more pronounced.

2.6 Solvolysis and Hydrolysis of Schiff Bases

Hydrolysis, which takes place even in absence of an acid but in warm aqueous solution, is the major drawback in the formation of schiff base chelating ligands. It is a two-step reaction that takes place by an attack of a water molecule at the electrophilic azomethine carbon atom as shown in Scheme 3 below.

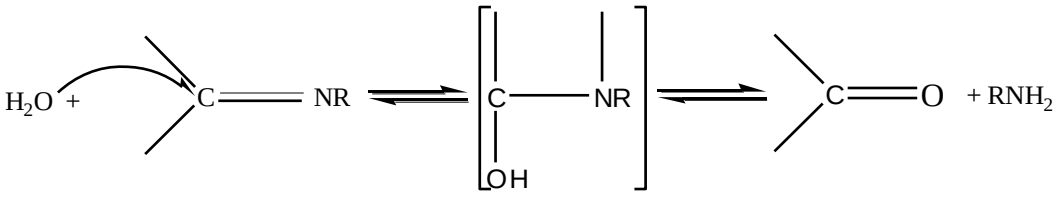

Scheme 3: Hydrolysis of Schiff Base

The unstable tetrahedral carbinolamine intermediate easily converts back to the initial aldehyde and amine. An experimental condition for the formation of the desired schiff base depends on the nature of the amine and especially the carbonyl compound, which determines the position of the equilibrium in the equation below.

$$RR^{I}CO + R^{II}NH_2 \rightleftharpoons RR^{I}=NR^{II} + H_2O$$

When R^I is an aryl group, it is generally advisable to remove water as it is formed by distillation using azeotropic solvents (Lutta *et al*., 1999). However, alkylaldehydes and dialkylketones can be condensed with primary amines without need to remove water from the equilibrium. One reason for this may be due to the electron withdrawing and donating capabilities of R^I group. Thus, the alkyl groups being electron releasing, may render the azomethine carbon atom less electrophilic and so less prone to hydrolysis while the aryl group being electron withdrawing shifts the electron density away from azomethine carbon thus making it electron deficient and hence susceptible to an attack by water and other nucleophilic molecules.

Hydrolysis of schiff bases can however be prevented by control of pH of the reaction media using a buffer system or addition of a weak base. Acetate salts have been useful in preparation of schiff base complexes since they offer advantage in the control of the pH by establishing acetate buffer action during the reaction.

Schiff bases may also undergo solvolysis in which a solvent molecule adds across the C=N linkages. For example, partial solvolysis in which an alcohol molecule adds across one of the imine linkages leaving the other one intact, has been observed in an attempt to prepare

copper complexes of N,N^{I}-bis (2-pyridylmethylene) ethane-1,2-diamine (Harris and Mckenzie, 1962). A case in which two moles of water adds across two azomethine linkages of schiff base, in the course of preparation of the copper schiff base complexes have also been observed (Bushby *et al*., 1995). Whereas aromatic aldehyde and aromatic or aliphatic ketones gives stable products with amines, aldehydes that contain CH_2CHO group easily undergo aldo-condensation to form polymers (Wagner, 1954). However, secondary aldehyde gives exclusively monomeric imines (Lutta, 1996). Other methods of synthesizing Schiff bases are widely reviewed by Dayagi and Degan (1970). All the above aspects were considered when designing the Schiff bases used in this work. Free Schiff bases were synthesized and isolated before being complexed with metals of interest to produce robust metal- Schiff base complexes.

2.7 Schiff Base Metal Complexes

Metal complexes of schiff bases represent an important and interesting class of co-ordination compounds (Syamal and Maurya, 1989), a situation manifested by the huge number of publications ranging from purely synthetic to modern physiochemical and biochemical relevant studies of schiff base complexes. A tremendous variety of stable chemical species containing transition, non-transition, inner transition, actinide metal ions and schiff base ligands have been synthesized (Holm *et al*., 1966). The doubly bonded nitrogen atom causes rather strong ligand field which leads to a large splitting of d-d orbital energies and consequently, a preferential occurrence of low spin configuration in such complexes (Jorgensen, 1963). Schiff base metal complexes have also played a significant role in the domains of stereochemistry structure, isomerism, magnetism,

spectroscopy, kinetics and mechanism of reactions, reaction of co-coordinated ligands, model systems of biochemical interest, analytical, catalysis, stabilizers, polymers, pigments and dyes, photography, electro-optical display and agriculture (Syamal and Maurya, 1989).

2.7.1 Historical Background of Schiff Base Metal Complexes

Preceding the work of Jorgensen, Ettling isolated a dark green crystalline product from the reaction of cupric acetate, salicylaldehyde and aqueous ammonia. The product 3 below was undoubtedly bis (salicylaldimine) Cu(II). The corresponding derivatives in which R=phenyl were isolated in 1869 by Schiff, who established the 1:2 metal ligand stoichiometry.

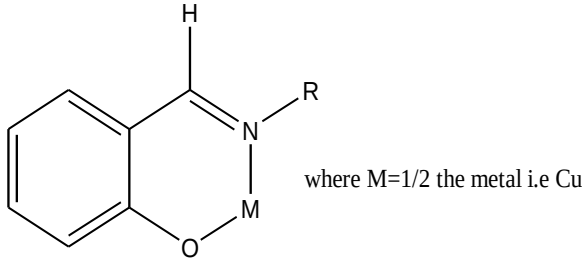

Figure 3: bis(salicylaldimine) Cu(II)

In his work, Schiff discovered the exceedingly important synthetic technique of preparing salicylaldimine complexes by reaction of the preformed metal salicylaldimine complexes with primary amines. Subsequently, he prepared complexes obtained from condensates of

urea and salicylaldehyde. Dele'pine prepared complexes depicted in 2 (R= methyl and benzyl) by reacting the metal acetate and salicylaldehyde in a 2:1 stoichiometry of ligand to metal acetate. After a period of relative inactivity, Pfeiffer and co-workers commenced the systematic synthetic study of schiff base complexes in 1931. Just prior to this, a cursory examination had revealed that transition metal ions formed coloured reaction products with a variety of substituted salicylaldehyde schiff bases. In 1931, Dubsky and Sokol isolated N, N'-bis (salicylidine) ethylenediamine Cu(II) and Ni (II) derivatives and correctly formulated their structures as 3, [B=$(CH_2)_2$, X = a halide, hydroxyl group and R= hydrogen or alkyl group].

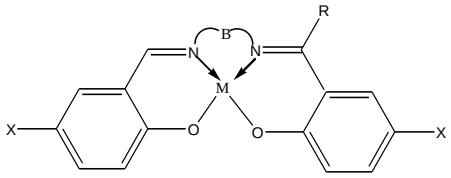

Figure 4: N,N'-bis (salicylidene) ethylene diamine metal complex

In the period 1931 – 1942, Pfeiffer and co-workers in a new classic series of papers produced a large number of complexes derived from schiff bases of salicylaldehyde and its substitution product (4), o-aminobenzaldehyde (5) and pyrrole-2-aldehyde (6).

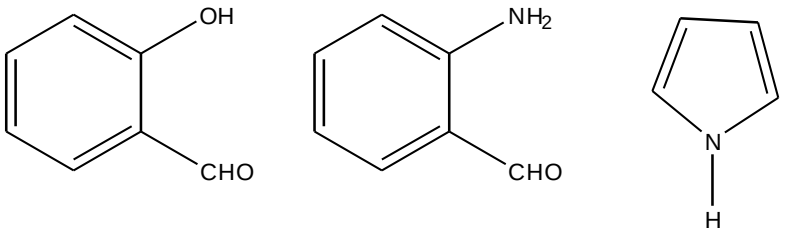

5 6 7

Figure 5: Complex from schiff bases and their substitution products

Figure 6: O-aminobenzaldehyde

Figure 7: Pyrrole-2-aldehyde

Of all schiff base complexes, those derived from salicylaldimine are by far the most thoroughly studied and therefore, their consideration comprises a major portion of the discussion.

2.7.2 General Preparative Methods for Schiff Base Metal Complexes

Schiff base metal complexes are readily prepared and easy to purify by recrystalisation (Speck *et al*., 1963). Procedures for preparation of the complexes can be broadly divided into two (Holm *et al*., 1966).

The first method involves reaction of metal ion and preformed schiff base ligand in the presence of an added base. The formation of the chelate complex proceeds by a conventional organic reaction and does not depend on the direct influence of the metal. These reactions are usually carried out homogenously in alcohol or aqueous alcohol solution with a base such as acetate or hydroxide. This method is useful for N-

arylsalicyaldimines but occasionally fails for N-alkyl complexes due to hydrolysis of the schiff base. In the second approach of reactions, the generation of the complexed product is influenced by the presence of a metal ion which acts as a template for crystallization reaction (Leussing and Stanfield, 1966). The mechanistic course of the reaction has not been precisely established but may be inferred from the reactions of the carbonyl groups and amines near neutral pH. A rapid nucleophilic attack of the carbonyl carbon by the amine first occurs followed by a slow rate determining step involving dehydration of the carbinolamine intermediate to yield the complex (Fujita *et al.,* 1996). This reaction mechanism is shown in Scheme 4.

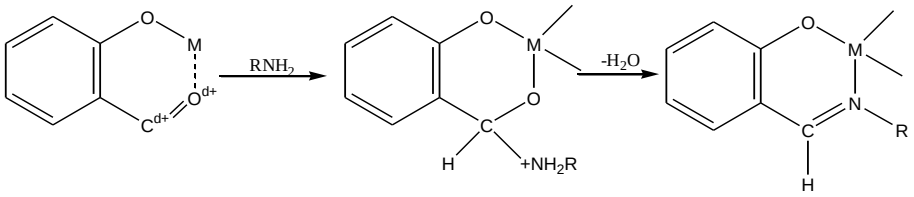

Scheme 4: Template synthesis of schiff metal complex.

The effect of the metal ions in promoting cyclization reactions as illustrated in scheme 3 has been recognized for a very long time (Leussing and Stanfield, 1966) and two possible roles for the metal ion in the template reaction have been delineated (Thompson *et al*., 1966). First, the metal ion may quench the cyclic product from an equilibrium mixture, between reactants and products. Here the chelate effect enhances the thermodynamic stability of the schiff base metal complexes and the metal ion is thus instrumental in shifting the position of equilibrium. Such a process has been termed as "thermodynamic template effect." Secondly, it is presumed that the polarization of the carbonyl group is

enhanced by the metal ion, thereby promoting nucleophilic attack on the carbonyl carbon by the amine. Although schiff base metal complexes synthesized in situ are expected to be highly unstable towards hydrolysis, this situation is expected to be overshadowed by other effects which result from coordination of the imine nitrogen to a metal ion (Culbertson *et al.*, 1935). The effects are two folds;

First, the metal having filled orbitals may suitably back donate electrons to the π acceptor orbitals on the amine carbon making it less electrophilic and thus less susceptible to hydrolysis. Second, the electron density associated with a C=N bond may shield, to some degree, the imine carbon from attacking nucleophiles. The metal ion is thus directing the steric course of condensation reactions such that the formation of the required product is facilitated. This process has been called "the kinetic effect." Examples of the operation of both types of effects have been documented (Lindoy, 1989).

2.7.3 Chiral Schiff Bases of Early Transition Metals

Schiff bases are widely used because they can control the coordination properties of the metal and form a coordination environment, similar to a metallocene. Schiff bases are moderate electron donors, with a chelating structure and a low electron counting number. Schiff base complexes of early transition metals are active catalysts for polymerization, provided that some simple criteria in the synthetic design are met. The coordination of phenoxy-imine to zirconium and titanium displays a distorted octahedral structure, with two nitrogen atoms and two chlorine atoms in cis position. The introduction of bulky groups in the phenoxy ring near to the oxygen is important, in order to stabilize these schiff bases and make them synthetically useful for polymerization. The octahedral and C_2-

symetric Ti- and Zr- bis (phenoxyimine) complexes are chiral at the metal, with the titanium assuming a fluxional Λ or Δ configuration.

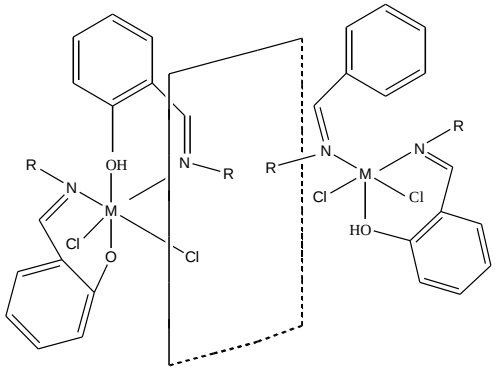

Λ-complex Δ-complex

Figure 8: Octahedral and C_2-symetric Ti and Zr-bis (phenoxyimine) complexes

2.7.3.1 The Chemistry of Cobalt

It always occurs in nature in association with Nickel and usually also with arsenic. It has an oxidation state ranging from –1 to –5. It is a hard bluish white metal (m.p 1493^0C b.p 1300^0C). It is ferromagnetic with curie temperature of 1121^0C. Cobalt (II), d^7 forms numerous complexes mostly either octahedral or tetrahedral but five-coordinate and square species are also known. There are more tetrahedral complexes of Co (II) than for other transition metal ions. This is in accord with the fact that for a d^7 ion, ligand field stabilization energies disfavour the tetrahedral configuration relative to the octahedral one to a smaller extent than for any other d^n ($1 \leq n \leq 9$) configuration. It should be noted that this argument is valid only in comparing the behaviour of one metal ion to another, not for assessing the absolute stabilities of the configurations for any particular ion. The only d^7 ion of common occurrence is Co^{2+} and planar complexes are formed with several bidentate

monoanions. Several neutral bidentate ligands also give planar complexes. Octahedral complexes are common with halides, pseudohalides and O-donors

(Cotton, 1980).

2.7.3.2 Biological Aspects of Cobalt

Cobalt is used as a stable low-spin state, Co (II), which has an exposed unpaired electron, d^7. It's a rare element and in nature most of it found in human body is in the corrin cobalt. The corrin cobalt complex is a vitamin of the lowest concentration in the body. The use of the metal is associated with the requirement for a free radical catalyst and the control of a free radical centre. Cobalt is paramagnetic and is sensitive to changes in its coordination geometry that appears in its visible absorption spectra. It is found in vitamin B_{12}, its only apparent biological site. Vitamin B_{12} deficiency causes the severe disease of pernicious anemia in humans, which indicates the critical role of cobalt.

2.7.3.3 Cobalt (Salen) as Useful Catalyst for Opening Epoxides

Achiral Co(salen) has a well- established ability to bind oxygen. The square pyramidal coordination geometry, imposed by the salen framework, is necessary for Co(salen) complexes to obtain the correct electronic configuration for oxygen binding. In particular, Co(salen) has been used for the preparative oxidation of phenols, indols, flavanols and amines. The complexation with a stronger donor molecule makes Co(salen) a stronger reducing agent. The binding ability of oxygen to Co(salen)-type complexes depends on the basicity of the axial ligand. Oxidation takes place via the coordination of the substrate to the cobalt. Organic substrates containing donor atoms (phenols, indols and amines) are more easily oxidized. Metallosalen cobalt complexes are useful for the transfer of carbene

and for opening epoxides. The Co (II) salen complexes are readily prepared by using $Co(OAc)_2$. The oxidation from Co (II) to Co(III) can be realized by treating Co (II) with air and acetic acid, or using various acids in the presence of air.

2.7.4 The Chemistry of Nickel

Nickel occurs in nature mainly in combination with arsenic, antimony and sulphur. It has the Oxidation State ranging from 0-4 and coordination number ranging from 2-6. Nickel (II) forms a large number of complexes with coordination numbers 3 to 6. A considerable number of neutral ligands, especially amines, displace some or all of the water molecules in the octahedral $[Ni(H_2O)_6]^{2+}$ ion. Magnetically, octahedral Ni (II) complexes have relatively simple behaviour. The magnetic moments ranging from 2.9 to 3.4 BM, depending on the magnitude of the orbital contribution. For regular or nearly regular tetrahedral complexes there are characteristic spectral and magnetic properties. Naturally, the more irregular the geometry of a paramagnet Ni (II) complex the less likely it is to conform to those specifications.

For the vast majority of four–coordinate Ni^{2+} complexes, planar geometry is preferred. This is a natural consequence of the d^8 configuration, since the planar ligand set causes one of the d orbitals (dx_2-y_2) to be uniquely high in energy and the eight electrons can occupy the other four d orbitals but leave this strongly antibonding one vacant. Almost all-planar complexes of Ni are thus diamagnetic. Trigonal complexes are rare for Ni^{2+}. Nickel forms organometallic complexes in the oxidation states 0, I and II; there are also a few examples of Ni^{3+} and Ni^{4+}.

It is known that nickel is an essential component in at least four types of enzymes and can exist under physiological conditions in the oxidation states I, II and III. Urease catalyzes the hydrolysis of urea to ammonium and carbonate ions; it appears to contain a redox-inactive Ni_2 unit in which the nickel atoms are octahedrally coordinated and probably act as Lewis acid for substrate binding (Cotton *et al;* 1999).

2.7.4.1 Biological Aspect of Nickel

Currently, there are only four proteins or enzymatic systems known in nature that contains functionally significant nickel. These are; ureases, hydrogenases, methyl coenzyme M, reductase cofactor F430 and carbonyl dehydrogenase. The distance and geometry of each ligand to nickel, the oxidation states used by nickel and the identity of the ligands in each of these enzymes must be determined. Ni^{2+} (d^8) is the common oxidation state in aqueous solution. It may be four or six –coordinate, square planar, tetrahedral or octahedral (cotton *et al;* 1999).

2.7.3.2 Nickel Metal Schiff Bases

Schiff bases have an important role to perform as polymerization catalysts, and are able to stabilize a relative cationic nickel complex. In order to stabilize cationic intermediate nickel complexes, the schiff bases are prepared using the reaction of hindered aromatic amine (2,6-diisopropylaniline) with diketones. Although Ni(salen) complexes have not found many applications in catalysis, their planar coordination geometry constitutes an interesting platform to coordinate other metals.

2.8 Polypyrazolyl Borate and Trispyrazolyl Borate

Research on coordination chemistry of pyrazole related ligands have progressed rapidly over the years following their discovery by Trofimenko (Trofimenko, 1999). They have a general formula $[RnB(Pz)_{4-n}]$ where n=0,1 or 2 and R is usually hydrogen or aryl group, Pz=pyrazole or substituted pyrazole. Uninegative tris(pyrazolyl) borate tripodal species are the most studied pyrazolyl ligands and has the formula $[RB(Pz)_3]^-$. They are stable in air and moisture (Daniel *et al*., 2000). They are prepared by reaction of pyrazole with an alkali-metal salt (Trofimenko, 1999). The extent of substitution in borohydride is controlled by temperature as illustrated in scheme 5 below. Ligands containing carbon constituents are prepared by using an appropriately substituted pyrazole in the reaction in Scheme 5. If 3,5-dimethyl pyrazole is reacted with BH_4^-, the reaction stops completely at the trisubstitution stage, probably crowding around the boron atom which cannot accommodate another large group.

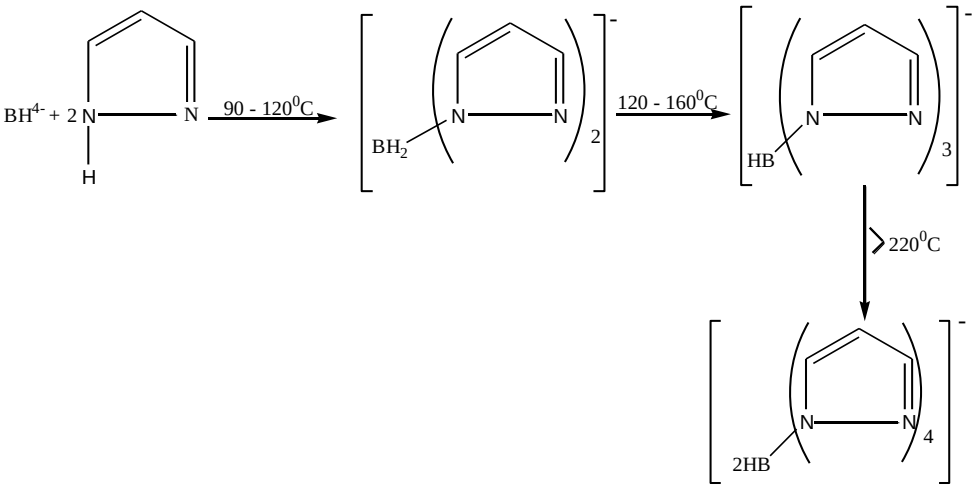

Scheme 5: Preparation of pyrazolyl borates.

The coordinating ability of these classes of ligands arises as a result of favourable geometrical factors and occurs via the nitrogen atoms at the two positions of each pyrazolyl ring. These ligands are uninegative and have C_{3v} symmetry. This combination of properties is unique because other ligands of C_{3v} symmetry are usually chargeless.

In developing the coordination chemistry of the ligands, Trofimenko noted the strong analogies between the behaviour of metal complexes containing trispyrazolylborato anion and those containing η^5-cyclopentadienyl (Daniel *et al*., 2000). The ligands are similar in the sense of formally occupying three coordination sites and supplying six electrons to the metal. However, the analogy between these two ligands is not ideal in that while cyclopentadienyl binds a metal by carbon-metal pi donation from the ring π-molecular orbitals, the tris(pyrazolyl) borato anion functions as a nitrogen sigma donor using appropriate combinations of sigma orbitals and a very weak π-acceptor. Also, the tris(pyrazolyl) borate is charged and has a three-fold symmetry whilst C_5H_5 is neutral and has a five fold symmetry (Trofimenko, 1999). Furthermore, the former has substantially greater steric bulk than the latter (Amitava *et al*., 1983).

The work described in this thesis involves the excessive use of the tris(3,5-methyl pyrazolyl)borato anion denoted by [HB(3,5-$Me_2C_3N_2H$)]- or [HB(DMPz)]- or T^* shown in figure 9.

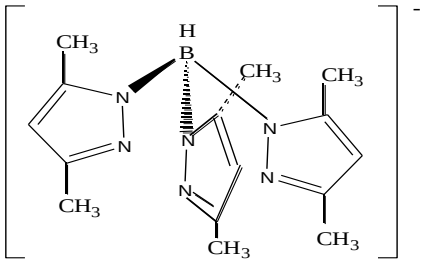

Figure 9: Tris(3,5-methyl pyrazolyl) borato anion

A derivative of the polypyrazolylborate ligand, tris(3,5-dimethylpyrazolyl) hydroborate, (9) was used in this study. It is prepared in the same way as the other polypyrazolyl-borates except that in this case, substitution stops at three 3,5-dimethylpyrazolyl rings. This is because boron is too crowded by the methyl groups to accommodate another large substituent. It is equally uninegative, tridentate and a six-electron donor, formally isoelectronic with η^5-$C_5H_5^-$. It is sterically bulky and thus usually confers greater stability on its complexes than the cyclopentadienyl ion (Trofimenko, 1993).

2.9 The Chemistry of Molybdenum.

It was discovered by Scheele in 1778, in molybdate MoS_2 which is its most important ore. Owing to its high melting point of 2622°C, molybdenum is usually obtained as a black powder, but if it is compressed and heated electrically nearly to its melting point it forms a coherent mass of a brilliant silver white colour. It has a boiling point of 3560°C and its specific conductivity at 0° is about one third of that of silver. It has a variety of stereochemistries in addition to oxidation states and its chemistry is among the most

complex of the transition elements. It can exist in six coordinated states (Cotton, 1999).

Molybdenum occurs chiefly as molybdenite (MoS_2) but also as molybdates such as $PbMoO_4$(Wulfenite). Molybdenum is used in a variety of catalysts combined with cobalt in desulfurization of petroleum; another major use is in alloy steels to which hardness and strength are imparted (Cotton *et al*., 1999).

2.9.1 Biological aspects of Molybdenum

Molybdenum is one of the biologically active transition elements. It is intimately involved in the functioning of enzymes called nitrogenases, which cause atmospheric nitrogen to be reduced to ammonia or its derivatives, in enzymes concerned with reduction of nitrate, and in still other biological processes (Cotton, *et al*., 1999). It is also found in enzymes such as xanthine oxidase, sulphite oxidase and nitrate reductase. The chemical reactions catalyzed by these enzymes all involve a change in the substrate and there is strong evidence that those enzymes possess a common molybdenum cofactor (Cleland *et al*., 1986).

Molybdenum is an essential trace element which is found in enzymes such as oxidase, sulphite oxidase and nitrate oxidase. The chemical reactions catalyzed by these enzymes all involve a change in the number of oxygen atoms in the substrate, and there is strong evidence that these enzymes possess a common molybdenum cofactor (Cramer and Stiefel, 1985). An overall chemical reaction cycle for oxo-molybdenum centres of such enzymes involving Mo(IV), Mo(V) and Mo(VI) is shown in the Scheme below.

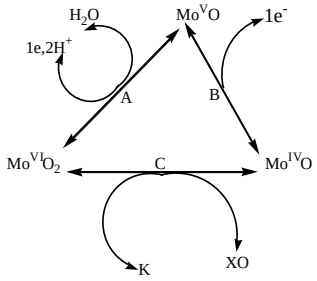

Scheme 6: Chemical reaction cycle for oxo-molybdenum centres.

Several chemical models for the oxo-transfer reaction between Mo(IV) and Mo(VI) represented by C of the scheme above have been demonstrated. The EPR signals of these Mo(V) states are observed upon reduction of the enzyme with substrate or dithionite and are usually present in equilibrium with both Mo(IV) and Mo(VI). Kinetic measurements have shown that the Mo(V) states are sufficiently long-lived to be intermediates in catalytic cycle. Present descriptions of the coordination environment of the molybdenum centres in enzymes rest upon comparisons of spectra obtained from the enzymes with those of well-characterized molybdenum complexes.

It is the only transition metal below the first series that is known to be essential in living systems. It is an essential trace element for many plants, probably entering them from the soil as molybdate ion. It also has a role in higher animals and humans. It is believed to be a necessary trace element in animal diets but its function and minimum levels have not been established. It is well established that nitrogen-fixing bacteria employ enzymes containing both Mo and Fe. It is best known for its essential role in various aspects of biological nitrogen chemistry (Cotton, 1980).

2.9.2 Molybdenum nitrosyl complexes of tris (3,5-dimethylpyrazolyl) hydroborate

Compounds containing the sterically hindered molybdenum nitrosyl tris(3,5-dimethyl-pyrazolyl) hydroborate group, Mo(NO)Tp*XY (**10**) have found application as a basic redox active metal fragment used as group I cation sensors, components of materials having non-linear optical properties and precursors for oligonuclear compounds exhibiting novel magnetic behaviour (McCleverty, 1989; Amoroso *et al.*, 1995).

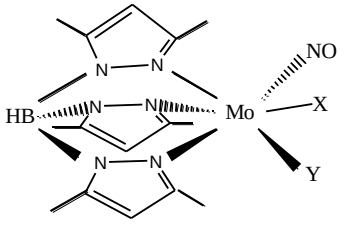

where X,Y = Cl, I, OAr, OR, NHR

Figure 10: Molybdenum nitrosyl tris (3, 5-dimethyl pyrazolyl) hydroborate metal fragment

They contain $Mo(NO)^{3+}$ species which is redox-active and readily undergoes one-electron reduction to $Mo(NO)^{2+}$ according to the equation below (Jones *et al.*, 1998).

$$Mo(NO)^{3+} + e^{-} \longrightarrow Mo(NO)^{2+}$$

This group of compounds where X, Y are halides, is prepared by first melting potassium borohydride and 3,5-dimethylpyrazole at 240°C. Hydrogen is given off while the product obtained, potassium tris(3,5-dimethylpyrazolyl) hydroborate, is refluxed with $Mo(CO)_6$ in toluene under nitrogen. This reaction yields carbon monoxide and a salt of potassium,

$K[MoTp^*(CO)_3]$ which on acidifying with ethanoic acid forms potassium ethanoate and $MoT_p^*(CO)_3H$. Nitrosylation with *N*-methyl-*N*-nitroso *p*-toluene sulphonamide (diazald) gives $Mo(NO)Tp^*(CO)_2$. *N*-methyl *p*-toluene sulphonamide and carbon monoxide are also formed. When $Mo(NO)Tp^*(CO)_2$ is halogenated with a benzyl halide under nitrogen gas, using iodine as a catalyst, $Mo(NO)Tp^*X_2$ is formed (Reynolds *et al*., 1985). A summary of the processes involved is shown below in Scheme 2.8.

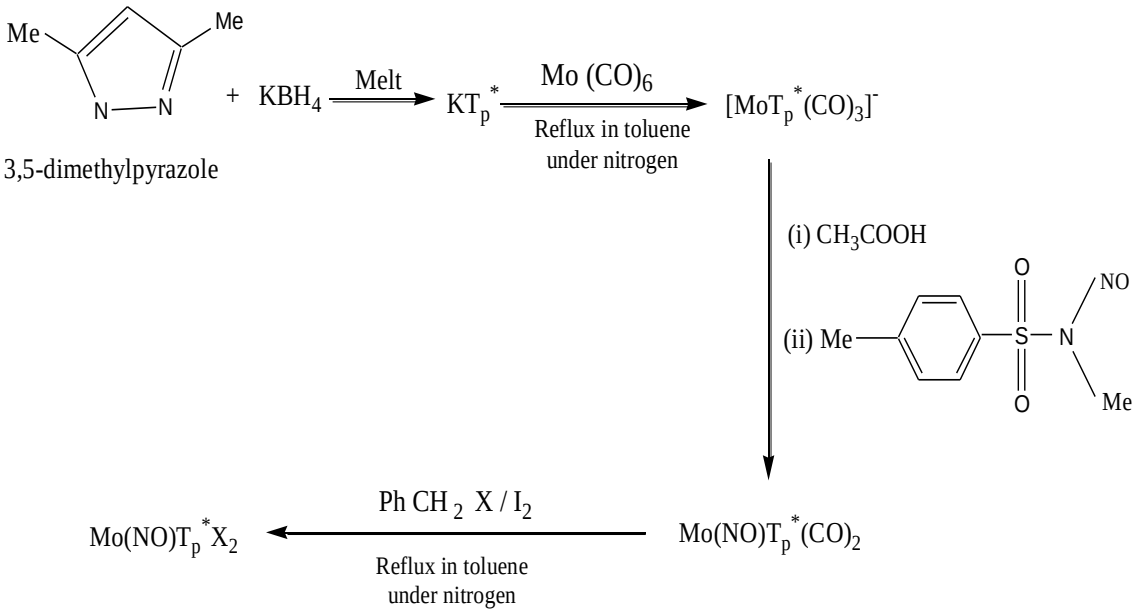

Scheme 7: Preparation of $Mo(NO)Tp^*X_2$

In this group of compounds, the most extensively studied halides are those where X = Cl or I (Briggs *et al*., 1985). The dichloride, $Mo(NO)Tp^*Cl_2$ is readily reduced electrochemically to the monoanion $[Mo(NO)Tp^*Cl_2]^-$, which is stable in solution and can be isolated by chemical reduction of the neutral precursor using triethylamine and triflouroethyl hydrazine. The diiodide, in contrast exhibits a much more complex behaviour. In dry THF,

the diiodide is reversibly reduced to the corresponding monoanion at a relatively anodic potential. However, if moisture is allowed into the system or if the neutral diiodide is exposed to water even in the absence of formally reducing conditions, reduction to $[Mo(NO)Tp^{*}I_2]^{-}$ is rapidly superceded by formation of a new reduced species, identified as $[Mo(NO)T_p^{*}I(solvent)_n]$, resulting from dissociation of I^{-} from $[Mo(NO)Tp^{*}I_2]^{-}$. For example, analogues of $[Mo(NO)Tp^{*}I(solvent)_n]$ where the 'solvent' is an amine, *viz* $[Mo(NO)Tp^{*}I(NHC_nH_{2n})]$ for n = 4 or 5 have been isolated and characterized. They readily get oxidized to $[Mo(NO)Tp^{*}I(NC_nH_{2n})]$ (Obaidi *et al*., 1986).

The compounds $Mo(NO)Tp^{*}XY$, where Y = OR, OAr, NHR, NHAr, SR and SAr, like their dihalide analogues, undergo one electron reductions and when X = Cl, the reduced species are stable to dissociation whereas $Mo(NO)T_p^{*}IY$ readily dissociates with I^{-} loss. This property can be very important not only for the electrochemical behaviour of this class of molybdenum complexes but also for the synthetic chemistry of this system. Substitution of halide in $Mo(NO)Tp^{*}Cl_2$, by primary alcohols and phenols to give in general, mono-alkoxides and aryloxides is carried out by heating the dihalide with the alcohol or phenol or by addition of triethylamine in the presence of a substrate (Reynolds *et al*., 1985).

The structures of representative members of the series $Mo(NO)Tp^{*}XY$ have been determined crystallographically (McCleverty, 1983). In all of them, the protective nature of the tris(3,5-dimethylpyrazolyl) hydroborate ligand is evident, the 5-methyl groups hanging down over the metal atom thus effectively enforcing six-coordination of these species

which normally prefer seven- or eight-coordination. In addition, the bond distances between the metal and the heteroatom of the Y group are short, indicating a substantial amount of p_π–d_π *or* d_π–d_π bonding between O, N or S and Mo. By this donation of charge from the 'hetero' ligand, the metal seeks to relieve its severe "electron deficiency", occasioned not just by the system's coordinative unsaturation, but also by the presence of the powerful π-acceptor NO and electronegative halogen ligands.

These factors undoubtedly contribute to the high stability of this class of compounds towards oxidative decomposition and to the facility with which they may be reduced. They are thus air- and moisture-stable, the unexpected robustness towards oxygen and water being attributed, at least in part, to the strongly protective nature of Tp^*. They are also monomeric in solution and in solid state and as such do not oligomerize, this being attributed to the steric bulkiness of the ligand. The chemistry of these tris(3,5-dimethyl-pyrazolyl) hydroborate nitrosyl species is, therefore, governed by a combination of both steric and electronic factors (McCleverty *et al*., 1998; Briggs *et al*., 1985).

The $E_{1/2}$ values of the reduction potentials of $Mo(NO)Tp^*XY$ are strongly influenced by the nature of X and Y (Obaidi *et al*., 1987).

2.9.3 Oxo-Molybdenum Complexes of Tris(3,5-Dimethyl-1-Pyrazolyl) Borato Anion

A major goal of coordination chemistry is to prepare multinuclear complexes in which the interactions between component parts lead to novel useful properties. Electrochemical, photochemical and magnetic interactions between remote metal centres all ultimately

depend on either transfer of one electron or interaction between two or more electrons, between the interacting centres. Usually, this interaction is mediated by a bridging ligand. It is of fundamental importance to understand the role of the bridging ligand and how it can modify or control the interactions across it. In this study, the precursor complex is oxo-molybdenum dichloride formulated $Mo(O)Tp^*Cl_2$, where Tp*= (3,5-dimethyl pyrazolyl) borato anion. This molecule has been described by Van and coworkers (Van *et al*., 1977).

The isolation and characterization of Mo(V) complexes that may be synthetic analogues of the Mo(V) states in enzymes are difficult because of propensity of oxo-Mo(V) complexes to form binuclear diamagnetic products in the presence of trace amounts of water. The approach to this problem has been to create a steric pocket for the molybdenum atoms in order to inbuilt (accommodate) such dimerization reactions. A simple pocket-shaped ligand is hydrotris(3,5-dimethyl-1-pyrazolyl) borate, TP* (Cleland *et al*., 1987).

Oxo-molybdenum complexes were first investigated by Cleland and co-workers who prepared a series of mononuclear complexes [Mo(O)(Tp*)ClX], where X= monodentate anionic ligand and determined their electrochemical and spectroscopic properties (Cleland *et el*., 1987). The complex was of particular appeal because;

i. It is electronically simple d^1.

ii. It is both redox-active and paramagnetic and so will lead itself to the study of electrochemical and magnetic interactions across bridging ligands.

iii. It is synthetically easy to use.

iv. The coordination chemistry and bioinorganic chemistry of oxo-molybdenum

(V) complexes have been extensively studied so their spectroscopic properties are fairly thoroughly understood (Cleland *et el*., 1987).

Complexes of the type [{Mo^{V}(O)(Tp*)Cl(μ-OO)}] where "OO" denotes a bridging ligand with two anionic phenolate-type donors have been prepared. These range from ligands with one aromatic ring, such as 1,3- and 1,4-dihydroxybenzene, to 4,4-dihydroxyquaterphenyl with four para-linked aromatic rings in the bridge. The research shows that there are strong electrochemical interactions which result in substantial splitting between the successive Mo(V)/Mo(VI) oxidations, and smaller splitting between the successive Mo(V)/Mo(IV) reductions (Cleland *et al*., 1987). The difference in the splittings between the two oxidations and the reduction is due to the fact that the oxidations are partly delocalized on to the bridging ligand such that the resonance form Mo(V)-(quinone)-Mo(V) contributes to the oxidized species, whereas reductions are essentially metal-localized. Electron paramagnetic resonance (EPR) spectra show that the magnetic exchange effects are present. This results in both line broadening at room temperature (solution), spectra that arise from the anisotropic interaction between the electrons and the appearance of the half-filled (ΔMs=2) transitions in the 77K (frozen) spectra that arise from the dipolar interaction between the electrons. The electrochemical interactions decreases as the bridging ligands become longer and also due to changing the substitution pattern of the bridge from *para* to *meta* or imposing a substantial dihedral twist between phenyl rings of the bridging ligand. The anisotropic interaction responsible for the line broadening in the EPR spectra is dependent on the nature of the π pathway between the metal centres in the same way (Van *et al*., 1997). Delocalization across the bridge will be

decreased by;

i. Increasing the length of the bridge.

ii. Imposition of a substantial dihedral twist between two aromatic rings within the bridge.

iii. Changing the substitution pattern from *para* to *meta* (Wlodarczyk *et al*., 1997).

2.9.4 Mo^{v} Oxo Species.

The isolation and characterization of Mo (V) complexes that may be synthetic analogues of the Mo (V) states in enzymes are difficult because of the propensity of oxo-Mo (V) complexes to form binuclear diamagnetic products in the presence of trace amounts of water. Some scientists have approached this problem by creating a steric pocket for the molybdenum atom in order to inhibit such dimerization reactions. A simple pocket shaped ligand is hydrotris (3,5-dimethyl-1-pyrazolyl) borates (Enemark., 1986).

An extensive range of Mo^{V} compounds can be obtained by the reduction of molybdates or MoO_3 in acid solution either chemically (for example by shaking with mercury) or electrolytically. They contain MoO_3^{3+}core with strong, short (1.6-1.7Å) bond to four other ligands forming the base of a square pyramid and a sixth weakly bound ligand (sometimes missing) trans to the MoO bond. An important species, often a source of material for preparation of other Mo^{V} compounds, is the emerald green ion $[MoOCl_5]^{2-}$ or the closely related $[MoOCl_4]^{-}$ and $[MoOCl_4(H_2O)]^{2-}$ ions all of which are readily interconverted by varying (or removing) the ligand trans to the Mo=O bond. There are also bromo and iodo analogues. These ions can be obtained by reduction of Mo^{VI} in aqueous HX, by oxidation

of $Mo_2(O_2CCH_3)_4$ in aqueous HX or by dissolving $MoOCl_5$in aqueous acid. Molybdenum pentachloride will also react with many organic compounds or solvents (such as Me_2SO or Ph_3PO) to abstract oxygen and form oxomolybdenum (v) complexes such as $MoOCl_3(OSMe_2)_2$.

Because of their possible presence in biological molecules and because they also exhibit remarkable fluorescence, the $[X_4MoO]^-$ions have been much studied spectroscopically and theoretically. The electron occupies the dxy orbital and the remaining orbitals are ordered in increasing energy (d_{xz}, d_{yz}), $d_{x^2-y^2}$, d_{z^2}. The fluorescence is due to the (xz-yz)xy. Many more complicated MoO^{3+} complexes are known, such as $HBPz_3$)(catechol)MoO and a peroxo species$[MoO(O_2)(Ox)]^{2-}$ with a roughly pentagonal pyramidal structure (Cotton *et al*.,1999).

Although the mononuclear complexes just mentioned are important, dinuclear complexes dominate the oxo chemistry of Mo^V. The dinuclear complexes of Mo^V are of two main types; singly bridged ones that exist in cis and trans enantiomers (a) and (b) and doubly bridged ones (c), which are cis. In most cases some or all ligands are chelating. Examples of this type are (a) $Mo_2O_3(S_2COEt)_4$and (b) $Mo_2O_3[S_2P(OEt)_2]_4$ and $Mo_2O_3(LL)_4$ in which represents O-thio-pyridine. The doubly bridged structure(c) is found in $[Mo_2O_4(C_2O_4)_2(H_2O]^{2-}$ where water molecules are only weakly bound trans to the Mo=O bonds. In all mono-and dinuclear oxo complexes of Mo^V ligands trans to Mo=O bonds are rather weakly bonded and are often entirely absent (Cotton *et al*., 1999).

2.10 The Transition Metal

Transition metals are the best candidates for the role of molecular switches, on account of the following peculiar properties (Fabbrizzi *et al.,* 1999).

i) They can form couples of consecutive oxidation states, A and B, easily interconverted through a fast and reversible one electron redox change.

ii) The one electron charge in most cases modifies drastically the properties of the metal centres.

The research involves the study of one metal, Nickel, against molybdenum. Molybdenum just like tungsten has a variety of stereochemistries in addition to oxidation states (Cotton, 1980). It can exist in six coordinated states. The higher oxidation states are mainly stable but Mo^{1} and Mo^{II} are unstable. Molybdenum is one of the biologically active transition elements. It is involved in the functioning of enzymes called nitrogenases, which cause atmospheric N_2 to be reduced to NH_3 or its derivatives and in enzymes concerned with reduction of nitrate. Cleland et al (1987) reported that molybdenum is also found in enzymes such as xanthine oxidase, sulphite oxidase and nitrate reductase. All chemical reactions catalyzed by these enzymes involve a change in the number of oxygen atoms in the sub-state, and it is evidenced that these enzymes posses a common molybdenum cofactor.

Transition metals can be used as structural compounds in the construction of molecular containers. Supramolecular chemistry, which is the formation of new chemical structures

by the assembly of molecular sub-units bound together by non-covalent interactions, is having a major impact on current chemical research. Transition metal centres incorporated as vertices in a macrocyclic structure offers ready access to square planar or octahedral geometries (Jones, 1998).

The majority of transition metal ion complexes contain six ligands surrounding the central ion octahedrally. Others contain four which are either arranged tetrahedrally or less frequently, at the corners of a square. The bonding between the ligand and the transition metal ion can either be predominantly electrostatic or predominantly covalent or in many cases intermediate between the two extremes (Liprot, 1974). The number of complexing agents, which are the ligands, will depend on the coordination number of the metal and on the number of the complexing groups on the ligand molecule (Christian, 1986). The complex formed by the coordination of polydentate ligand to a metal atom is called a "chelate complex" (Jolly, 1985). Chelating ligands tend to form thermodynamically more stable complexes than comparable non-chelating ligands. The coordination of chelating ligands necessarily leads to the formation of rings and five or six membered rings are most common (Smith, 1990).

The incorporation of transition metal centres into cyclophane like structures introduces new functionality. This may contribute to the binding of guest molecules by the macrocycle and can give rise to novel electron transfer, luminescence or magnetic properties (Jones, 1998).

2.10.1 Transition Metals in Molecular Containers

Early examples of supramolecular assemblies have been provided by 'host-guest' compounds in which a larger 'host' molecule includes a smaller 'guest' molecule within a cavity in its structure (Cram *et al*., 1994). One well-studied example is provided by tetra-p-tert-butylcalix [4] arene (b cal H_4). The inclusion of toluene into the hydrophobic cavity of bcalH_4 provides an example of an 'inclusion compound' (Jones, 1998). Because they contain molecular cavities, and have the capacity to include organic molecules as guests, cyclophanes have played a central role in the development of such 'host-guest' chemistry. The incorporation of transition metal centres into such structures can confer new properties on those potential host molecules. In particular, transition metal centres might introduce Lewis acidity, magnetism, and redox activity or luminescence properties into the macrocyclic structures (McQuillan *et al.*, 1996). This may have important implications for the chemical reactivity or physical properties of a cyclophane host; for example optically driven charge transfer process between the metal centres and ligands in the macrocycle structure may lead to novel electro-optical properties.

Further, far-reaching aspects of the metal ions in supramolecular chemistry arise from the particular structural features associated with transition metal centres and the range of thermodynamic and kinetic stabilities their complexes display. The incorporation of transition metal centres as vertices in a macrocyclic centre offers ready access to square planar or octahedral geometries. A consideration of crystal field theory tells us that in the presence of strong field ligands, the use of d^5 electron configurations as in Co^{3+} should favour an octahedral geometry. Transition metal complexes containing suitably oriented

ligands which can be substituted by a polyfunctional ligand capable of linking metal centres provides a means of forming macrocycles in a single reaction step (Fujita *et al.,* 1996). Apart from these structural features, the variety of thermodynamic and kinetic properties exhibited by transition metal centres allows access to a range of reactivities, which may be exploited during macrocycle synthesis. The use of kinetically more inert metal centres provides access to those macrocyclic products, which form most rapidly, whilst with kinetically labile metal centres the thermodynamically most stable macrocyclic products will be obtained (Fujita *et al*., 1996).

2.10.2 Redox Active Transition Metal Complexes.

Multi-metallic complexes containing two or more redox active metal centres display distinctive physical and chemical properties. In binuclear complexes, which contain reducible and / or oxidizable peripheral fragments connected by a multi-atom bridge, the redox properties of one centre can efficiently be communicated through the bridging ligands to the neighboring redox centres. This is particularly so in compounds containing bipyridyls or quinines, where the ligands themselves are capable of redox activity (Lutta *et al*., 1999).

Research is being carried out in the study of the redox responsive binuclear metal complexes with emphasis on investigation and study of the mechanisms of transmission of electronic effects from one redox metal centre to another. Electronic interactions between redox canters are the basis on which the rate of intramolecular electron transfer is determined. One major aim in this area has been to investigate how bridging ligand

structure controls the magnitude of such interactions (Obaidi *et al*., 1986, Charsley *et al*., 1988).

There has been strong research interest in the relationship between the electrochemical behaviour and structure of transition metal complexes. Emphasis in this field has mainly been placed on two aspects;

i. Evaluation of the effect of changes in degree and type of substitution on the redox response of metal complexes.
ii. Investigation and study of the mechanism of transmission of electronic effects of one redox metal centre to another.

Early work of redox active transition metal systems include 1,2-dithiolene complexes (11) containing the basic $[M(S_2C_2R_2)_2]^2$ or $[M(S_2C_2R_2)_3]^3$ coordination site, which undergo facile, usually reversible, e^- transfer;

$$[M(S_2C_2R_2)_2]^0 \underset{-e^-}{\overset{+e^-}{\rightleftharpoons}} [M(S_2C_2R_2)_2]^+ \underset{-e^-}{\overset{+e^-}{\rightleftharpoons}} [M(S_2C_2R_2)_2]^{2-}$$

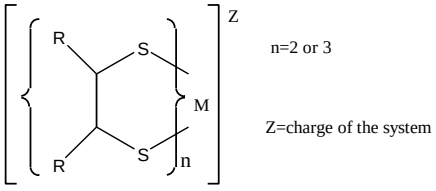

Figure 11: 1,2-dithiolene complexes

In simple dithiolene complexes (Fabbrizzi *et al*., 1999), the decreasing stability of the dianions has been found to be of the order; R=CN>CF_3>Ph>H>Me. This order reflects the

nature of the R-group, which shows that the dianions are least stable towards oxidation when R is an electron-releasing group.

A comprehensive study of complexes of (11) (where M=Ni, Pd, Pt and R=CN, CF_3, P-C_6H_4Cl, C_6H_5, H, C_6H_4Me, P-C_6H_4-OMe, Me, Et, normal and iso-pr) reveals a linear relationship between polarographic halfwave, $E_{1/2}$ and the inductive substituent constant.

Similar electrochemical behaviour has been observed (Hawkes et al., 1966) in the related arene 1,2-dithiolene complexes $[M(S_2C_6X_2Y_2)_2]$ (12) (M=Co, Ni, Cu; X=Y=H, Me, Cl; X=H, Y=Me) where $E_{1/2}$ for the couple $[M(S_2C_6X_2Y_2)_2]^{2-}$ are strongly dependent on the electronic nature of X and Y.

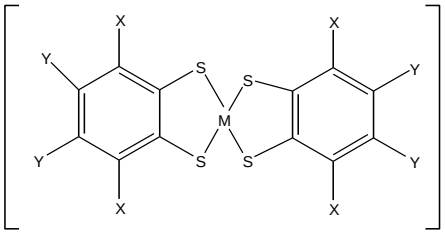

Figure 12: arene 1,2-dithiolene complex

Electron releasing substituents form more stable monoanionic complexes whereas electron withdrawing ones favors the dianionic form. Synthesis and electrochemical studies have also been done on redox active mononitrosyl complexes as shown below.

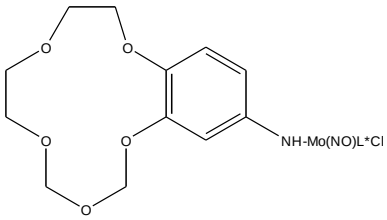

Figure 13: Redox active mononitrosyl complex

Besides crown ethers, compounds containing redox active molybdenum mononitrosyl centres, novel trimetallic compounds containing two metallocene redox centres have also been studied fully (Obaidi *et al*., 1986).

2.10.3 Transition Metals in Enzyme Catalysis

Most industrially important reactions are carried out with the aid of catalysts, transition metals or transition metal compounds. Many biologically important reactions take place with the aid of proteins in which transition metal atoms play important roles. For example, a cobalt atom lies at the heart of the vitamin B_{12} coenzymes. Both molybdenum and iron are contained in nitrogen fixing enzymes. The transition metal atoms in catalysts act as sites for holding the reacting species in conformations favourable for reaction and act as sources of, or sink for, electrons. These functions are obviously aided by the abilities of the transition metals to form complexes that undergo oxidation-reduction reactions (Jolly, 1985).

Transition metals are often involved in catalysis due to their electronic structures. Several properties of transition metals make them useful in catalysis. Metal ions provide a high

concentration of positive charge that is especially useful in binding small molecules. Because transition metals act as Lewis acids, they are effective electrophiles. Their directed valences allow them to interact with two or more ligands, metal ions help orient the substrate within the active site. As a consequence, the substrate-metal ion complex polarizes the substrate and promotes catalysis (Trudy *et al*., 2003).

2.11 Mixed Valence Compounds

These are materials that contain same metal in two different oxidation states (Robin and Day, 1967). They have been thoroughly studied by chemists particularly in their quest to understand electron transfer process between metal centres (Callahan *et al.,* 1975). The earliest example of this type of compound is Prussian blue which was discovered in 1724. The blue substance is thought to be basically $KCN.Fe(CN)_2.Fe(CN)_3$ in which iron is in +2 and +3 oxidation states. The intense blue colour of this bimetallic salt arises because visible light absorption induces electron transfer from Fe^{2+} to Fe^{3+}, a phenomenon possible in mixed valence compounds where the interacting metal ions are in close proximity. Cruetz and Taube (1973) deliberately synthesized and studied mixed-valence compounds a short time after the first publication on mixed-valence compounds appeared in 1967 (Robin and Day, 1967). Traditional approach to work in this area has been to synthesize complexes containing two or more metal ion each with their appropriate complement of external ligands and one or more shared entities referred to as bridging groups.

Electronic interactions in such systems are usually propagated through orbitals on the bridging group in an inner sphere fashion (Taube, 1978) though outer-sphere “through

space" coupling is also known especially if the metals are in close proximity (Sullivan and Meyer, 1980). By systematically varying the bridging group and holding the metals and co-ligands constant chemists have studied the nature and extent of metal-metal communication. On the other hand, both the bridging and co-ligands can be held constant while systematically varying the metal ions. Mochizuki and co-workers synthesized and studied electrochemical properties of heterobimetallic copper(II) and Ni (II) complexes of type 14 shown below (Mochizuki *et al.*, 1982).

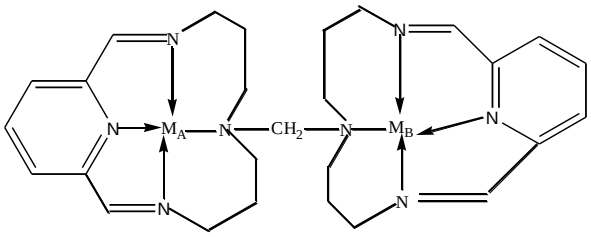

Figure 14: Heterobimetallic Cu(II) and Ni (II) complexes

Where M_A= Ni^{2+}, M_B=Cu^{2+} or M_A=Ni^{2+}, M_B=Ni^{2+} or M_A=Cu^{2+}, M_B=Cu^{2+}.

Their results revealed that the differential pulse polarogram of $[CuNiL]^{+4}$ is the sum of $[Cu_2L]^{+4}$ and $[Ni_2L]^{+4}$ [L= bis (tetrazamacrocycle) moieties indicating no interaction between the metal centres]. Utilizing complexes of type 15 below, Gagne and co-workers studied metal-metal interactions with copper in the M_A site while M_B was varied across the series {M_B= Mn^{2+}, Fe^{2+}, Ni^{2+}, Cu^{2+} and Zn^{2+}}. The observed changes in the electrochemical properties at the M_A site have been attributed to some form of metal-metal communication with remote metal M_B via intramolecular coupling of the two metal ions in sites M_A and M_B. This argument is plausible since the ligand remains constant (Andrea *et*

al., 2004).

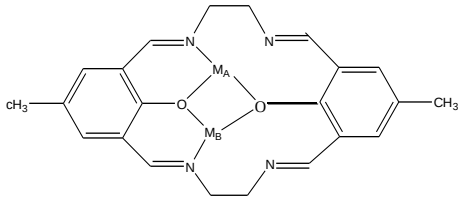

Figure 15: metal-metal interactions with Cu and metals across the series

However, the most thoroughly studied mixed valence compound has been the controversial yet highly celebrated Cruetz-Taube ion $[(Ru\{NH_3\}_5)_2$ pyrazine$]^{5+}$ and its analogue $[\{Ru(bpy)Cl\}_2$ pyrazine$]^{3+}$ complex both of which formally contain ruthenium in +2 and +3 oxidation state (Cruetz and Taube, 1993). Interests in the systems of this kind are the need to investigate whether the valencies of +2 and +3 are localized (trapped) at each end thus making the whole molecule unsymmetrical. The Cruetz-Taube ion has not been empirically proved to be either a localized or delocalized system. Thus its physical description remains controversial (Day, 1981).

Robin and Day classified mixed-valence compounds into three categories depending on the magnitude of electronic interactions between the two centres (Robin and Day, 1967). On the extreme ends are classes I and III compounds while class II lies between the two. Basically, when metal-metal interactions through a connecting bridging ligand are weak such that the metal centres have electronic and chemical properties of isolated monomeric complexes, then the system constitutes class I. the valencies of the centres are trapped (localized) and the property of the polymeric system is the sum of the monomeric units. An example of the molecule in this class is diruthenium complex (16) shown below.

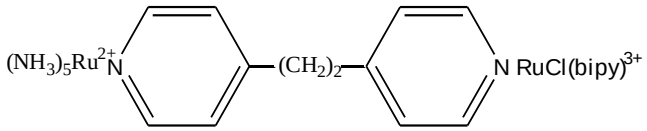

Figure 16: Diruthenium complex

No intervalence charge transfer band was observed for the complex above because the orbital pathway between the metal centres is blocked by saturated $–CH_2CH_2-$ linkage (Callahan *et al.*, 1975).

Class III compounds may be regarded as fully delocalized systems and interaction between the two centres is so great that the two behave as a single unit. An example of this system is oxo-bridged complexes of [Ru(III), $Bipy_2XRuORuXBipy]^{2+}$ where Bipy = 2,2-bipyridine and X is Cl or NO_2.

Class (II) compounds exhibit slightly perturbed metal centres. Here some degree of metal-metal interaction occurs, which may be accompanied by some electronic exchange between the metal centres. The compounds also exhibit some properties not attributed to the isolated metal centres but still not truly delocalized.

2.12 Examining the Extent of Metal-Metal Interactions

If there is an orbital pathway between metal centres in a complex, a light induced electron

transfer occurs between metal centres in different oxidation states and the band due to this transition is called intervalence charge transfer (IVCT). It is observed in the visible or near IR region (Callahan *et al.,* 1975). There have been developed a theoretical treatment for IVCT transition and found that the energy, intensity and shape of this band have much to say about the degree to which the redox active centres communicate via the bridging ligand.

In molecules where each metal centre undergoes reversible one-electron reduction processes, the extent of metal-metal interaction can also be estimated from the separation in reduction potentials (ΔE) between two reduction waves associated with each metal on the cyclic voltammetry time scale. Systems having ΔE between 500 and 1000mV indicate strong interactions, while those having ΔE=100mV and less indicate intermediate and weak metal-metal interaction, respectively (McCleverty *et al.,* 1988).

2.13 Factors Affecting Magnitude of Metal-Metal Electronic Interactions

There are several factors that control the rate of electron transfer between redox active centres (Callahan, 1975). These include;

2.13.1 Nature of the bridging ligand

As the length and degree of saturation of the bridging ligand increases, the redox coupling between metal centres decreases (Creutz and Taube, 1973). This was reported by Jing Jer and coworkers (1979) who investigated electron transfer processes in $(NC)_5Fe^{II}LCo^{III}(NH_3)_5$; where [L is bis (4-bipyridyl) methane, (BPM), n=2], [bis (4-

pyridyl) ethylene, (BPE), n=3], [bis(4-bipyridyl) ethane,(BPE), n=4] and [bis(4-pyridyl) ethylene,(BPE)]. They came up with a trend which showed how the bridging ligand controls the rate of electron transfer. They reported that the rate of intramolecular electron transfer increased in the order BPM>BPA>BPP. This demonstrated that as the length of the bridging ligand increases, the electronic interaction decreases. Studies on mixed valence compounds involving Ru(II) /Ru(III) amines showed that the degree of interaction between metal centres decreases exponentially as the size of the bridging ligand increases (Creutz and Taube, 1983). For pyridine ligands, the size of methylene bridge between pyridyl groups strongly decreases the metal-metal interaction (Sulton and Taube, 1981).

2.13.2 Nature of ligating atom

These are the atoms on the ligand that coordinates the ligands directly to the central metal ion. They can stabilize a particular metal oxidation state and affect its redox potential. Substitution of two thioethers for two amine donors results in increased values of Cu(II)/Cu(I) potentials by 300-700mV cathodically in the corresponding pairs of bis (pyridyl) dithio and bis (pyridyl) diaza complexes (Nikles *et al*., 1983). Their results were in agreement with previous observations that thioether donors produce high values for the Cu(II)/Cu(I) couple, an effect which is quantitatively attributed to the ability of the thioether donor to accept electron density into vacant 3*d* orbitals and stabilize the Cu(I) state (Dockal *et al*., 1976; Sakaguchi and Addison, 1979). McCleverty (1983), also worked on bimetallic complexes of type $M(NO)T_p^*X\text{-}Q\text{-}XM(NO)T_p^*Y$ for M, M′= Mo; X, Y = Cl; Q = OC_6H_4O, NHC_6H_4NH and found that complexes in which Q = NHC_6H_4NH reduced at potentials some 500 mV more cathodic than their counterparts in which Q = OC_6H_4O.

Patterson and coworkers reported high values for Cu(II)/Cu(I) potential using ligands with thioether. This effect was attributed to the ability of the thioether to stabilize Cu^{+} state via π acceptor interaction (Patterson *et al*., 1975).

2.13.3 Other factors

Besides the above factors, the type of the metal comprising the redox active centres as well as the geometry of redox centre affects metal-metal interactions. Metal ions usually prefer formation of three stereochemistries namely octahedral, tetrahedral and square planar. The preferred geometry around a metal centre depends on the emerging crystal field stabilization energy and whether such geometry can also stabilize oxidation state of the central metal. This affects its redox property and the rate of electron transfer.

CHAPTER THREE

EXPERIMENTAL

3.1 Introduction

Standard reagent materials were obtained from commercial sources and used as supplied without any further purification. The compound $Mo(O)Tp^*Cl_2$ was prepared according to the literature method (Cleland *et al*., 1987). All synthetic reactions except those involving preparation of schiff base ligands and their nickel and cobalt derivatives were carried out under nitrogen. Silica gel 60(70–230 mesh) was used for column chromatography while dichloromethane and hexane were employed as eluents.

An extensive series of $Mo(O)Tp^*XY$ (X,Y=Cl, I, OAr, OR, NHR) complexes can be prepared by several routes from the common precursor $Mo(O)Tp^*Cl_2$ first reported by Trofimenko (1972) as a product of the reaction of $[Tp^*Mo(CO)_3]$- with $SOCl_2$. A more convenient and improved preparation of $Mo(O)Tp^*Cl_2$ and to related oxo-Mo(V) mononuclear complexes have been developed. This is through the reaction of $MoCl_5$ with THF under anaerobic conditions which yields the known $Mo(O)Cl_3(THF)_2$, presumably by abstraction of an oxygen atom from the solvent.

$$MoCl_5 \xrightarrow{THF} MoOCl_3(THF)_2 \xrightarrow{Tp^*} Mo(O)Tp^*Cl_2$$

Addition of Tp* to the reaction mixture and moderate heating affords $Mo(O)Tp^*Cl_2$ as a green precipitate, which can be recrystalized from hot dichloromethane or 1,2-dichloroethane as bright green crystals. The complex is stable in air and water and is unchanged at 200°c (Cleland *et al.,* 1987).

Detailed experimental procedures are described in Scheme 8 below.

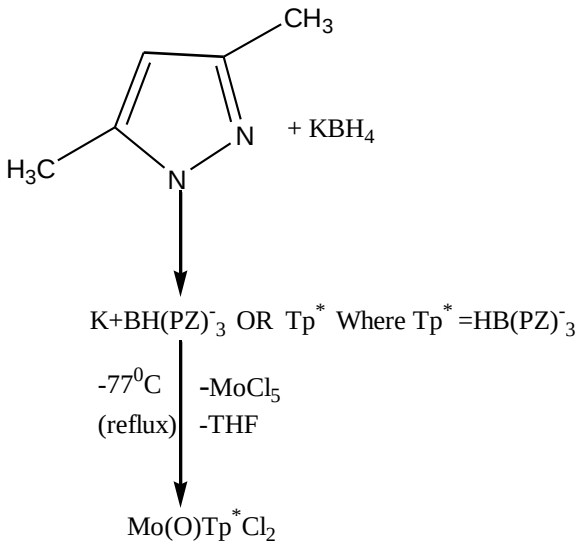

Scheme 8: Preparation of precursor molecule, Mo(O)Tp*Cl_2

Schiff bases (*meta* and *para* with respect to OH at position 2 in the benzene ring) were prepared by reacting *m*- or *p*-hydroxybenzaldehyde, salicylaldehyde and a variety of diamines in ethanol. They were then refluxed with metal salts (Ni (II) chloride and Co (II) chloride) to form metal Schiff base complexes which on refluxing with Mo(O)Tp^*Cl_2 yielded the desired bimetallic complexes. After each stage of preparation, the yield of the products obtained was determined and percentage yield calculated on the basis of the moles of the limiting reactant. Their physical properties as well as spectra were also determined at each stage of synthesis after which electrochemical studies were conducted on the monometallic and bimetallic complexes (Lutta and Kagwanja, 2000; 2001). A summary of the synthetic processes involved in this study is shown in Scheme 9 below.

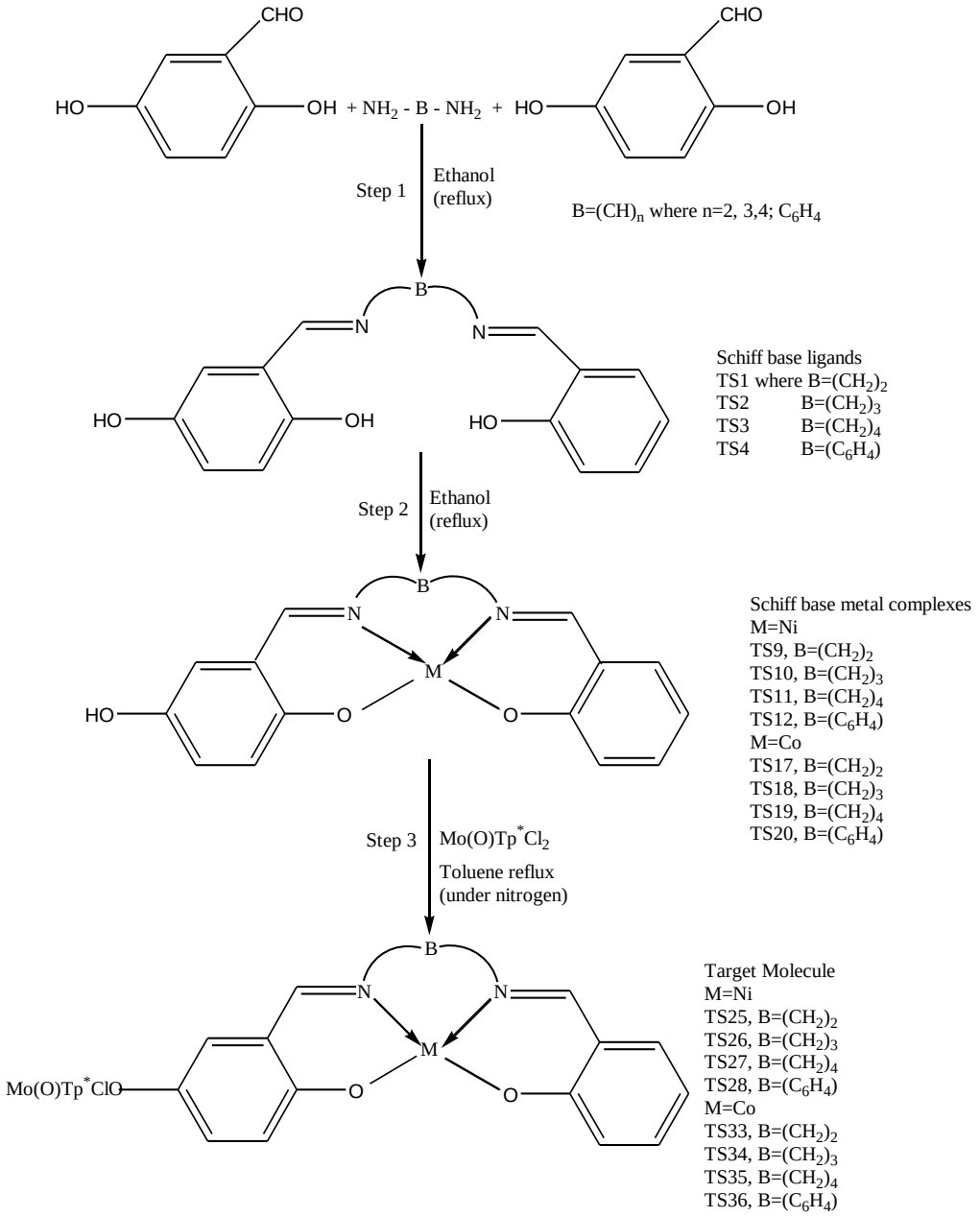
CHO
HO
OH
+ NH2 - B - NH2 +
CHO
HO
OH
Step 1
Ethanol
(reflux)
B=(CH)n where n=2, 3,4; C6H4
B
N
N
HO
OH
HO
Schiff base ligands
TS1 where B=(CH2)2
TS2 B=(CH2)3
TS3 B=(CH2)4
TS4 B=(C6H4)
Step 2
Ethanol
(reflux)
B
N
N
M
HO
O
O
Schiff base metal complexes
M=Ni
TS9, B=(CH2)2
TS10, B=(CH2)3
TS11, B=(CH2)4
TS12, B=(C6H4)
M=Co
TS17, B=(CH2)2
TS18, B=(CH2)3
TS19, B=(CH2)4
TS20, B=(C6H4)
Step 3
Mo(O)Tp*Cl2
Toluene reflux
(under nitrogen)
B
N
N
M
Mo(O)Tp*ClO
O
O
Target Molecule
M=Ni
TS25, B=(CH2)2
TS26, B=(CH2)3
TS27, B=(CH2)4
TS28, B=(C6H4)
M=Co
TS33, B=(CH2)2
TS34, B=(CH2)3
TS35, B=(CH2)4
TS36, B=(C6H4)

Scheme 9: Preparation of Schiff base ligands, monometallic and bimetallic complexes

3.2 Chemicals and Starting Materials

Molybdenum pentachloride, diamines, salicylaldehyde and triethylamine were obtained from Aldrich chemicals Co. Ltd. (U.K) and were used as supplied. Nickel chloride and cobalt acetate, 3,5-dimethylpyrazole, potassium borohydride, 2,4- and 2,5-dihydroxybanzeldehyde were dried for 24 hours in a dessicator over phosphorus (v) oxide before use.

Except for acetonitrile, which was an AR grade, all the other solvents namely, hexane, toluene, diethyl ether, tetrahydrofuran (THF) and ethanol were distilled before use to increase purity.

3.2.1 Glassware Cleaning

The glasswares were cleaned with liquid detergent and tap water. The glassware were then soaked overnight in chromic acid cleaning mixture and then rinsed with distilled water. Finally, the glassware were rinsed with acetone and then stored in an electric oven maintained at 105°c. The U.V and I.R cells were cleaned and rinsed with the same solvents as used to run the experiments.

3.3 Synthetic Procedures

All the weighing and measurements of solid samples were carried out on analytical balance while liquid samples were measured in graduated pipettes. Preparation of precursor molecule (Scheme 8) is in accordance to the literature method (Cleland *et al*., 1987).

3.4 Preparation of Schiff Bases

3.4.1 Schiff Base TS1; [B= $(CH_2)_2$]

To a solution of 2,5-dihydroxybenzaldehyde (1g, 7.24mmoles) and salicylaldehyde (0.9g, 7.24 mmoles) in absolute ethanol (30ml) was added dropwise to a solution of ethylene diamine (0.5ml, 7.24 mmoles) in absolute ethanol (5ml). The solution mixture was refluxed for three hours and then filtered when hot. The filtrate was transferred into a 250ml beaker and the solution was kept standing overnight at room temperature. The yellow crystals formed were isolated by filtration. The crystals were recrystalized in ethanol, filtered and washed thrice with 50ml n-hexane. The crystals were dried in air for 2days.

3.4.2 Schiff Base TS2; [B= $(CH_2)_3$]

To a solution of 2,5-dihydroxybenzaldehyde (1.0g, 7.24 mmoles) and salicylaldehyde (0.9g, 7.24 mmoles) in absolute ethanol (30ml) was added dropwise a solution of propylene diamine (0.6g, 7.24 mmoles) in 5ml of absolute ethanol. The mixture was refluxed for 3hours. The solution was filtered while hot and excess solvent evaporated in vacuo to give red oil. To the red oil was added diethyl ether to afford yellow solid that was thoroughly washed with diethyl ether and dried in air for 2 days.

3.4.3 Schiff Base TS3; [B= $(CH_2)_4$]

To a solution of 2,5-dihydroxybenzaldehyde (1.0g, 7.24 mmoles) and salicylaldehyde (0.9g, 7.24mmoles) in absolute ethanol (30ml) was added dropwise a solution of 1,4-diaminobutane (0.73g, 7.24 mmoles) in 5ml of absolute ethanol. The mixture was refluxed for 3hours and then filtered when hot. The yellow filtrate was cooled and excess solvent evaporated in vacuo. On cooling, a yellow solid was obtained. The solid was isolated by filtering and washed thrice with 50ml diethyl ether. The solid was dried in air for 2 days.

3.4.4 Schiff Base TS4; [B=C_6H_4]

To a solution of 2,5-dihydroxybenzaldehyde (1.0g, 7.24 mmoles) and salicylaldehyde (0.9g, 7.24mmoles) in absolute ethanol (30ml) was added dropwise a solution of o-phenylene diamine (0.78g, 7.24 mmoles) in 5ml of absolute ethanol. The mixture was refluxed for 3hours. The solution was filtered while hot, and the solvent evaporated *in vacuo* to give red oily liquid which was triturated with diethyl ether to yield a red solid. The solid was thoroughly washed with diethyl ether and then dried in air for 2 days.

3.4.5 Schiff Base TS5; [B= $(CH_2)_2$]

To a solution of 2,4-dihydroxybenzaldehyde (1.0g, 7.24 mmoles) and salicylaldehyde (0.9g, 7.24 mmoles) in absolute ethanol (30ml) was added dropwise a solution of ethylene diamine (0.5ml, 7.24 mmoles) in absolute ethanol (5ml). The solution mixture was refluxed for three hours and then filtered while hot. The filtrate was transferred into a 250ml beaker. The solution was kept standing overnight at room temperature and yellow crystals formed which were isolated by filtration. The crystals were recrystalized in ethanol

filtered and washed thrice with 50ml n-hexane. The crystals were dried in air for 2days.

3.4.6 Schiff Base TS6; [B= $(CH_2)_3$]

To a solution of 2,4-dihydroxybenzaldehyde (1.0g, 7.24 mmoles) and salicylaldehyde (0.9g, 7.24 mmoles) in absolute ethanol (30ml) was added dropwise a solution of propylene diamine (0.6ml, 7.24 mmoles) in 5ml of absolute ethanol. The mixture was refluxed for 3hours. The solution was filtered while hot and excess solvent evaporated in vacuo to give red oil. To the red oil was added 30ml diethyl ether to afford yellow solid which was thoroughly washed with diethyl ether and dried in air for 2 days.

3.4.7 Schiff Base TS7; [B= $(CH_2)_4$]

To a solution of 2,4-dihydroxybenzaldehyde (1.0g, 7.24 mmoles) and salicylaldehyde (0.9g, 7.24mmoles) in absolute ethanol (30ml) was added dropwise a solution of 1,4-diaminobutane (0.73ml, 7.24 mmoles) in 5ml of absolute ethanol. The mixture was refluxed for 3hours and then filtered when hot. The yellow filtrate was cooled and excess solvent evaporated in vacuo. On cooling, a yellow solid was obtained. The solid was isolated by filtering and washed thoroughly with diethyl ether (3x50ml). The solid was dried in air for 2 days.

3.4.8 Schiff Base TS8; [B= C_6H_4]

To a solution of 2,4-dihydroxybenzaldehyde (1.0g, 7.24 mmol) and salicylaldehyde (0.9g, 7.24mmoles) in absolute ethanol (30ml) was added dropwise a solution of o-phenylene diamine (0.78g, 7.24 mmol) in 5ml of absolute ethanol. The mixture was refluxed for

3hours and then filtered while hot. The solvent was evaporated *in vacuo* yielding a red oily liquid which was then triturated with diethylether. A red solid obtained was thoroughly washed with diethylether and dried in air for 2 days.

3.5 Preparation of Monometallic Complexes

3.5.1 Preparation of Precursor Complex

The precursor metal complex [Mo(O)Tp*Cl_2] used in this study has the general formula Mo(O)Tp*XY, (**1**) where Tp* = tris(3,5-dimethylpyrazolyl) hydroborate, X and Y are halogens . Complexes of this type are prepared in a series of steps as indicated in Scheme 8. The following synthetic procedures were employed in preparing the target precursor complex.

3.5.1.1 Preparation of potassium hydrotris (3,5-dimethyl pyrazolyl) borate [$KHB(Me_2N_2C_3H)_3$]=Tp*

A mixture of potassium borohydride was heated on a hot plate in a 250ml-refluxing flask connected to a bubbler. The reaction temperature was raised to 238°C, the melting temperature of the mixture and maintained above 255°C until bubbling stopped. This served as an indication that the reaction was complete. The melt was then cooled to 100°C, poured into 100ml of freshly distilled toluene and stirred with a glass rod until it attained the room temperature. A white precipitate formed which was filtered and washed thrice with 50ml n-hexane and left to dry on a filter paper overnight.

3.5.1.2 Preparation of Tris(3,5-Dimethyl Pyrazolyl) Borato Molybdenum(V)

($Mo(O)Tp^*Cl_2$).

Although the final reaction product is air stable, the intermediates are oxygen sensitive. This reaction was therefore carried out under nitrogen. To 9.8g (35.7 mmoles) of $MoCl_5$ in a 200ml airless flask at –77°C was slowly added 120ml of tetrahydrofuran (also at –77°C) with vigorous stirring. Near room temperature, an exothermic reaction begun, the colour changed from dark red-brown to green and a green precipitate subsequently formed. To the resulting slurry was added 12g, (35.7mmoles) of Tp* and the mixture was separated from the dark-red supernatant by filtration, washed several times with acetonitrile and dried in vacuo. The crude product was dissolved in approximately one litre of refluxing 1,2-dichloroethane, and the solution was filtered to remove potassium chloride and evaporated to dryness in vacuo. The green product was washed with acetonitrile several times to remove a red impurity and then dried in vacuo.

3.5.2. Preparation of *p*-Schiff base – metal complexes

3.5.2.1 Schiff base – Ni (II) complex TS9;(M=Ni, M'= H, B= $(CH_2)_2$]

A solution of nickel chloride (0.25g, 1.06 mmoles) in absolute ethanol was added dropwise to a solution of TS1 (0.3g, 1.06mmoles) in absolute ethanol (30ml). The solution turned green and a green precipitate was formed. The mixture was refluxed for 24 hours, cooled and then filtered. The residue was washed thrice with 50ml ethanol and then dried in air to afford a green solid.

3.5.2.2 Schiff base – Ni (II) complex TS10 ;(M=Ni, M'= H, B= $(CH_2)_3$]

This compound was prepared in an identical manner to TS9 using nickel chloride (0.32g,

1.35mmol) and TS2 (0.4g, 1.35mmoles). A green precipitate was formed which was isolated by filtration. The solid was thoroughly washed thrice with 50ml ethanol. It was then washed thrice with 50ml diethyl ether and dried in air.

3.5.2.3 Schiff base – Ni (II) complex TS11 ;(M=Ni, M'= H, B= $(CH_2)_4$]

This compound was prepared in an identical manner to TS10 using nickel chloride (3.23g, 14mmol) and TS3 (0.7g, 14mmoles). A green precipitate was formed which was isolated by filtration. The solid was thoroughly washed thrice 50ml ethanol. It was then washed thrice with 50ml diethyl ether and dried in air to afford a green solid.

3.5.2.4 Schiff base – Ni (II) complex TS12 ;(M=Ni, M'= H, B= C_6H_4]

This compound was prepared in an identical manner to TS11 using nickel chloride (0.35g, 1.46mmol) and TS4 (0.3g, 1.46mmoles). A wine red precipitate was formed which was isolated by filtration. The solid was thoroughly washed thrice with 50ml ethanol. It was then washed thrice with 50ml diethyl ether and dried in air to afford a green solid.

3.5.2.5 Schiff base – Co (II) complex TS13 ;(M=Co, M'= H, B= $(CH_2)_2$]

A solution of cobalt acetate (0.27g, 1.1mmol) in absolute ethanol (30ml) was added dropwise to a solution of TS1 (0.3g, 1.1mmoles) in absolute ethanol (30ml). The solution turned dark-green and a grayish precipitate was formed. The mixture was refluxed for 24hours, cooled and then filtered. A grey residue was obtained which was thoroughly washed thrice with 50ml ethanol and diethyl ether and then dried in air.

3.5.2.6 Schiff base – Co (II) complex TS14 ;(M=Co, M'= H, B= $(CH_2)_3$]

This complex was prepared in an identical manner to TS13 using cobalt acetate (0.72g, 2.9mmol) and TS2 (0.4g, 2.9mmoles) in absolute ethanol (30ml). A grayish precipitate was formed which was isolated by filtration. The solid was thoroughly washed thrice with ethanol and diethyl ether and dried in air.

3.5.2.7 Schiff base – Co (II) complex TS15 ;(M=Co, M'= H, B= $(CH_2)_4$]

This complex was prepared in an identical manner to TS14 using cobalt acetate (2.61g, 3.5mmoles) and TS3 (0.3g, 3.5mmol) in absolute ethanol (30ml). A grayish precipitate was formed which was isolated by filtration. The solid was thoroughly washed thrice with 50ml ethanol and diethyl ether and dried in air.

3.5.2.8 Schiff base – Co (II) complex TS16 ;(M=Co, M'= H, B= (C_6H_4)]

This complex was prepared in an identical manner to TS15 using cobalt acetate (0.57g, 0.946mmoles) and TS4 (0.3g, 0.946mmoles) in absolute ethanol (30ml). A grayish precipitate was formed which was isolated by filtration. The solid was thoroughly washed thrice with 50ml ethanol and diethyl ether and dried in air.

3.5.3 Preparation of *m*-Schiff base – metal complexes

3.5.3.1 Schiff base – Ni (II) complex TS17; (M=Ni, M'= H, B= $(CH_2)_2$]

A solution of nickel chloride (0.25g, 1.06 mmoles) in absolute ethanol was added dropwise to a solution of TS5 (0.3g, 1.06mmoles) in absolute ethanol (30ml). The solution turned green and a green precipitate was formed. The mixture was refluxed for 24hours, cooled

and then filtered. Green residue was obtained. The residue was washed thrice with 50ml ethanol and then dried in air.

3.5.3.2 Schiff base – Ni (II) complex TS18; (M=Ni, M'= H, B= $(CH_2)_3$]

This compound was prepared in an identical manner to TS17 using nickel chloride (0.32g, 1.35mmol) and TS6 (0.4g, 1.35mmoles). A green precipitate was formed which was isolated by filtration. The solid was thoroughly washed with 50ml ethanol and diethyl ether and dried in air.

3.5.3.3 Schiff base – Ni (II) complex TS19; (M=Ni, M'= H, B= $(CH_2)_4$]

The compound was prepared in an identical manner to TS18 using nickel chloride (3.23g, 14mmoles) and TS7 (0.7g, 14mmoles). A green precipitate was formed which was isolated by filtration. The solid was thoroughly washed with 50ml ethanol and diethyl ether and dried in air.

3.5.3.4 Schiff base – Ni (II) complex TS20; (M=Ni, M'= H, B= C_6H_4]

This compound was prepared in an identical manner to TS19 using nickel chloride (0.35g, 1.46mmoles) and TS8 (0.3g, 1.46mmoles). A wine red precipitate was formed which was isolated by filtration. The solid was thoroughly washed with 50ml ethanol and diethyl ether and dried in air.

3.5.3.5 Schiff base – Co (II) complex TS21; (M=Co, M'= H, B= $(CH_2)_2$]

A solution of cobalt acetate (0.27g, 1.1mmoles) in absolute ethanol (30ml) was added dropwise to a solution of TS5 (0.3g, 1.1mmoles) in absolute ethanol (30ml). The solution

turned dark-green and a grayish precipitate was formed. The mixture was refluxed for 24hours, cooled and then filtered. A grey residue was obtained. The residue was thrice washed with 50ml ethanol and diethyl ether and then dried in air.

3.5.3.6 Schiff base – Co (II) complex TS22; (M=Co, M'= H, B= $(CH_2)_3$]

This complex was prepared in an identical manner to TS21 using cobalt acetate (0.72g, 2.9mmoles) and TS6 (0.4g, 2.9mmoles) in absolute ethanol (30ml). A grayish precipitate was formed which was isolated by filtration. The solid was thoroughly washed with 50ml ethanol followed by diethyl ether and dried in air.

3.5.3.7 Schiff base – Co (II) complex TS23; (M=Co, M'= H, B= $(CH_2)_4$]

This complex was prepared in an identical manner to TS22 using cobalt acetate (2.61g, 3.5mmoles) and TS7 (.3g, 3.5mmoles) in absolute ethanol (30ml). A grayish precipitate was formed which was isolated by filtration. The solid was thoroughly washed with 50ml ethanol and diethyl ether and dried in air.

3.5.3.5 Schiff base – Co (II) complex TS24; (M=Co, M'= H, B= C_6H_4]

This complex was prepared in an identical manner to TS23 using cobalt acetate (0.57g, 0.946mmol) and TS8 (0.3g, 0.946mmoles) in absolute ethanol (30ml). A grayish precipitate was formed which was isolated by filtration. The solid was thoroughly washed with 50ml ethanol and diethyl ether and dried in air.

3.6 Preparation of bimetallic complexes

3.6.1 Preparation of *p*-bimetallic complexes

3.6.1.1 Mo – Ni (II) complex TS25; [M = Ni, M´ = Mo(O)Tp*Cl, B = $(CH_2)_2$]

To a suspension of TS9 (0.12g, 0.336mmoles) in dry toluene (30ml) was added a few drops of triethylamine. To this suspension was added Mo(O)Tp*Cl_2 (0.15g, 0.336mmoles) in dry toluene. The mixture was refluxed for 8 days under nitrogen in which time a wine red solution was obtained. The solution was filtered when hot and the filtrate cooled. The filtrate was evaporated in vacuo affording an orange solid. The solid was dissolved in a minimum amount of dichloromethane and chromatographed on a column packed with silica gel 60 (70 – 230 mesh). The first fraction was eluted using n-hexane though it was discarded because it was unreacted Mo(O)Tp*Cl_2. The second major green fraction was eluted using 10% hexane in DCM. The solvent was allowed to evaporate for two days after which green crystals formed. They were then washed with n-hexane and allowed to dry for two day.

3.6.1.2 Mo – Ni (II) complex TS26; [M = Ni, M´ = Mo(O)Tp*Cl, B = $(CH_2)_3$]

To a suspension of TS10 (0.12g, 0.336mmoles) in dry toluene (30ml) was added a few drops of triethylamine. To this suspension was added Mo(O)Tp*Cl_2 (0.15g, 0.336mmoles) in dry toluene. The mixture was refluxed for 8 days under nitrogen in which time a wine red solution was obtained. The solution was filtered when hot and the filtrate cooled. The filtrate was evaporated in vacuo affording an orange solid. The solid was dissolved in a minimum amount of dichloromethane and chromatographed on a column packed with silica gel 60 (70 – 230 mesh). The first fraction was eluted using n-hexane and discarded.

The second major green fraction was eluted using 5% hexane in DCM. The solvent was allowed to evaporate for two days after which green crystals formed. They were then washed with n-hexane and allowed to dry for two days.

3.6.1.3 Mo – Ni (II) complex TS27; [M = Ni, M´ = Mo(O)Tp*Cl, B = $(CH_2)_4$]

To a suspension of TS11 (0.12g, 0.336mmoles) in dry toluene (30ml) was added a few drops of triethylamine. To this suspension was added Mo(O)Tp*Cl$_2$ (0.15g, 0.336mmoles) in dry toluene. The mixture was refluxed for 8 days under nitrogen in which time a wine red solution was obtained. The solution was filtered when hot and the filtrate cooled. The filtrate was evaporated in vacuo affording an orange solid. The solid was dissolved in a minimum amount of dichloromethane and chromatographed on a column packed with silica gel 60 (70 – 230 mesh). The first fraction was eluted using n-hexane and discarded. The second major green fraction was eluted using 10% hexane in DCM. The solvent was allowed to evaporate for two days after which green crystals formed. They were then washed with n-hexane and allowed to dry for two days.

3.6.1.4 Mo – Ni (II) complex TS28; [M = Ni, M´ = Mo(O)Tp*Cl, B = C_6H_4]

To a suspension of TS12 (0.12g, 0.336mmoles) in dry toluene (30ml) was added a few drops of triethylamine. To this suspension was added Mo(O)Tp*Cl$_2$ (0.15g, 0.336mmoles) in dry toluene. The mixture was refluxed for 8 days under nitrogen in which time a wine red solution was obtained. The solution was filtered when hot and the filtrate cooled. The filtrate was evaporated in vacuo affording an orange solid. The solid was dissolved in a minimum amount of dichloromethane and chromatographed on a column packed with silica gel 60 (70 – 230 mesh). The first fraction was eluted using n-hexane and discarded.

The second major green fraction was eluted using 5% hexane in DCM. The solvent was allowed to evaporate for two days after which green crystals formed. They were then washed with n-hexane and allowed to dry for two days.

3.6.1.5 Mo – Co (II) Complex TS29; [M = Co, M´ = Mo(O)Tp*Cl, B = $(CH_2)_2$]

To a suspension of TS13 (0.12g, 0.336mmoles) in dry toluene (30ml) was added a few drops of triethylamine. To this suspension was added Mo(O)Tp*Cl$_2$ (0.15g, 0.336mmoles) in dry toluene. The mixture was refluxed for 8 days under nitrogen in which time a wine red solution was obtained. The solution was filtered when hot and the filtrate cooled. The filtrate was evaporated in vacuo affording an orange solid. The solid was dissolved in a minimum amount of dichloromethane and chromatographed on a column packed with silica gel 60 (70 – 230 mesh). The first fraction was eluted using n-hexane and discarded. The second major green fraction was eluted using 10% hexane in DCM. The solvent in the eluate was evaporated in the air for 2 days. The solid obtained was washed with *n*–hexane and then dried for 2 days.

3.6.1.6 Mo – Co (II) Complex TS30; [M = Ni, M´ = Mo(O)Tp*Cl, B = $(CH_2)_3$]

To a suspension of TS14 (0.12g, 0.336mmoles) in dry toluene (30ml) was added a few drops of triethylamine. To this suspension was added Mo(O)T*Cl$_2$ (0.15g, 0.336mmoles) in dry toluene. The mixture was refluxed for 8 days under nitrogen in which time a wine red solution was obtained. The solution was filtered when hot and the filtrate cooled. The filtrate was evaporated in vacuo affording an orange solid. The solid was dissolved in a minimum amount of dichloromethane and chromatographed on a column packed with silica gel 60 (70 – 230 mesh). The first fraction was eluted using n-hexane and discarded.

The second major green fraction was eluted using 10% hexane in DCM. The solvent in the eluate was evaporated in the air for 2 days. The solid obtained was washed with *n*–hexane and then dried for 2 days.

3.6.1.7 Mo – Co (II) Complex TS31; [M = Co, M´ = Mo(O)Tp*Cl, B = $(CH_2)_4$]

To a suspension of TS15 (0.12g, 0.336mmoles) in dry toluene (30ml) was added a few drops of triethylamine. To this suspension was added Mo(O)Tp*Cl$_2$ (0.15g, 0.336mmoles) in dry toluene. The mixture was refluxed for 8 days under nitrogen in which time a wine red solution was obtained. The solution was filtered when hot and the filtrate cooled. The filtrate was evaporated in vacuo affording an orange solid. The solid was dissolved in a minimum amount of dichloromethane and chromatographed on a column packed with silica gel 60 (70 – 230 mesh). The first fraction was eluted using n-hexane and discarded. The second major green fraction was eluted using 5% hexane in DCM. The solvent in the eluate was evaporated in the air for 2 days. The solid obtained was washed with *n*–hexane and then dried for 2 days.

3.6.1.8 Mo – Co (II) Complex TS32; [M = Co, M´ = Mo(O)Tp*Cl, B = C_6H_4]

To a suspension of TS16 (0.12g, 0.336mmoles) in dry toluene (30ml) was added a few drops of triethylamine. To this suspension was added Mo(O)Tp*Cl$_2$ (0.15g, 0.336mmoles) in dry toluene. The mixture was refluxed for 8 days under nitrogen in which time a wine red solution was obtained. The solution was filtered when hot and the filtrate cooled. The filtrate was evaporated in vacuo affording an orange solid. The solid was dissolved in a minimum amount of dichloromethane and chromatographed on a column packed with silica gel 60 (70 – 230 mesh). The first fraction was eluted using n-hexane and discarded.

The second major green fraction was eluted using 5% THF in DCM. The solvent in the eluate was evaporated in the air for 2 days. The crystals obtained were washed with *n*–hexane and then dried for 2 days.

3.6.2 Preparation of *m*-bimetallic complexes

3.6.2.1 Mo – Ni (II) complex TS33; [M = Ni, M´ = Mo(O)Tp*Cl, B = $(CH_2)_2$]

To a suspension of TS17 (0.12g, 0.336mmoles) in dry toluene (30ml) was added a few drops of triethylamine. To this suspension was added Mo(O)Tp*Cl_2 (0.15g, 0.336mmoles) in dry toluene. The mixture was refluxed for 8 days under nitrogen in which a wine red solution was obtained. The solution was filtered when hot and the filtrate cooled. The filtrate was evaporated in vacuo affording an orange solid. The solid was dissolved in a minimum amount of dichloromethane and chromatographed on a column packed with silica gel 60 (70 – 230 mesh). The first fraction was eluted using n-hexane and was discarded. The second major green fraction was eluted using 10% hexane in DCM. The solvent was allowed to evaporate for two days after which green crystals formed. They were then washed with n-hexane and allowed to dry for two days.

3.6.2.2 Mo – Ni (II) complex TS34; [M = Ni, M´ = Mo(O)Tp*Cl, B = $(CH_2)_3$]

To a suspension of TS18 (0.12g, 0.336mmoles) in dry toluene (30ml) was added a few drops of triethylamine. To this suspension was added Mo(O)Tp*Cl_2 (0.15g, 0.336mmoles) in dry toluene. The mixture was refluxed for 8 days under nitrogen in which time a wine red solution was obtained. The solution was filtered when hot and the filtrate cooled. The filtrate was evaporated in vacuo affording an orange solid. The solid was dissolved in a

minimum amount of dichloromethane and chromatographed on a column packed with silica gel 60 (70 – 230 mesh). The first fraction was eluted using n-hexane and was discarded. The second major green fraction was eluted using 10% hexane in DCM. The solvent was allowed to evaporate for two days. The green crystals formed were then washed with n-hexane and allowed to dry for two days.

3.6.2.3 Mo – Ni (II) complex TS35; [M = Ni, M´ = Mo(O)Tp*Cl, B = $(CH_2)_4$]

To a suspension of TS19 (0.12g, 0.336mmoles) in dry toluene (30ml) was added a few drops of triethylamine. To this suspension was added Mo(O)Tp*Cl_2 (0.15g, 0.336mmoles) in dry toluene. The mixture was refluxed for 8 days under nitrogen in which time a wine red solution was obtained. The solution was filtered when hot and the filtrate cooled. The filtrate was evaporated in vacuo affording an orange solid. The solid was dissolved in a minimum amount of dichloromethane and chromatographed on a column packed with silica gel 60 (70 – 230 mesh). The first fraction was eluted using n-hexane and was discarded. The second major green fraction was eluted using 5% hexane in DCM. The solvent was allowed to evaporate for two days after which green crystals formed. They were then washed with n-hexane and allowed to dry for two days.

3.6.2.4 Mo – Ni (II) complex TS36; [M = Ni, M´ = Mo(O)Tp*Cl, B = C_6H_4]

To a suspension of TS20 (0.12g, 0.336mmoles) in dry toluene (30ml) was added a few drops of triethylamine. To this suspension was added Mo(O)Tp*Cl_2 (0.15g, 0.336mmoles) in dry toluene. The mixture was refluxed for 8 days under nitrogen in which time a wine red solution was obtained. The solution was filtered when hot and the filtrate cooled. The

filtrate was evaporated in vacuo affording an orange solid. The solid was dissolved in a minimum amount of dichloromethane and chromatographed on a column packed with silica gel 60 (70 – 230 mesh). The first fraction was eluted using n-hexane and was discarded. The second major green fraction was eluted using 5% THF in DCM. The solvent was allowed to evaporate for two days. The green crystals formed were then washed with n-hexane and allowed to dry for two days.

3.6.2.5 Mo – Co (II) Complex TS37; [M = Co, M´ = Mo(O)Tp*Cl, B = $(CH_2)_2$]

To a suspension of TS21 (0.12g, 0.336mmoles) in dry toluene (30ml) was added a few drops of triethylamine. To this suspension was added Mo(O)Tp*Cl_2 (0.15g, 0.336mmoles) in dry toluene. The mixture was refluxed for 8 days under nitrogen in which time a wine red solution was obtained. The solution was filtered when hot and the filtrate cooled. The filtrate was evaporated in vacuo affording an orange solid. The solid was dissolved in a minimum amount of dichloromethane and chromatographed on a column packed with silica gel 60 (70 – 230 mesh). The first fraction was eluted using n-hexane and discarded. The second major green fraction was eluted using 10% hexane in DCM. The solvent in the eluate was evaporated in the air for 2 days. The crystals obtained were washed with *n*–hexane and then dried for 2 days.

3.6.2.6 Mo – Co (II) Complex TS38; [M = Co, M´ = Mo(O)Tp*Cl, B = $(CH_2)_3$]

To a suspension of TS22 (0.12g, 0.336mmoles) in dry toluene (30ml) was added a few drops of triethylamine. To this suspension was added Mo(O)Tp*Cl_2 (0.15g, 0.336mmoles) in dry toluene. The mixture was refluxed for 8 days under nitrogen in which time a wine

red solution was obtained. The solution was filtered when hot and the filtrate cooled. The filtrate was evaporated in vacuo affording an orange solid. The solid was dissolved in a minimum amount of dichloromethane and chromatographed on a column packed with silica gel 60 (70 – 230 mesh). The first fraction was eluted using n-hexane and discarded. The second major green fraction was eluted using 10% hexane in DCM. The solvent in the eluate was evaporated in the air for 2 days. The crystals obtained were washed with *n*–hexane and then dried for 2 days.

3.6.2.7 Mo – Co (II) Complex TS39; [M = Co, M´ = Mo(O)Tp*Cl, B = $(CH_2)_4$]

To a suspension of TS23 (0.12g, 0.336mmoles) in dry toluene (30ml) was added a few drops of triethylamine. To this suspension was added Mo(O)Tp*Cl_2 (0.15g, 0.336mmoles) in dry toluene. The mixture was refluxed for 8 days under nitrogen in which time a wine red solution was obtained. The solution was filtered when hot and the filtrate cooled. The filtrate was evaporated in vacuo affording an orange solid. The solid was dissolved in a minimum amount of dichloromethane and chromatographed on a column packed with silica gel 60 (70 – 230 mesh). The first fraction was eluted using n-hexane and discarded. The second major green fraction was eluted using 5% hexane in DCM. The solvent in the eluate was evaporated in the air for 2 days. The crystals obtained were washed with *n*–hexane and then dried for 2 days.

3.6.2.8 Mo – Co (II) Complex TS38; [M = Co, M´ = Mo(O)Tp*Cl, B = C_6H_4]

To a suspension of TS12 (0.12g, 0.336mmoles) in dry toluene (30ml) was added a few drops of triethylamine. To this suspension was added Mo(O)Tp*Cl_2 (0.15g, 0.336mmoles)

in dry toluene. The mixture was refluxed for 8 days under nitrogen in which time a wine red solution was obtained. The solution was filtered when hot and the filtrate cooled. The filtrate was evaporated in vacuo affording an orange solid. The solid was dissolved in a minimum amount of dichloromethane and chromatographed on a column packed with silica gel 60 (70 – 230 mesh). The first fraction was eluted using n-hexane and discarded. The second major green fraction was eluted using 5% THF in DCM. The solvent in the eluate was evaporated in the air for 2 days. The crystals obtained were washed with *n*–hexane and then dried for 2 days.

3.7 Physical property tests

3.7.1 Solubility Test

This was performed on all the unknown compounds prepared in this study. The tests were extremely important in determining suitable solvent for solution analysis. In all cases about 1mg of solid `was added to $2cm^3$ of solvent in a test tube. The mixture was shaken vigorously and in some cases warmed in case it did not dissolve. The schiff base ligands (TS1–TS8) were soluble in ethanol, chloroform, dichloromethane, DMF, DMSO, acetonitrile and methanol at room temperature. Bimetallic complexes (TS25-TS40) were soluble in dichloromethane, DMSO and acetonitrile.

3.7.2 Melting Point Determination

This was done to provide information on purity of compounds. Pure samples have sharp melting point range ± (0-2°C). The melting points of the samples were determined using electronic melting point apparatus. A glass capillary tube containing the sample was inserted into the heating block. Preliminary melting points determinations were done rapidly but the actual melting points were determined by heating the samples rapidly to temperatures about 10°C below their expected melting points, then slowly the rate of temperature rise increased to about 1°C per minute. This ensured that the sample and the block were at thermal equilibrium. If the compound melted over a wide temperature range, it was re-crystallized and the melting point determination repeated.

3.7.3 Conductance Measurements

Conductance measurements were obtained to provide information on whether the

complexes were electrolytic or non-electrolytic. The measurements were obtained in DMSO, acetonitrile and ethanol. In all cases, ca 1x 10^{-3} $moldm^{-3}$ solutions of sample were prepared and conductivity measured using model **WTW** conductometer.

3.8 Spectral Studies

3.8.1 U.V-Visible Absorption Spectral Studies

U.V-visible absorption spectra were recorded using rectangular Pyrex cell with a 1.00cm path length. The electronic spectra for schiff base ligands were run in ethanol. The electronic spectra for mono- and bimetallics were run in DMSO and dichloromethane respectively.

3.8.2 F.T.I.R Spectral Studies

The spectra were recorded on a HYPER I.R at room temperature. 2mg of the compound was ground with 100mg of dry KBr in a mortar. The powder was crushed to form a disk in a hand press which was mounted on the spectrophotometer and spectrum obtained.

3.8.3 Cyclic Voltammetry Studies

This was carried out using Autolab Gpes polarographic analyzer/ stripping voltameter. Solutions in DMSO, acetonitrile and dichloromethane were mixed while $[Bu^{n}_{4}N][PF_{6}]$ was used as the base electrolyte. Ag/AgCl was used as the reference electrode while the working and the counter electrodes were glassy carbon and platinum foil respectively. Electrochemical studies were done for monometallic and bimetallic complexes.

CHAPTER FOUR

RESULTS AND DISCUSSIONS

4.1 Synthetic Studies

The synthetic strategy for the production of bimetallic species was initially to prepare appropriate tetradentate schiff base ligands (TS1-TS8) capable of accommodating two metal centres. The first was type A, p-Schiff base ligands (TS1-TS4)[M'=H, B=(CH_2)n, n=2-4, C_6H_4] (**1**) and the other one was type B, m-Schiff base ligands (TS5-TS8) [M'=H, B=(CH_2)n, n=2-4, C_6H_4] (**1**). They were reacted with an appropriate metal acetate or chloride in a 1:1 mole ratio in ethanol, affording metal-Schiff base complexes, type **A,** *p*-nickel schiff base complexes (TS9-TS12) [M'=H, M=Ni, B=(CH_2)n, n=2-4, C_6H_4], p-cobalt schiff base complexes (TS13-16) [M'=H, M=Co, B=(CH_2)n, n=2-4, C_6H_4] and type B, *m*-nickel schiff base complexes (TS17-TS20) [M'=H, M=Ni, B= $(CH_2)_n$, n=2-4, C_6H_4], *m*-cobalt schiff base complexes (TS21-24) [M'=H, M=Co, B= (CH_2)n, n=2-4, C_6H_4]. The general synthesis of bimetallic complexes (TS25-TS40) involved the addition of the appropriate metal schiff base complex to precursor molecule Mo(O)Tp*Cl in 1:1 molar ratio in presence of an excess of triethylamine, which facilitates the deprotonation of the phenolic hydroxyl groups of the schiff base as well as extracting the hydrogen chloride gas liberated as a triethylammonium salt, $Et_3NH^+Cl^-$. The mixture was refluxed for eight days to ensure completion of the reaction. The nickel bimetallic complexes of type A and B [M'=Mo(O)Tp*Cl, M=Ni, B=$(CH_2)_n$, n=2-4, C_6H_4] yielded green precipitates as the major products and wine red precipitates as the minor products. Similarly, cobalt bimetallic complexes of type A and B [M'=Mo(O)Tp*Cl, M=Co, B=$(CH_2)_n$, n=2-4, C_6H_4] yielded green precipitate as the major products and wine-red precipitates as the minor products.

The general reaction for the formation of bimetallic complexes is summarized in Scheme 9, Chapter Three.

4.2 Physical property

4.2.1 Solubility

All the Schiff bases were soluble in common organic solvents such as chloroform, EtOH, DCM, DMSO, ACN and methanol at room temperature. All the metal-Schiff base complexes were soluble in DMSO, while the bimetallic complexes were soluble in DCM, DMSO, ACN and chloroform at room temperature.

4.2.2 Melting point

The Schiff bases exhibited melting points in the range of 122 – 195°C. The melting points of the monometallic and bimetallic complexes were above 400°C (at this temperature, they were still in solid state). The values obtained are given in Tables 1 and 2.

Table 1: Data of physical properties for *p*-compounds (Ω^{-1} cm^2 mol^{-1})

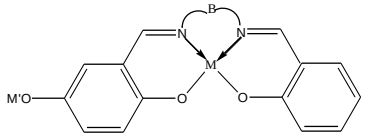

M'	B	M	Colour	M.P^{0}c	%Yield	I.R ($\nu_{C=N}$)	I.R (ν_{B-H})	I.R ($\nu_{Mo=O}$)
H	$(CH_2)_2$	H	Yellow	193-195	45.8	1636		
H	$(CH_2)_3$	H	Yellow	126-127	58.0	1632		
H	$(CH_2)_4$	H	Yellow	124-126	60.0	1634		
H	(C_6H_4)	H	Yellow	151-153	61.0	1654		
H	$(CH_2)_2$	Ni	Green	>400	81.0	1622		
H	$(CH_2)_3$	Ni	Green	>400	39.0	1629		
H	$(CH_2)_4$	Ni	Green	>400	43.9	1625		
H	(C_6H_4)	Ni	Green	>400	80.6	1624		
H	$(CH_2)_2$	Co	Grey	>400	69.4	1600		
H	$(CH_2)_3$	Co	Grey	>400	25.1	1612		
H	$(CH_2)_4$	Co	Grey	>400	31.0	1608		
H	(C_6H_4)	Co	Grey	>400	65.4	1612		
Mo(O)Tp*Cl	$(CH_2)_2$	Ni	Green	>400	43.7	1637	2557	960
Mo(O)Tp*Cl	$(CH_2)_3$	Ni	Green	>400	48.1	1654	2555	960
Mo(O)Tp*Cl	$(CH_2)_4$	Ni	Green	>400	46.9	1651	2557	960
Mo(O)Tp*Cl	(C_6H_4)	Ni	Green	>400	35.0	1654	2557	960
Mo(O)Tp*Cl	$(CH_2)_2$	Co	Green	>400	38.9	1635	2559	962
Mo(O)Tp*Cl	$(CH_2)_3$	Co	Green	>400	44.4	1610	2554	960
Mo(O)Tp*Cl	$(CH_2)_4$	Co	Green	>400	47.4	1614	2532	960
Mo(O)Tp*Cl	(C_6H_4)	Co	Green	>400	45.0	1612	2553	933

Table 2: Data of physical properties for *m*-complexes (Ω^{-1} cm^2 mol^{-1})

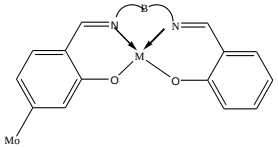

M'	B	M	Colour	M.P^{0}c	%Yield	I.R ($\upsilon_{C=N}$)	I.R (ν_{B-H})	I.R $\nu_{Mo=O}$)
H	$(CH_2)_2$	H	Yellow	132-134	46.0	1632		
H	$(CH_2)_3$	H	Yellow	161-163	60.0	1631		
H	$(CH_2)_4$	H	Yellow	124-126	58.2	1636		
H	(C_6H_4)	H	Yellow	122-124	59.3	1616		
H	$(CH_2)_2$	Ni	Green	>400	89.1	1622		
H	$(CH_2)_3$	Ni	Green	>400	39.0	1627		
H	$(CH_2)_4$	Ni	Green	>400	73.1	1625		
H	(C_6H_4)	Ni	Green	>400	60.0	1612		
H	$(CH_2)_2$	Co	Grey	>400	72.2	1622		
H	$(CH_2)_3$	Co	Grey	>400	79.3	1608		
H	$(CH_2)_4$	Co	Grey	>400	34.9	1620		
H	(C_6H_4)	Co	Grey	>400	76.3	1612		
Mo(O)Tp*Cl	$(CH_2)_2$	Ni	Green	>400	32.8	1652	2557	960
Mo(O)Tp*Cl	$(CH_2)_3$	Ni	Green	>400	42.8	1652	2557	960
Mo(O)Tp*Cl	$(CH_2)_4$	Ni	Green	>400	46.9	2557	1652	960
Mo(O)Tp*Cl	(C_6H_4)	Ni	Green	>400	35.0	2557	1652	960
Mo(O)Tp*Cl	$(CH_2)_2$	Co	Green	>400	44.4	1651	2526	981
Mo(O)Tp*Cl	$(CH_2)_3$	Co	Green	>400	38.9	1651	2557	966
Mo(O)Tp*Cl	$(CH_2)_4$	Co	Green	>400	42.1	1629	2555	948
Mo(O)Tp*Cl	(C_6H_4)	Co	green	>400	40.0	1652	2557	960

4.2.3 Conductance Measurement

Conductance measurements were done for both the monometallic and bimetallic complexes in DMSO, acetonitrile and ethanol solvents and their values compared with literature values of complexes at 1.0 x 10^{-3} M quoted by various authors for all types of electrolytes. In general, the values obtained for all compounds were less than those quoted by Sear *et al.,* (1959) for 1:1 electrolyte suggesting that the complexes were non-electrolytic in nature. In ethanol, the values were below 40.5 $\Omega^{-1}cm^2mol^{-1}$, which is the lowest acceptable value for a 1:1 electrolyte (Evans *et al*., 1968). In DMSO, conductances values for the complexes were generally below 60 $\Omega^{-1}cm^2mol^{-1}$, which is the least value suggested by Greenwood *et al.,* (1968) for 1:1 electrolytes in DMSO.

Similar observations were made in acetonitrile in which the complexes had values less than 65.0 $\Omega^{-1}cm^2mol^{-1}$, which is the least value for 1:1 electrolytes in this solvent. It was also observed that the conductance values of mono- and bimetallic complexes of Co (II) were generally much lower than those of the corresponding complexes of Ni (II). Conductance data for the complexes are summarized in Tables 3 and 4.

Table 3: Conductance measurements data for *p*-complexes (Ω^{-1} cm^2 mol^{-1})

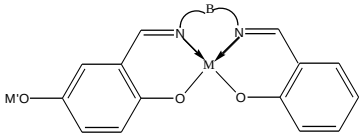

COMPOUND			SOLVENT		
M'S'	B	M	EtOH	DMSO	CAN
H	$(CH_2)_2$	Ni	35	50	40
H	$(CH_2)_3$	Ni	20	60	40
H	$(CH_2)_4$	Ni	20	50	30
H	(C_6H_4)	Ni	30	50	40
H	$(CH_2)_2$	Co	10	30	20
H	$(CH_2)_3$	Co	10	40	30
H	$(CH_2)_4$	Co	20	50	30
H	(C_6H_4)	Co	10	40	30
Mo(O)Tp*Cl	$(CH_2)_2$	Ni	40	43	42
Mo(O)Tp*Cl	$(CH_2)_3$	Ni	26	41	41
Mo(O)Tp*Cl	$(CH_2)_4$	Ni	25	38	33
Mo(O)Tp*Cl	(C_6H_4)	Ni	36	39	41
Mo(O)Tp*Cl	$(CH_2)_2$	Co	13	23	22
Mo(O)Tp*Cl	$(CH_2)_3$	Co	15	37	32
Mo(O)Tp*Cl	$(CH_2)_4$	Co	17	40	33
Mo(O)Tp*Cl	(C_6H_4)	Co	14	33	34

Table 4: Conductance measurements data for *m*-complexes (Ω^{-1} cm^2 mol^{-1})

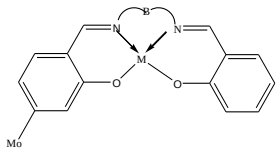

COMPOUND			SOLVENT		
M''	B	M	EtOH	DMSO	CAN
H	$(CH_2)_2$	Ni	20	50	40
H	$(CH_2)_3$	Ni	20	60	50
H	$(CH_2)_4$	Ni	30	50	40
H	(C_6H_4)	Ni	30	60	50
H	$(CH_2)_2$	Co	10	40	20
H	$(CH_2)_3$	Co	20	40	30
H	$(CH_2)_4$	Co	10	30	20
H	(C_6H_4)	Co	30	60	30
Mo(O)Tp*Cl	$(CH2)_2$	Ni	22	43	42
Mo(O)Tp*Cl	$(CH2)_3$	Ni	23	47	41
Mo(O)Tp*Cl	$(CH2)_4$	Ni	34	42	33
Mo(O)Tp*Cl	(C6H4)	Ni	34	45	41
Mo(O)Tp*Cl	$(CH2)_2$	Co	12	31	22
Mo(O)Tp*Cl	$(CH2)_3$	Co	24	32	32
Mo(O)Tp*Cl	$(CH2)_4$	Co	14	26	33
Mo(O)Tp*Cl	(C6H4)	Co	36	44	34

4.3 Spectral studies

4.3.1 UV/VIS spectral data

Electronic spectra of *p*-schiff base ligands, TS1-TS4 [M'=H, M=H, B=C_6H_4, $(CH_2)_n$] and *m*-schiff base ligands, TS5-TS8 [M'=H, M=H, B=C_6H_4, $(CH_2)_n$] (**17** and **18**) were carried out in ethanol, DMSO and acetonitrile. A single band between 192-195nm for *p*-schiff base ligands and 190-192nm for *m*-schiff base ligands were observed, which can be assigned to intraligand transition of n - σ*. The bands at 221-228nm for *p*-schiff base and 221-225nm for *m*-schiff base are an indication of intraligand transitions of π - π*. This could be as a result of C=N chromophore. The bands appearing in the range of 253-256nm for *p*-schiff base and 252-253nm for *m*-schiff base can be associated with the characteristic of compounds containing aromatic structures as was reported by Silverstein *et al*., (1991). Bands appearing between 271-333nm for p-schiff base and 264-318nm for m-schiff base ligands can presumably be assigned to charge transfer transitions of n - π*. In general, the absorption maximum of schiff base ligands is generally not sensitive to the length of the polymethylene chain (Lutta and Kagwanja, 2000). The electronic spectra of schiff base ligands are summarized in Table 3 and 4 and Figs. 17 and 18.

Figure 17: UV-Vis absorption spectra of TS1 (source: author, 2013**)**

Figure 18: UV-Vis absorption spectra of TS5 (source: author, 2013**)**

Table 5: Electronic data for the compounds of Type A

M'	B	M	[a] (λmax)[b](ε)
H	$(CH_2)_2$	H_2	265.0(9730)
H	$(CH_2)_3$	H_2	266.0(17920)
H	$(CH_2)_4$	H_2	320.0(20120)
H	C_6H_4	H_2	271.5(27730)
H	$(CH_2)_2$	Ni	337.5 (23750)
H	$(CH_2)_3$	Ni	200.0 (16550)
H	$(CH_2)_4$	Ni	260.0 (10190)
H	C_6H_4	Ni	267.0 (16170)
H	$(CH_2)_2$	Co	252.5 (3100)
H	$(CH_2)_3$	Co	355.0 (1350)
H	$(CH_2)_4$	Co	259.5 (10080)
H	C_6H_4	Co	266.5 (7790)
Mo(O)Tp*Cl	$(CH_2)_2$	Ni	269.5 (1170)
Mo(O)Tp*Cl	$(CH_2)_3$	Ni	281.0 (23800)
Mo(O)Tp*Cl	$(CH_2)_4$	Ni	193.0 (2120)

Mo(O)Tp*Cl	C_6H_4	Ni	223.0 (2270)
Mo(O)Tp*Cl	$(CH_2)_2$	Co	205.0 (19950)
Mo(O)Tp*Cl	$(CH_2)_3$	Co	225.5 (1370)
Mo(O)Tp*Cl	$(CH_2)_4$	Co	268.5 (9700)
Mo(O)Tp*Cl	C_6H_4	Co	194.0 (9150)

[a] in nm

[b] in $mol^{-1}\ dm^{-3}\ cm^{-3}$

Table 6: Electronic Data for the compounds of Type B

M'	B	M	[a] (λmax)[b](ε)
H	$(CH_2)_2$	H_2	282.5 (25910)
H	$(CH_2)_3$	H_2	316.5 (8000)
H	$(CH_2)_4$	H_2	310.5 (12640)
H	C_6H_4	H_2	318.0 (14680)
H	$(CH_2)_2$	Ni	272.0 (29140)
H	$(CH_2)_3$	Ni	250.5 (18720)
H	$(CH_2)_4$	Ni	197.0 (19090)
H	C_6H_4	Ni	319.5 (27490)
H	$(CH_2)_2$	Co	246.5 (15780)
H	$(CH_2)_3$	Co	261.5 (12600)
H	$(CH_2)_4$	Co	267.0 (9940)
H	C_6H_4	Co	259.5 (10080)
Mo(O)Tp*Cl	$(CH_2)_2$	Ni	192.0 (910)
Mo(O)Tp*Cl	$(CH_2)_3$	Ni	223.5 (1890)
Mo(O)Tp*Cl	$(CH_2)_4$	Ni	264.5 (1100)
Mo(O)Tp*Cl	C_6H_4	Ni	269.5 (1530)
Mo(O)Tp*Cl	$(CH_2)_2$	Co	274.5 (21320)
Mo(O)Tp*Cl	$(CH_2)_3$	Co	269.5 (2660)
Mo(O)Tp*Cl	$(CH_2)_4$	Co	265.5 (1660)
Mo(O)Tp*Cl	C_6H_4	Co	191.0 (950)

[a] in nm

[b] in $mol^{-1}\ dm^{-3}\ cm^{-3}$

Electronic spectra for monometallic complexes were expected to show bands due to d-d transitions, charge transfer, intraligand and combination vibrations. They all exhibited a broad absorption band in the visible region, which can be assigned to a metal-to-ligand charge transfer (M.L.C.T) process. All the electronic spectra of type A monometallic complexes had bands appearing between 190-194nm which can be assigned to an

intraligand transition of n - σ* type. The intense bands in the region 207 - 267nm and 304 - 396nm for nickel and 211 - 266nm and 355nm for cobalt schiff base complexes can presumably be assigned to charge transfer transitions or intraligand transition π - π* and n - π*. The spectra also contain a transition near 580nm whose constancy suggests a d-d transition, probably enhanced by intensity borrowing from adjacent charge transfer bands. The electronic spectra of monometallic complexes of type A are summarized in Table 5 and Figs. 19 and 20. There was a hypsochromic shift of C=N bond for the monometallic complexes in reference to the schiff bases. This shift has an average of 10nm in *para* and 4nm in *meta* cobalt complexes. This is higher than that of nickel complexes, which shows a shift of 7nm and 3nm for *para* and *meta* complexes respectively.

The electronic spectra for type B monometallic complexes had bands appearing at 191-194nm and 190-192nm for nickel and cobalt respectively, which can be assigned to intraligand transition of n - σ*. The intense bands in the region 209-285nm and 304-355nm for nickel and 221-267nm and 355nm for cobalt can presumably be assigned to charge transfer transitions or intraligand transition π - π* and n - π*. The spectra also contain a transition near 580.0nm whose constancy suggests a d-d transition, probably enhanced by intensity borrowing from adjacent charge transfer bands. The electronic spectra of monometallic complexes of type B are summarized in table 6 and Fig. 21.

Figure 19: UV-Vis absorption spectra of TS10 (source: author, 2013**)**

Figure 20: UV-Vis absorption spectra of TS13 (source: author, 2013**)**

Figure 21: UV-Vis absorption spectra of TS22 (source: author, 2013**)**

Spectra for bimetallic complexes of type A were dominated by high intensity bands in the region 190-199nm, medium intensity band in the region 205-355nm and low intensity band

in the region 482-580nm. The bands in the region 190-199nm for both nickel and cobalt bimetallic complexes are due to π - π* transition in C=N. The bands in the region 205-355nm may be associated with n - π* transition of the conjugated imine chromophore. The presence of an intense band at 482nm is a strong evidence for the presence of a Mo=O core as observed by other workers like Van *et al*., (1996). The band appearing in the region 580nm is an indication of a pure d-d transition. The electronic spectra of bimetallic complexes of type A are summarized in Table 5 and Fig. 21.

Type B bimetallic complexes exhibited a band in the region 190-192nm which can be assigned to π - π* due to the presence of C=N. The bands in the region 220-355nm can be assigned to n - π* transition of the conjugated imine chromophore. The band in the region 482.0 portrays a clear evidence for the presence of Mo=O core as observed by other workers (Fabbrizzi *et al*., 1999). Band appearing in the region 580nm is assigned to pure d-d transition. Electronic spectra for the bimetallic complexes of type B are summarized in table 6.

Figure 22: UV-Vis absorption spectra of TS29

4.3.2 Infrared spectral Studies

The i.r of the schiff base ligands of type A were characterized by azomethine stretching vibrations $\upsilon_{C=N}$ in the region 1608–1636cm^{-1}. These values fall within the range of typical stretching frequency of Schiff bases reported by other workers (Lutta *et al*., 2001). It has been observed that $\upsilon_{C=N}$ is not sensitive to the change in polymethylene carbon chain to a great extent. However, $\upsilon_{C=N}$ of the schiff base when B is a butylene group occurs at a higher frequency than when B is ethylene, propylene and O-phenylene. The strong band appearing at around 1542cm^{-1} can be assigned to the C=C antisymmetric vibrations. The C-C ring stretching bands of benzene occurred at frequencies 1496-1492cm^{-1}. The multiple vibrations υ_{C-N}, υ_{C-O} and υ_{C-C} stretches are assigned to a large number of bands occurring between 1346-1008cm^{-1}. N-H stretching frequency which appears around 3350cm^{-1} (2.99μ) and 3150cm^{-1} (3.17μ) was absent. This is significant since it is a clear indication that the amino groups in the diamines completely condensed with the carbonyl groups of the salicylaldehyde and hydroxybenzaldehyde. A representative i.r spectrum for the schiff

base ligands of type A is shown in Fig.22 and summary of spectral data in Table 1.

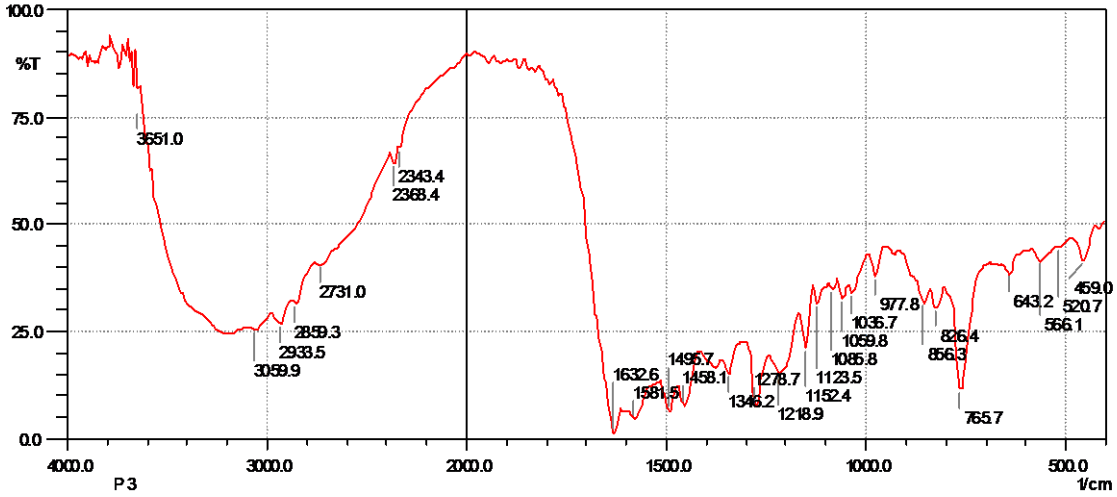

Figure 22: i.r spectrum for the schiff base ligand of type A; p$(CH_2)_3$

(Source: author, 2013**)**

For the i.r of schiff base ligands of type B, the characteristic azomethine stretching vibrations $\upsilon_{C=N}$ were observed in the region 1636-1616 cm^{-1}. This is within the range expected as reported by other workers (Lutta and Kagwanja, 2001). It is observed that $\upsilon_{C=N}$ as in schiff base of type A is not sensitive to the change in polymethylene carbon chain to a great extent. The frequency decreases as the number of carbon increases except for the case where B is a butylene group that occurs at a higher frequency than in cases where B is ethylene, propylene and o-phenylene diamine. The absence of N-H stretching frequency band which, generally occurs in the region 3000-3100cm^{-1} is significant since it shows that the amino groups in the diamines completely condensed with the carbonyl groups of the salicylaldehyde and hydroxybenzaldehyde. The strong band appearing at 1543-1542cm^{-1} is a confirmation for the C=C antisymmetric vibrations. The band at

1488cm^{-1} is one of the typical bands for C-C ring stretching of benzene while C-H stretching modes of methylene groups appear in the region 2976–2853cm^{-1}. Aromatic C-H stretch vibration bands are observed within the frequency range of 3015–3063cm^{-1}, which is within the accepted range of 3100–3000cm^{-1}. The bending vibrations of C-H bonds of methylene groups occurred as medium intensity group of bands in the range 1459–1456cm^{-1}. This is in agreement with what had been reported by other workers (Kipkemboi *et al*., 2003). υ_{C-N}, υ_{C-O} and υ_{C-C} stretches have various vibration bands appearing in all schiff bases of type B in the frequency range 1342–1013cm^{-1}.

In general, N-H stretching frequency, which appears at about 3350cm^{-1} and 3150cm^{-1} was absent. This is significant since it shows that the amino groups in the diamines completely condensed with the carbonyl groups of the salicylaldehyde and hydroxybenzaldehyde. A representative i.r spectrum for the schiff base ligands of type B is shown in Fig.23 and summary of spectral data in Table 2.

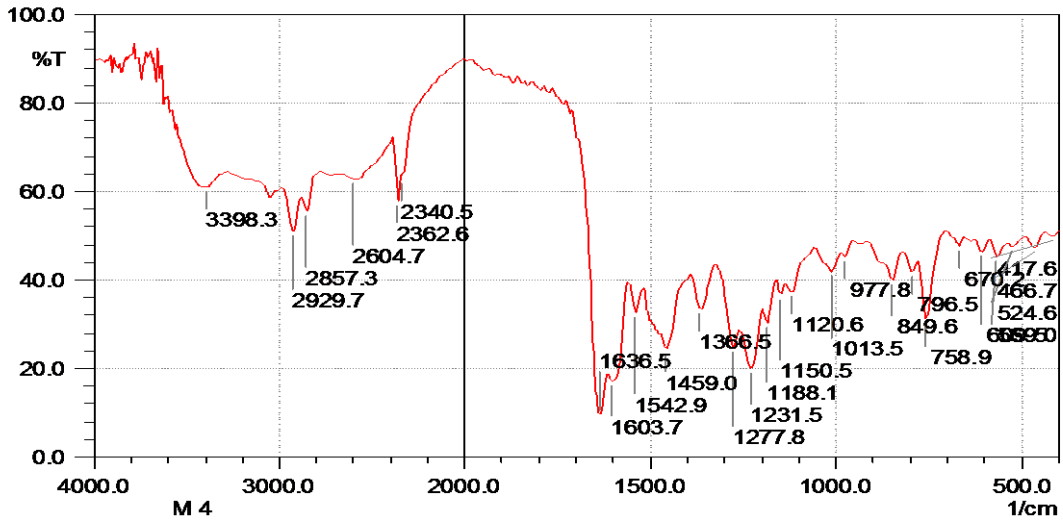

Figure 23: i.r spectrum for the schiff base ligand of type B; m$(CH_2)_4$ (source: author, 2013)

The nickel-schiff base complexes of type A were characterized by the azomethine stretching vibration $\upsilon_{C=N}$ occurring as strong band at 1624-1609cm^{-1}. This vibration compared to the one in the schiff base ligands indicates a bathochromic shift of about 20cm^{-1} being an indication that a co-ordinate bond is formed between nitrogen of the azomethine group of the schiff bases and the central metal atom, in this case nickel. The C-H stretch had absorption bands at 2933-2854cm^{-1} and CH bend of methylene and methyl groups at 1452 and 1373cm^{-1} respectively. The C=C antisymmetric vibrations in all complexes had strong bands appearing at 1542cm^{-1}. The 1400-1500cm^{-1} spectral region shows sharp distinct band at 1452.3cm^{-1}, which is assigned to CH_3 antisymmetric deformations which is in agreement with what had been observed by other workers (Kipkemboi *et al*.,2003). The large number of bands occurring at 1340-1006cm^{-1} in all complexes is assigned to υ_{C-C}, υ_{C-N} and υ_{C-O} vibrations. A representative i.r spectrum for the Nickel schiff base complexes of type A is shown on Figure 24 and the summary of spectral data in Table 1.

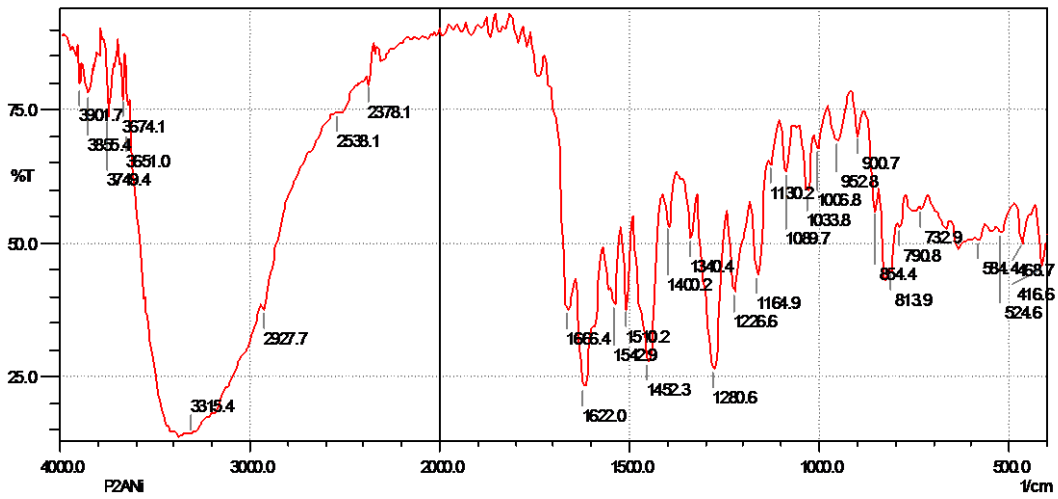

Figure 24: i.r spectra for nickel schiff base complex of type A. (source: author, 2013**)**

All i.r spectra of *para*-cobalt schiff base complexes were characterized by azomethine stretching vibrations, $\upsilon_{C=N}$, in the range of 1612-1600cm^{-1}. The corresponding $\upsilon_{C=N}$ vibrations in the schiff base occurred at 1636.5cm^{-1} which in response to the schiff base complexes shows a bathochromic shift to lower energy by 25cm^{-1} indicating that a co-ordinate bond is formed between nitrogen and the central metal. The C-H stretch absorption bands are observed in the region 2929-2854cm^{-1} and C-H bend of methylene and methyl groups at 1458-1446cm^{-1} and 1392-1380cm^{-1}, respectively. The strong bands appearing at 1554-1541cm^{-1} is due to C=C antisymmetric vibrations. The various vibration bands appearing in all cobalt schiff base complexes of type A at wavelengths of 1338-1026cm^{-1} are assigned υ_{C-N}, υ_{C-O} and υ_{C-C} vibration bands.

A representative i.r spectrum for the cobalt schiff base complex of type A is shown in Fig. 25 and summary of spectral data in Table 1.

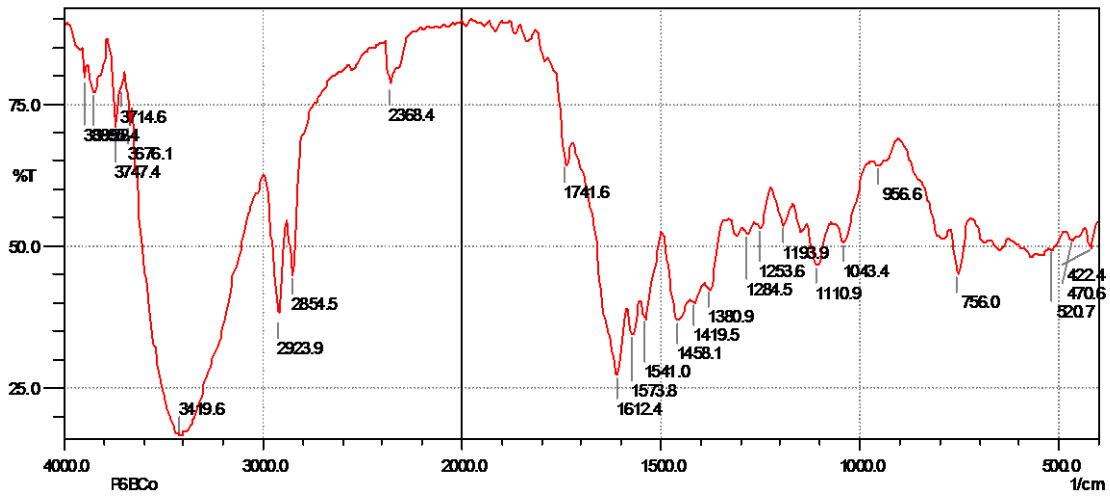

Figure 25: i.r spectra for cobalt schiff base complex of type A. (source: author, 2013**)**

Type B nickel schiff base complexes have a characteristic azomethine stretching vibrations, $\upsilon_{C=N,}$ within the range of 1627-1612cm^{-1}. In response to the azomethine vibrations of the schiff base complexes of type B, which occurred at 1636.5-1616.2cm^{-1}, there is a shift to the lower energy by 9cm^{-1}, an indication that a co-ordinate bond is formed between nitrogen of the schiff base and the central metal. C-H stretch absorption band occurred in the region of 2931cm^{-1} and CH bend of methylene and methyl groups at 1460-1440cm^{-1}. C=C antisymmetric vibrations are assigned to the strong bands appearing at frequencies of 1546-1542cm^{-1}. The various vibration bands at frequencies of 1340-1008cm^{-1} are assigned to $\upsilon_{C-N,}$ υ_{C-O} and υ_{C-C} vibration bands. All these agrees with what had been observed by other researchers (Kipkemboi *et al*., 2003)

A representative i.r spectrum for the cobalt schiff base complex of type B is shown in Fig. 26 and summary of spectral data in Table 2.

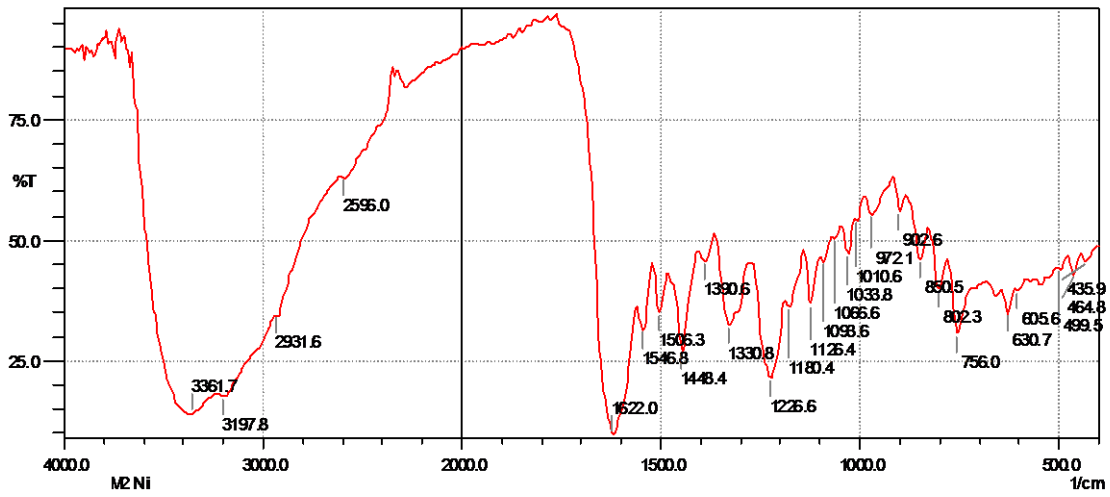

Figure 26: i.r spectra for Nickel schiff base complex of type B. (source: author, 2013**)**

Meta-cobalt Schiff base complexes had a characteristic azomethine stretching vibrations, $\upsilon_{C=N}$, at 1622-1608cm^{-1}. This indicates a shift of 15cm^{-1} to the lower energy in comparison to the vibrations observed in the schiff base complexes of type B. This is an indication that a co-ordinate bond is formed between nitrogen of the schiff base and the central metal, in this case cobalt. The C-H stretch absorption bands occurred in the region of 2925-2856cm^{-1} and CH bend of methylene and methyl groups at 1454-1421cm^{-1} and 1383cm^{-1} respectively. C=C antisymmetric vibrations are assigned to the strong bands appearing at frequencies of 1552-1542cm^{-1}. O-H vibrations are found in the region centred around 3446cm^{-1}. Various vibration bands appearing at frequencies of 1336-1037cm^{-1} are assigned to $\upsilon_{C-N,}$ υ_{C-O} and υ_{C-C} vibration bands.

A representative i.r spectrum for the cobalt schiff base complex of type B is shown in Figure 27 and summary of spectral data in Table 2.

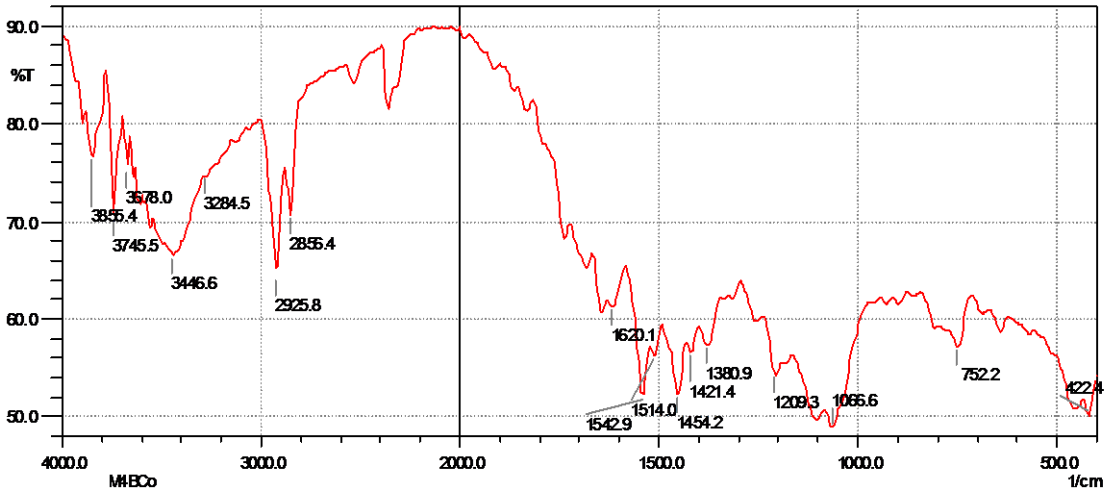

Figure 27: i.r spectra for cobalt schiff base complex of type B. (source: author, 2013**)**

The i.r spectra of nickel bimetallic complexes of type A were all characterized by υ_{B-H} vibrations at frequencies of 2557.4cm^{-1}. Azomethine stretching vibrations, $\upsilon_{C=N,}$ occurred at the range of 1654-1651cm^{-1}. From these frequencies, it was observed that $\upsilon_{C=N}$ frequencies of all bimetallic species of type A nickel experienced a hyperchromic shift towards the higher frequencies by 25cm^{-1}. The characteristic absorption band of Mo=O occurred in the frequency range of 960-931cm^{-1} and this agreed with the findings of other workers (Cleland *et al*., 1987). These frequencies acted as the spectroscopic handle to monitor the coordination of molybdenum in the complex formation. The C=C antisymmetric vibrations in all complexes had strong bands occurring at 1541cm^{-1}. In addition to these, vibration bands of pyrazolyl ligand occurred within the range of 1448-1382cm^{-1}. Absorption bands for C-H stretch appeared in the range of 2925-2853cm^{-1}. υ_{C-N}, υ_{C-C} and υ_{C-O}, which occurred as various absorption bands were observed at 1359-

1041cm^{-1}.

A representative i.r spectrum of the nickel bimetallic complexes is shown in Fig. 28 and summary of their spectral data in table 1.

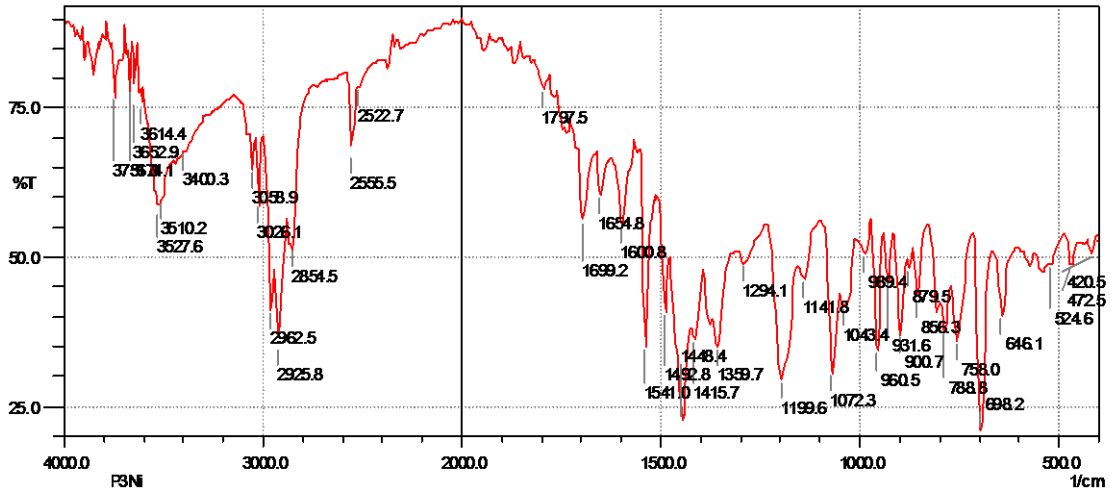

Figure 28: i.r spectra for nickel bimetallic complex of type A. (source: author, 2013**)**

Bimetallic complexes of cobalt type A had a characteristic vibration of υ_{B-H} at 2526cm^{-1}. C=N vibrations were observed at the region of 1651cm^{-1} thus, indicating a hyperchromic (blue) shift towards the higher frequencies for all cobalt bimetallic compounds. The band appearing at the frequencies of 981-962cm^{-1} are assigned to Mo=O vibrations thereby acting as a proof that coordination of molybdenum in the complex formation has occurred. The strong band appearing 1593-1541cm^{-1} is a confirmation for C=C antisymmetric vibrations. The pyrazolyl ligand band appeared at the frequencies of 1461-1380cm^{-1}. Various vibration bands at frequencies of 1355-1010cm^{-1} are assigned to $\upsilon_{C-N,}$ υ_{C-C} and υ_{C-O} in all complexes. This is in agreement with what had been observed by other researchers

(Kipkemboi *et al*., 2003)

A representative i.r spectrum for cobalt bimetallic complexes of type A is shown in Fig. 29 and summary of their spectral data in Table 1.

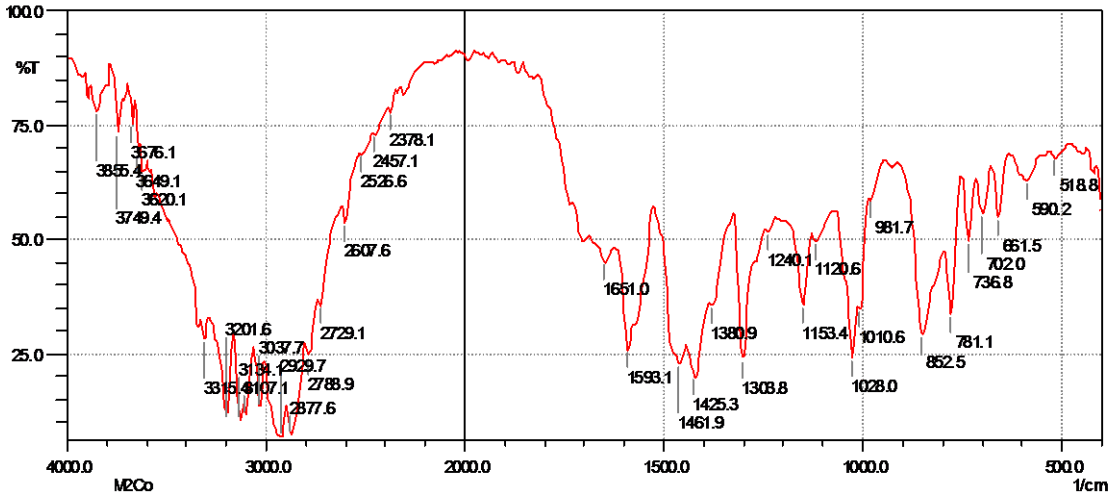

Figure 29: i.r spectra for cobalt bimetallic complex of type A. (source: author, 2013**)**

The i.r spectra of bimetallic complexes of nickel type of B had a characteristic $\upsilon_{B\text{-}H}$ vibrations at 2557cm^{-1}. Azomethine $\upsilon_{C=N}$ stretching vibrations appeared at the range of 1652cm^{-1} thereby exhibiting a hyperchromic shift towards the higher frequencies in all complexes compared to their monometallic counterparts. Mo=O vibration bands were observed at frequencies of 960cm^{-1} and this agreed with the findings of other workers (Cleland *et al*., 1987). The 2927-2852cm^{-1}, frequency region comprises fundamental vibrations due to the CH_3 stretching oscillations. A distinct band at about 1541cm^{-1} is assigned to C=C antisymmetric vibrations while the band in the frequency region of 1446-1384cm^{-1} is for the pyrazolyl ligand. The various vibrations $\upsilon_{C\text{-}N,}$ $\upsilon_{C\text{-}C}$ and $\upsilon_{C\text{-}O}$ in all

complexes are assigned to the number of bands occurring within the range of 1359-1043cm^{-1}.

A representative i.r spectrum for nickel bimetallic complexes of type B is shown in Figure 30 and summary of their spectral data in Table 2.

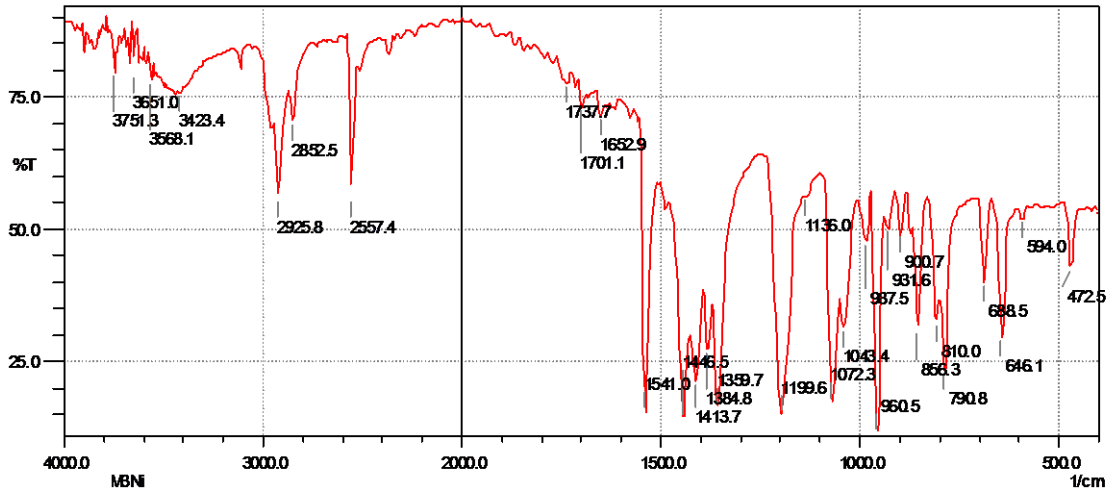

Figure 30: i.r spectra for Nickel bimetallic complex of type B. (source: author, 2013**)**

All the i.r spectra of bimetallic complexes of cobalt of type B had a υ_{B-H} band at 2557cm^{-1}. C=N vibration band appeared at 1652-1651^{-1} for all complexes hence indicating a shift to the higher frequencies. The Mo=O band occurs at the frequencies of 960cm^{-1}. The vibrations due to CH_3 stretching were observed at the range between 2925-2852cm^{-1}. A strong band appearing at the frequencies of 1541cm^{-1} in all complexes can be assigned to C=C antisymmetric vibrations. The band for pyrazolyl ligand was observed at the frequency range of 1456-1377cm^{-1}.

A representative i.r spectrum for cobalt bimetallic complexes of type B is shown in Fig. 31 and summary of their spectral data in Table 2.

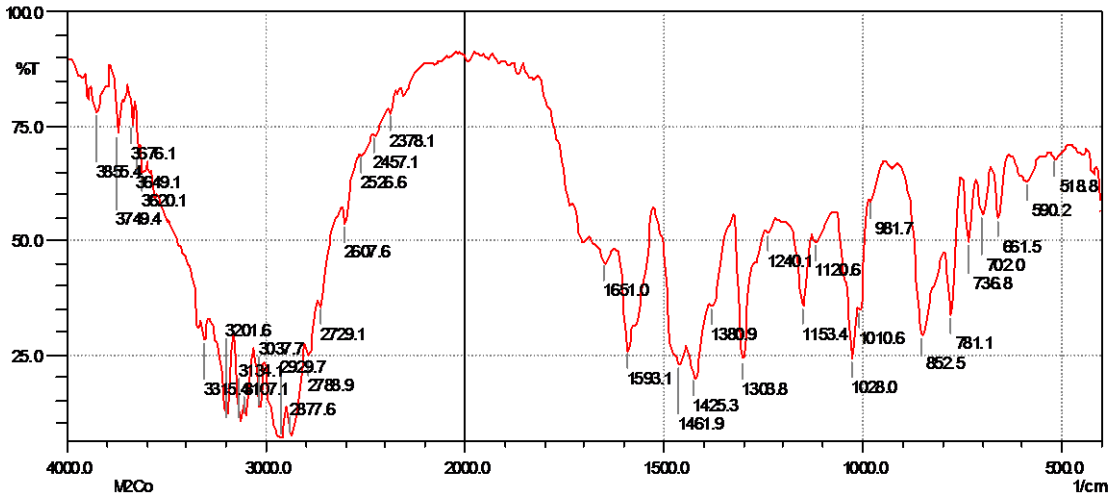

Figure 31: i.r spectra for cobalt bimetallic complex of type B. (source: author, 2013**)**

4.4 Electrochemical Studies

4.4.1 Cyclic voltammetric Studies

The electrochemical studies of monometallic and bimetallic complexes were investigated by cyclic voltammetry in the potential window –1.5 to +1.5V vs Ag\AgCl at room temperature. Electrochemical behaviour of the monometallic complexes could only be obtained in DMSO, the only solvent in which the compounds were soluble. However, electrochemical properties of the bimetallic complexes were performed in DCM and ACN to establish whether their redox properties were solvent dependent. Platinum wire was used as the counter electrode (CE) and glassy carbon as the working electrode (WE).

Ferrocene was used as the internal standard while 0.1M tetra(n-butyl)ammonium hexafluorophosphate [n-Bu_4N][PF_6] was used as the supporting electrolyte. Deoxygenation

of the solutions was also done using ultra high purity nitrogen gas, which had been purified by passing through a chromous perchloric acid scrubber.

4.4.1.1 CV of monometallic complexes of type B

When all the *m*-monometallic complexes of nickel (II), TS17 – TS20 [M'=H, M=Ni, B=C_6H_4, $(CH_2)_n$; n=2-4] were scanned in DMSO from -1.5V to 0.0 and back, identical voltammograms were observed. Reversible peak potentials falling in the range -0.735 to -0.754 were recorded. The cathodic peaks may be due to $Ni^{2+} + e^- \rightarrow Ni^+$ while the anodic peaks may be associated with $Ni^+ \rightarrow Ni^{2+} + e^-$ processes. Peak potential separations between cathodic and anodic peaks were within the range of 64-79 mV of which they are within the expected theoretical value of ΔE=59mV for a reversible one-electron transfer process. The small deviations from 59 mV may however be due to uncompensated solution internal and non-ideal cell geometry. On addition of ferrocene to the analyte solution under investigation, ΔE_F, values narrowed to the range of 59-69mV. The $E_{1/2}$ values for the complexes shifted cathodically by about 20mV as the polymethylene carbon chain of the schiff base backbone lengthened. On scanning from 0.0 to 1.5V and reversing the scan direction, similar anodic peaks which may be attributed to $Ni^{2+} \rightarrow Ni^{3+} + e^-$ process for all the complexes were observed in the range of 0.635 to 0.834 V. A typical voltammogram for *m*-monometallic complexes is shown in figure 32

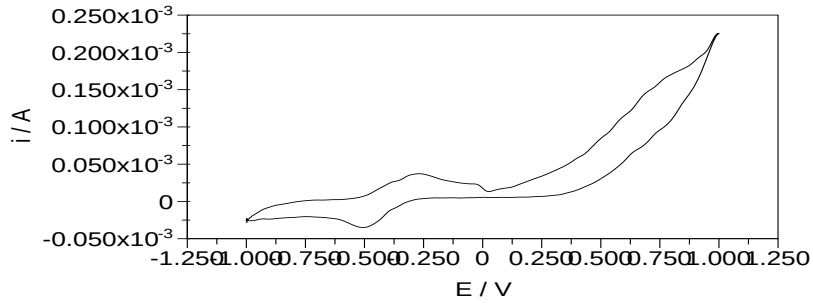

Figure 32: cyclic voltammogram of monometallic complex TS20 [M'=H, M=Ni, B=C_6H_4, $(CH_2)_n$; n=2-4] in DMSO at scan rate of 500mV/s and a current range of 10mA. **(**source: author, 2013**)**

for *m*-cobalt complexes, TS21-TS24 [M'=H, M=Co, B=C_6H_4, $(CH_2)_n$; n=2-4] on scanning from 0.0 to -1.5 V and reversing the scan polarity in DMSO, similar reduction waves for all the complexes with the reduction potentials falling in the range of -0.351 to -0.381V were observed. The cathodic waves may be attributed to $Co^{2+} + e^- \rightarrow Co^+$ reduction processes while the corresponding anodic peaks may be due to $Co^+ \rightarrow Co^{2+} + e^-$ oxidation processes. There was a shift of 30mV in the reduction potential values as the polymethylene carbon chain of the schiff base backbone lengthened. Scanning from 0.0 to 1.5V and back produced similar anodic peaks associated with $Co^{2+} \rightarrow Co^{3+} + e^-$ processes, which were observed between 0.584 to 0.769 V [Table 7]. There were no corresponding cathodic peaks. These oxidation potentials increased as the polymethylene carbon chain of the schiff base lengthened thereby suggesting that the oxidation orbitals may be ligand based.

Table 7: Redox potentials for *m*-monometallic complexes in DMSO.

M'	B	M	$(E^{1,2})_{1/2}$	$\Delta E^{1,2}$	ΔE_{FC}	$E_a^{3,4}$
H	$(CH_2)_2$	Ni	-0.738	79	70	0.820
H	$(CH_2)_3$	Ni	-0.744	73	63	0.799
H	$(CH_2)_4$	Ni	-0.754	66	66	0.834
H	C_6H_4	Ni	-0.735	64	59	0.635
H	$(CH_2)_2$	Co	-0.379	70	67	0.727
H	$(CH_2)_3$	Co	-0.381	69	65	0.769
H	$(CH_2)_4$	Co	-0.375	67	64	0.590
H	C_6H_4	Co	-0.351	61	63	0.584

[1]Reduction potential (in volts) for the process $Ni^{2+} + e^- \rightarrow Ni^+$

[2]Reduction potential (in volts) for the process $Co^{2+} + e^- \rightarrow Co^+$

[3]Oxidation potential (in volts) for the process $Ni^{2+} \rightarrow Ni^{3+} + e^-$

[4]Oxidation potential (in volts) for the process $Co^{2+} \rightarrow Co^{3+} + e^-$

Ea= Anodic peak potential

$E_{1/2} = (E_{cathodic} + E_{anodic})/2$

$\Delta E = |E_{cathodic} - E_{anodic}|$ in mV

$\Delta E_{FC} = E_{cathodic} - E_{anodic}$ for Ferrocene

4.4.1.2 CV of monometallic complexes of type A

When all the *p*-monometallic complexes of nickel, TS9-TS12 [M'=H, M=Ni, B=C_6H_4, $(CH_2)_n$; n=2-4] were scanned from -1.5v to 0.0v and back in DMSO, Similar reduction waves were observed with the reduction potentials for all the complexes falling in the range of -0.733 to -0.759V. The shift was not more than 7mV and increased as the length of the polymethylene carbon chain of the schiff base backbone, $(CH_2)_n$ lengthens from n = 2, 3,4 or C_6H_4, (Table 8). This implies that the reduction orbitals of these Ni (II) complexes could be ligand-based. However, compared to the reduction potentials of their corresponding m-analogues, these E-values were slightly more cathodic by about 2-5mV

thus showing the effect of changing the position of substitution in the benzene ring. The cathodic peak may be due to $Ni^{2+} + e^- \rightarrow Ni^+$ process while the anodic peaks may be attributed to $Ni^+ \rightarrow Ni^{2+} + e^-$ process. The peak potential separations between cathodic and anodic peaks were within the range of 60-76 mV of which these values are within the expected theoretical value of ΔE=59mV for a reversible one electron transfer process. The small deviations from 59mV may, however, be due to uncompensated solution internal resistance and non-ideal cell geometry. When ferrocene was added to the analyte solution under investigation, $\Delta E_{ferrocene}$ values narrowed within the range of 61 to 72 mV.

After scanning the potential from 0.0 to 1.5V and back, similar anodic waves which may be associated with $Ni^{2+} \rightarrow Ni^{3+} + e^-$ were observed with anodic peak potentials in the range of 0.461 to 0.576V. There were no corresponding cathodic peaks observed which probably may be due to the instability of Ni^{3+} ions in solution. The anodic shift was of about 115mV and increased as the polymethylene carbon chain of the schiff base backbone lengthened (Table 8).

The *p*-monometallic complexes of cobalt, TS13-TS16 [M'=H, M=Co, B=C_6H_4, $(CH_2)_n$; n=2-4] were scanned from 0.0 to -1.5V and reversing the scan polarity in DMSO. They exhibited voltammograms similar to their corresponding *m*-analogues except that the reduction potentials observed between -0.371 to -0.388V were more cathodic by about 7mV. By scanning from 0.0 to 1.5V and back, voltammograms similar to those of their m-analogues were also observed. The anodic peak potentials for all the complexes fell in the range of 0.554 to 0.707V [Table 8] the value being less anodic by about 32mV. There were

no observable reverse cathodic peaks

Table 8: Redox potentials for *p*-monometallic complexes in DMSO

M'	B	M	$(E^{1,2})_{1/2}$	$\Delta E^{1,2}$	ΔE_{FC}	$E_a^{3,4}$
H	$(CH_2)_2$	Ni	-0.736	76	72	0.537
H	$(CH_2)_3$	Ni	-0.744	74	67	0.543
H	$(CH_2)_4$	Ni	-0.759	67	64	0.576
H	C_6H_4	Ni	-0.733	61	61	0.461
H	$(CH_2)_2$	Co	-0.371	73	65	0.584
H	$(CH_2)_3$	Co	-0.384	70	63	0.645
H	$(CH_2)_4$	Co	-0.388	60	59	0.707
H	C_6H_4	Co	-0.372	66	61	0.554

[1]Reduction potential (in volts) for the process $Ni^{2+} + e^- \rightarrow Ni^+$

[2]Reduction potential (in volts) for the process $Co^{2+} + e^- \rightarrow Co^+$

[3]Oxidation potential (in volts) for the process $Ni^{2+} \rightarrow Ni^{3+} + e^-$

[4]Oxidation potential (in volts) for the process $Co^{2+} \rightarrow Co^{3+} + e^-$

Ea= Anodic peak potential

$E = (E_{cathodic} + E_{anodic})/2$

$\Delta E = |E_{cathodic} - E_{anodic}|$ in mV

$\Delta E_{Fc} = E_{cathodic} - E_{anodic}$ for ferrocene

4.4.1.3 CV of Bimetallic Complexes of Type B

Electrochemical studies for the bimetallic complexes were examined in both acetonitrile (ACN) and dichloromethane (DCM) solvents in order to establish the effect of solvent on their redox potentials. When *m*-bimetallic complexes of Ni (II), TS33-TS36, [M'=Mo(O)Tp*Cl, M=Ni, B=C_6H_4, $(CH_2)_n$; n=2-4] were investigated in ACN by scanning from 0.0 to -1.5V and back, two reversible reduction peaks were observed with the reduction potentials for all complexes falling in the range of -0.762 to -0.793V and -0.572 to -0.589V [Table 9]. Compared to the voltammograms of the *m*-monometallic

complexes of nickel, the potential at -0.762 to -0.793V may be associated with $Ni^{2+} + e^{-} \rightarrow Ni^{+}$ reduction process of bimetallic complexes though it is more cathodic by about 27-39mV than in the corresponding monometallic complexes. This shows that the presence of molybdenum centre modifies the electron distribution of the central Ni (II) ion to the tetradentate schiff base cavity. The potential at -0.572 to -0.589 V range for all the complexes may be attributed to the $Mo(O)^{3+} + e^{-} \rightarrow Mo(O)^{2+}$ reduction process.

By scanning from 0.0 to 1.5V and reversing the scan direction, a well-defined anodic wave was observed in the range of 1.097 to 1.195V for all the complexes. This had no corresponding cathodic wave. The peaks may be attributed to $Ni^{2+} \rightarrow Ni^{+} + e^{-}$ oxidation process. Since molybdenum centre is electron deficient, it withdraws electrons from the nickel centre thus making it harder to oxidize. This may serve as an explanation to why the oxidation potential of nickel (II) becomes more anodic in the bimetallic than in the corresponding monometallic complexes.

Table 9: Redox potentials for *m*-bimetallic complexes in ACN

M'	B	M	$(E^{1,2})_{1/2}$	$\Delta E^{1,2}$	E^3	ΔE^3	E_a
Mo(O)Tp*Cl	$(CH_2)_2$	Ni	-0.762	63	-0.572	63	1.097
Mo(O)Tp*Cl	$(CH_2)_3$	Ni	-0.773	65	-0.579	67	1.102
Mo(O)Tp*Cl	$(CH_2)_4$	Ni	-0.793	68	-0.589	69	1.148
Mo(O)Tp*Cl	C_6H_4	Ni	-0.776	67	-0.575	61	1.195
Mo(O)Tp*Cl	$(CH_2)_2$	Co	-0.472	61	-0.531	74	1.010
Mo(O)Tp*Cl	$(CH_2)_3$	Co	-0.472	65	-0.533	60	1.048
Mo(O)Tp*Cl	$(CH_2)_4$	Co	-0.484	63	-0.535	69	1.179
Mo(O)Tp*Cl	C_6H_4	Co	-0.496	61	-0.548	64	1.111

[1]Reduction potential (in volts) for the process $Ni^{2+} + e^- \rightarrow Ni^+$

[2]Reduction potential (in volts) for the process $Co^{2+} + e^- \rightarrow Co^+$

[3]Reduction potential (in volts) for the process $Mo(O)^{3+} + e^- \rightarrow Mo(O)^{2+}$

E_a = anodic peak potential (in volts) for oxidation of metal ion.

When the same complexes [M'=Mo(O)Tp*Cl, M=Ni, B=C_6H_4, $(CH_2)_n$; n=2-4] were examined in DCM, almost similar voltammograms were obtained although the peaks were broader. Scanning from 0.0 to -1.5V and back gave cathodic waves associated to the reduction of Ni (II) in the range of -0.754 to -0.785V and -0.541 to -0.547 for all the complexes. Cathodic waves falling in the range of -0.541 to -0.547V for all the complexes are associated with $Mo(O)^{3+} + e^- \rightarrow Mo(O)^{2+}$ process [Table 10].

On scanning from 0.0 to 1.5V and back, two irreversible oxidation peaks were observed with the anodic peaks for all the complexes appearing in the range of 0.989 to 1.109V and

1.156 to 1.235V [Table 10]. Waves observed in the range of 0.989 to 1.109V may be attributed to $Ni^{3+} \rightarrow Ni^{2+} + e^-$ oxidation process. This is more anodic than in the corresponding monometallic complexes showing that the oxidation of nickel in the bimetallic complexes is influenced by the proximity of the highly electro deficient Mo(O)Tp*Cl group. The other peaks at 1.156 to 1.235V may be due to the ligand oxidation. The results obtained are summarized in Table 10 below and a representative cyclic voltammogram of nickel bimetallic complexes is shown in Figure 33 below.

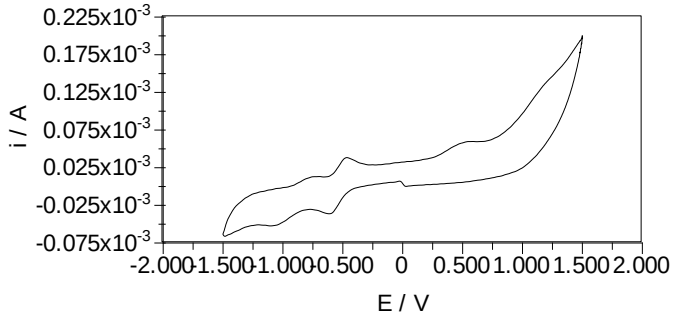

Figure 33: Cyclic voltammogram of TS27 in ACN at the scan rate of 500mV

(source: author, 2013**)**

Table 10: Redox potentials for the *m*-bimetallic complexes in DCM

M'	B	M	$(E^{1,2})_{1/2}$	E^3	ΔE^3	$E^{4,5}$	E^6
Mo(O)Tp*Cl	$(CH_2)_2$	Ni	-0.754	-0.547	69	0.995	1.176
Mo(O)Tp*Cl	$(CH_2)_3$	Ni	-0.784	-0.543	75	1.109	1.235
Mo(O)Tp*Cl	$(CH_2)_4$	Ni	-0.785	-0.543	67	1.064	1.156
Mo(O)Tp*Cl	C_6H_4	Ni	-0.773	-0.541	73	0.989	1.193
Mo(O)Tp*Cl	$(CH_2)_2$	Co	-0.448	-0.542	60	0.740	1.095
Mo(O)Tp*Cl	$(CH_2)_3$	Co	-0.449	-0.533	64	0.779	1.256
Mo(O)Tp*Cl	$(CH_2)_4$	Co	-0.452	-0.531	59	0.759	1.357
Mo(O)Tp*Cl	C_6H_4	Co	-0.456	-0.537	69	0.764	1.295

[1]Cathodic peak potential (in volts) for the process $Ni^{2+} + e^- \rightarrow Ni^+$

[2]Cathodic peak potential (in volts) for the process $Co^{2+} + e^- \rightarrow Co^+$

[3]Reduction potential (in volts) for the process $Mo(O)^{3+} + e^- \rightarrow Mo(O)^{2+}$

[4]Anodic peak potential (in volts) for the process $Ni^{2+} \rightarrow Ni^{3+} + e^-$

[5]Anodic peak potential (in volts) for the process $Co^{2+} \rightarrow Co^{3+} + e^-$

[6]Anodic peak potential (in volts) for oxidation of ligand

Multiple scans at varying scan rates yielded nearly superimposable voltammograms indicating marked stability of the reduction process of both Ni (II) and molybdenum centres.

When ferrocene was added to the complexes as an internal standard, no peaks corresponding to ferrocene/ferrocenium (Fc/Fc^+) couple were observed. The presence of Ferrocene enhanced the reversible reduction waves of the molybdenum centre so that they

became sharper while the waves due to reduction of nickel (II) were not visible. An overlay of the voltammogram in ACN solvent is given in Figures 34.

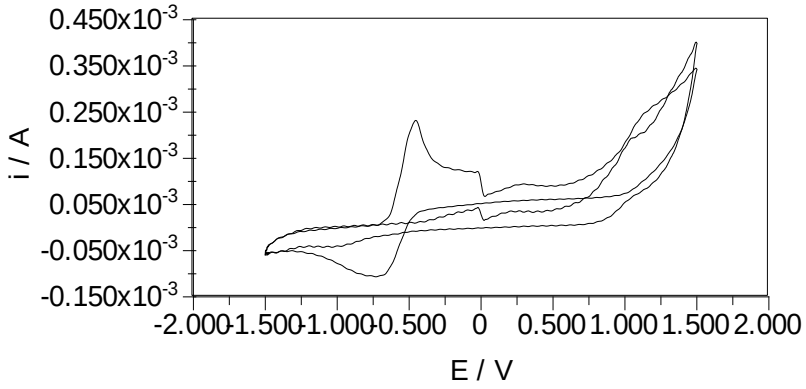

Figure 34: cyclic voltammograms obtained before (a) and after (b) addition of Ferrocene in TS26 in ACN at the scan rate of 400mV/s. (source: author, 2013**)**

By comparing the voltammograms obtained in both ACN and DCM, a number of differences are observed. Only one anodic wave is observed on scanning from 0.0 to 1.5V in ACN while in DCM, two anodic waves were observed. The reduction of nickel (II) in ACN is reversible; ΔE for this process fall in the range of 63-68mV but in DCM, this process is irreversible with ΔE falling in the range of 137-198mV. These observations show that the redox potentials are solvent dependent.

When *m*-bimetallic complexes of cobalt, TS37-TS40 [M'=Mo(O)Tp*Cl, M=Co, B=C_6H_4, $(CH_2)_n$; n=2-4] were scanned from -1.5V to 0.0v and back in ACN, two reversible reduction waves ranging between -0.472 to -0.496V and -0.531 to -0.548V [Table 9].

Compared to the voltammograms of the corresponding m-monometallic complexes of cobalt, the potentials falling in the range of -0.472 to -0.496V may be associated with $Co^{2+} + e^- \rightarrow Co^+$ reduction processes. The reduction potential values shifted cathodically by about 24mV as the polymethylene carbon chain of the schiff base ligand lengthened. The potentials falling in the range of -0.531 to -0.542V may be attributed to the $Mo(O)^{3+} + e^- \rightarrow Mo(O)^{2+}$ process. This reduction potential shifts slightly cathodically by about 11mV as the length of the polymethylene carbon chain of the schiff base ligand increases. Comparing with the corresponding *m*-analogues of nickel (II), the potential value for *m*-bimetallic complexes of cobalt becomes more anodic by about 31mV as the carbon chain length increases. This shows that the type of metal incorporated in the schiff base cavity has some influence on the reduction potential of the molybdenum centre. ΔE values for the reduction processes are in the range of 64-74mV while for ferrocene falls in the range of 63-69mV. These values are consistent with the expected theoretical value of ΔE=59mV for a one-electron transfer process.

On scanning from 0.0 to 1.5V and reversing the scan direction, one irreversible anodic wave with a peak potential in the range of 1.010 to 1.179V was observed. This could be due to one-electron transfer processes that may be associated with the oxidation of Co (II) to cobalt (III).

By investigating m-bimetallic cobalt (II) complexes in DCM on scanning from 0.0 to -1.5V and reversing the scan direction, the reduction wave associated with

$Co^{2+} + e^- \rightarrow Co^+$ process appeared as cathodic waves only in the range of -0.448 to-0.456V for all the complexes [Table 10]. In comparison to the corresponding E-values in ACN, these values were less cathodic by about 24 - 40mV. Reversible reduction waves which may be associated with $Mo(O)^{3+} + e^- \rightarrow Mo(O)^{2+}$ processes were also observed with the reduction potentials for all the complexes falling in the range of -0.533 to -0.542V [Table 10], which when compared with the values observed when using ACN were slightly lower by about 6mV.

On scanning from 0.0 to 1.5V and back for all the complexes, two irreversible oxidation waves associated with $Co^{2+} \rightarrow Co^{3+} + e^-$ and a ligand based oxidation processes were observed in the potential ranges of 0.740 to 0.779V and 1.095 to 1.357V [Table 10] respectively. In ACN, only one single wave was observed. This is a confirmation that the redox potentials for these types of complexes are solvent dependent. In the corresponding *m*-analogues of nickel, when ferrocene was added, it did not show the characteristic waves associated with Fc/Fc^+ couple. This appears to have enhanced the reversible reduction waves of the molybdenum centre making them sharper instead.

4.4.1.4 CV of bimetallic complexes of type A

The electrochemical studies of *p*-analogues of Ni (II) and Co (II) bimetallic complexes were conducted in both ACN and DCM in order to study the effect of substitution on the benzene ring and the effect of solvent on the redox potentials. When *p*-bimetallic complexes of nickel, TS25-TS28, [M'=Mo(O)Tp*Cl, M=Ni, B=C_6H_4, $(CH_2)_n$; n=2-4] were scanned in ACN from 0.0 to -1.5V and the scan polarity reversed, two reversible

reduction waves associated with the reduction of nickel (II) and $Mo(O)^{3+}$ were observed with the reduction potentials for all the complexes ranging between -0.765 to -0.791V and -0.561 to -0.590V, respectively [Table 11]. When this was compared with the reduction potentials of their m-analogues, nickel (II) was less cathodic by about 7mV but that of the molybdenum centre shifted by about 10mV. This indicates that the *p*-complexes are easier to reduce, which could be due to the fact that LUMO's of the *p*-analogues have less electron density than those of the *m*-analogues.

Scanning from 0.0 to 1.5V and reversing the scan polarity gave one irreversible oxidation wave associated with nickel (II) oxidation processes with the electrode potential falling in the range of 1.098 to 1.204V for all the complexes. However, these potentials were more anodic than the corresponding m-analogues by about 42mV. This shows that shifting the position of Mo(O)Tp*Cl from meta to para in the benzene ring of the schiff base framework creates some influence on the redox potentials of both nickel (II) and $Mo(O)^{3+}$ centres.

Table 11: Redox potentials for *p*-bimetallic complexes in ACN.

M'	B	M	$(E^{1,2})_{1/2}$	$\Delta E^{1,2}$	E^3	ΔE^3	E_a
Mo(O)Tp*Cl	$(CH_2)_2$	Ni	-0.779	66	-0.561	64	1.152
Mo(O)Tp*Cl	$(CH_2)_3$	Ni	-0.785	65	-0.581	62	1.204
Mo(O)Tp*Cl	$(CH_2)_4$	Ni	-0.787	69	-0.590	67	1.131
Mo(O)Tp*Cl	C_6H_4	Ni	-0.769	74	-0.570	71	1.098
Mo(O)Tp*Cl	$(CH_2)_2$	Co	-0.468	71	-0.551	68	1.097
Mo(O)Tp*Cl	$(CH_2)_3$	Co	-0.471	67	-0.558	65	1.048
Mo(O)Tp*Cl	$(CH_2)_4$	Co	-0.473	69	-0.559	63	1.065
Mo(O)Tp*Cl	C_6H_4	Co	-0.476	65	-0.559	62	1.195

[1]Reduction potential (in volts) for the process $Ni^{2+} + e^- \rightarrow Ni^+$

[2]Reduction potential (in volts) for the process $Co^{2+} + e^- \rightarrow Co^+$

[3]Reduction potential (in volts) for the process $Mo(O)^{3+} + e^- \rightarrow Mo(O)^{2+}$

Ea= Anodic peak potential (in volts) for oxidation of the metal ion.

By investigating the *p*-complexes of nickel [M'=Mo(O)Tp*Cl, M=Ni, B=C_6H_4, $(CH_2)_n$; n=2-4] in DCM and scanning from 0.0 to -1.5V and back, one irreversible cathodic wave associated with the reduction of nickel (II) was observed in the potential range of -0.737 to -0.745V. A reversible wave associated with the reduction of molybdenum centre was also observed at the potential range -0.520 to -0.543V for all the complexes. These reduction potentials were below the values obtained when ACN was used by about 32-40mV for nickel (II) and 40-47mV for molybdenum centres. Similar observations were made in the corresponding m-complexes. As the polymethylene carbon chain lengthened, it was observed that the reduction potentials for both nickel (II) and molybdenum centres became

more cathodic.

On scanning from 0.0 to 1.5V and reversing the scan direction, two irreversible oxidation waves falling in the potential ranges of 0.521 to 0.740V and 1.082 to 1.205V for all the complexes were observed. These waves are attributed to nickel (II) and ligand based oxidation processes, respectively. The potentials were found to be more anodic than their corresponding m-analogues by 10-26mV.

When *p*-analogues of cobalt bimetallic complexes, TS29-TS32 [M'=Mo(O)Tp*Cl, M=Co, B=C_6H_4, $(CH_2)_n$; n=2-4] were studied in ACN, two reversible reduction waves on scanning from 0.0 to -1.5V and back were recorded. The potential waves appearing in the range of -0.468 to -0.476V may be attributed to $Co^{2+} + e^- \rightarrow Co^+$ reduction processes for all the p-cobalt complexes. The E-values as compared to the corresponding m-analogues are more cathodic by 4-20mV. This served as a confirmation that incorporation of the molybdenum centre into the cobalt schiff base complexes affects the reduction potential of cobalt. This was also observed in the complexes of type B. The other reversible reduction waves were in the range of -0.551 to -0.559V, which are associated to $Mo(O)^{3+} + e^- \rightarrow Mo(O)^{2+}$ reduction processes. The E-values were more cathodic by almost 15mV than the corresponding *m*-analogues. This shows that the position of substitution of the molybdenum centre on the benzene ring of the schiff base affects reduction potential. These reduction potentials were very close as the polymethylene carbon chain lengthened, a condition similar to that observed in the *m*-analogues.

Scanning from 0.0 to 1.5V and reversing the scan direction, one irreversible oxidation wave was observed with the anodic peak potential appearing in the range of 1.048 to

1.295V for all the complexes. These peaks may be associated with $Co^{2+} + e^{-} \rightarrow Co^{+}$ reduction processes. The values were more anodic than for the corresponding *m*-analogues.

p-bimetallic complexes of cobalt, TS29-TS32 [M'=Mo(O)Tp*Cl, M=Co, B=C_6H_4, $(CH_2)_n$; n=2-4], were also investigated in DCM. On scanning from 0.0 to -1.5V and back, one irreversible reduction wave attributed to $Co^{2+} + e^{-} \rightarrow Co^{+}$ processes appeared in the range of -0.423 to -0.445V. A reversible wave associated with the reduction of the molybdenum centre also appeared in the range of -0.563 to -0.571V. From these results, the reduction potential values for cobalt (II) and molybdenum centre were more cathodic than in their *m*-analogues, an observation also made in their corresponding monometallic complexes.

On scanning from 0.0 to 1.5V and reversing the scan polarity, two irreversible oxidation waves associated with cobalt (II) and a ligand based oxidation processes appeared in the ranges of 1.105 to 1.263 and 1.152 to 1.365V, respectively [Table 12]. In DCM, these reduction waves were broader as compared to the ones in ACN. Only one irreversible wave associated with cobalt (II) process was observed in ACN while two irreversible waves associated with the same process were observed in DCM. This is a confirmation that these redox processes are solvent dependent.

The effects on the redox potentials of the metal centres using different solvents and changing the position of substitution on the benzene ring are quite clear. In CAN solvent, the reduction of Ni (II) and Co (II) are reversible while in DCM they are irreversible. *P*-

complexes of both the monometallic and bimetallic complexes of both Ni (II) and Co (II) were found to have more cathodic reduction potentials than their corresponding *m*-complexes.

Table 12: Redox potentials for *p*-bimetallic complexes DCM.

M'	B	M	$(E^{1,2})_{1/2}$	$\Delta E^{1,2}$	ΔE^{3}	E^{3}	$E^{4,5}$	E^{6}
Mo(O)Tp*Cl	$(CH_2)_2$	Ni	-0.737	71	-0.531	63	0.999	1.082
Mo(O)Tp*Cl	$(CH_2)_3$	Ni	-0.739	67	-0.539	61	1.115	1.163
Mo(O)Tp*Cl	$(CH_2)_4$	Ni	-0.745	62	-0.543	68	1.135	1.205
Mo(O)Tp*Cl	C_6H_4	Ni	-0.737	63	-0.520	65	1.129	1.183
Mo(O)Tp*Cl	$(CH_2)_2$	Co	-0.438	65	-0.569	68	1.263	1.152
Mo(O)Tp*Cl	$(CH_2)_3$	Co	-0.439	63	-0.569	70	1.157	1.182
Mo(O)Tp*Cl	$(CH_2)_4$	Co	-0.445	61	-0.571	69	1.189	1.252
Mo(O)Tp*Cl	C_6H_4	Co	-0.423	63	-0.563	67	1.105	1.365

[1]Cathodic peak potential (in volts) for the process $Ni^{2+} + e^- \rightarrow Ni^+$

[2]Cathodic peak potential (in volts) for the process $Co^{2+} + e^- \rightarrow Co^+$

[3]Reduction potential (in volts) for the process $Mo(O)^{3+} + e^- \rightarrow Mo(O)^{2+}$

[4]Anodic peak potential (in volts) for the process $Ni^{2+} \rightarrow Ni^{3+} + e^-$

[5]Anodic peak potential (in volts) for the process $Co^{2+} \rightarrow Co^{3+} + e^-$

[6]Anodic peak potential (in volts) for oxidation of ligand

$\Delta E = |E_{cathodic} - E_{anodic}|$ in mV

4.4.2 Differential Pulse Voltammetric Studies

The electrochemical properties of the monometallic and bimetallic complexes were also investigated by differential pulse voltammetric (DPV) technique. Monometallic complexes were studied using DMSO while the bimetallic complexes were studied using ACN and DCM solvents. DPV produced well-defined peaks as compared with the cyclic voltammetry. Monometallic complexes of Ni (II) of type B [M'=H, M=Ni, B=C_6H_4, $(CH_2)_n$; n=2-4] in DMSO produced peaks in the range of –0.743 to –0.762V for all the complexes [Table 13] while for type A complexes, the peak potential range was –0.743 to –0.761V [Table 14]. Monometallic complexes of cobalt of type B and A [M'=H, M=Co, B=C_6H_4, $(CH_2)_n$; n=2-4] produced peaks in the range of –0.484 to –0.502V and –0.485 to –0.501V, respectively.

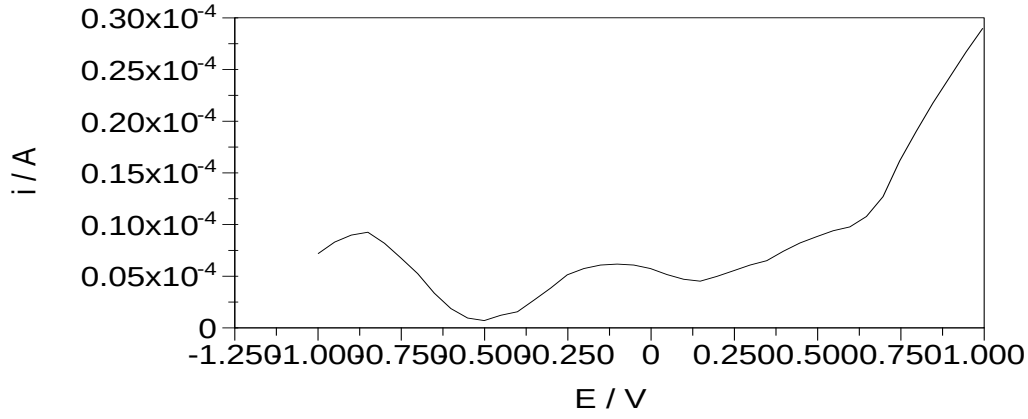

Figure 35: Differential pulse voltammogram of TS22, in DMSO. (source: author, 2013**)**

Table 13: DPV reduction potentials for *m*-monometallic complexes in DMSO

M'	B	M	E(V)	Electrode reaction
H	$(CH_2)_2$	Ni	-0.745	$Ni^{2+} + e^- \rightarrow Ni^+$
H	$(CH_2)_3$	Ni	-0.747	$Ni^{2+} + e^- \rightarrow Ni^+$
H	$(CH_2)_4$	Ni	-0.762	$Ni^{2+} + e^- \rightarrow Ni^+$
H	C_6H_4	Ni	-0.743	$Ni^{2+} + e^- \rightarrow Ni^+$
H	$(CH_2)_2$	Co	-0.484	$Co^{2+} + e^- \rightarrow Co^+$
H	$(CH_2)_3$	Co	-0.484	$Co^{2+} + e^- \rightarrow Co^+$
H	$(CH_2)_4$	Co	-0.502	$Co^{2+} + e^- \rightarrow Co^+$
H	C_6H_4	Co	-0.495	$Co^{2+} + e^- \rightarrow Co^+$

Table 14: DPV reduction potentials for *p*-monometallic in DMSO

M'	B	M	E(V)	Electrode reaction
H	$(CH_2)_2$	Ni	-0.745	$Ni^{2+} + e^- \rightarrow Ni^+$
H	$(CH_2)_3$	Ni	-0.752	$Ni^{2+} + e^- \rightarrow Ni^+$
H	$(CH_2)_4$	Ni	-0.761	$Ni^{2+} + e^- \rightarrow Ni^+$
H	C_6H_4	Ni	-0.743	$Ni^{2+} + e^- \rightarrow Ni^+$
H	$(CH_2)_2$	Co	-0.485	$Co^{2+} + e^- \rightarrow Co^+$
H	$(CH_2)_3$	Co	-0.501	$Co^{2+} + e^- \rightarrow Co^+$
H	$(CH_2)_4$	Co	-0.499	$Co^{2+} + e^- \rightarrow Co^+$
H	C_6H_4	Co	-0.492	$Co^{2+} + e^- \rightarrow Co^+$

All bimetallic complexes were examined in both ACN and DCM for the purpose of determining the effect of solvent on their redox potentials. Nickel (II) complexes of type B exhibited two peaks in the range of -0.753 to -0.759 V and -0.551 to -0.560V. The peak observed in the range of -0.753 to -0.759V is associated with the reduction of nickel (II)

while that in the range of -0.551 to -0.560V is for the reduction of molybdenum centre (Table 15). Type A complexes, TS24-TS28, gave similar voltammograms with the corresponding peaks falling in the ranges of -0.755 to -0.764V and -0.552 to -0.565V respectively (Table 16). Cobalt (II) complexes of type B, TS37-TS40, exhibited peaks associated with the reduction of cobalt (II) in the range of -0.342 to -0.359V while peaks associated with the reduction of molybdenum centre were observed in the range of -0.546 to -0.553V (Table 15). Bimetallic complexes of cobalt type A, TS33-TS36 had their corresponding peaks between -0.346 to -0.359V and -0.546 to -0.553V (Table 16).

In DCM, the fact that the redox potentials of this type of complexes are solvent dependent was confirmed by the fact that the reduction potentials of Ni (II) was observed to be more cathodic in DCM than in ACN. Type B complexes of nickel (II), TS29-TS32, exhibited peaks associated with the reduction of nickel (II) in the potential range of -0.747 to -0.762V while the peaks associated with the reduction of molybdenum centre was observed in the potential range of -0.552 to -0.556V [Table 15). Type A complexes of nickel (II), TS25-TS28, had their corresponding voltammograms in the potential range of -0.343 to -0.355V and -0.547 to -0.565V, respectively [Table 16].

Cobalt complexes of type B, TS37-TS40, in DCM exhibited their redox potential peaks in the range of -0.345 to -0.351V, which is associated with the reduction of cobalt (II) and -0.548 to -0.550V associated with the reduction of molybdenum centre [Table 15]. Their corresponding peaks for type A complexes falls in the range of -0.343 to -0.355V and -0.547 to -0.565V, respectively [Table 16]. The potential values for the reduction of cobalt

and molybdenum centres in type A complexes were found to be more cathodic than type B complexes. This is a clear indication that the position of substitution on the benzene ring affects the redox potentials of this type. The results obtained are summarized in tables 15 and 16 and a representative voltammogram of bimetallic complexes shown in the Figure 36.

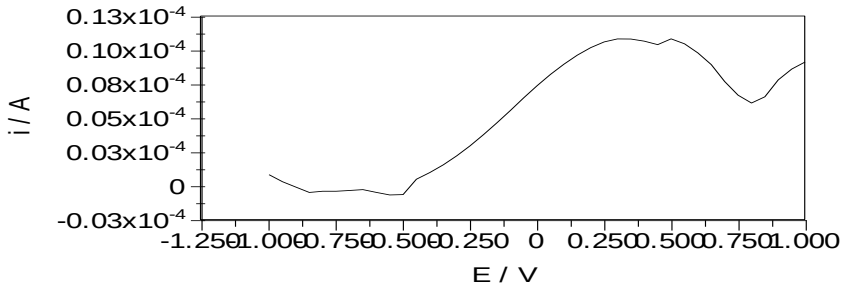

Figure 36: DPV reduction potentials for TS27, in ACN. (source: author, 2013**)**

Table 15: DPV reduction potentials for *m*-bimetallic complexes in ACN and DCM

			CAN			DCM		
M'	B	M	E(V)[1,2]	E(V)[3]	ΔE(mV)[4,5]	E(V)[1,2]	E(V)[3]	ΔE(mV)[4,5]
Mo(O)Tp*Cl	$(CH_2)_2$	Ni	-0.756	-0.553	203	-0.749	-0.553	196
Mo(O)Tp*Cl	$(CH_2)_3$	Ni	-0.757	-0.555	202	-0.754	-0.556	198
Mo(O)Tp*Cl	$(CH_2)_4$	Ni	-0.759	-0.560	199	-0.762	-0.553	209
Mo(O)Tp*Cl	C_6H_4	Ni	-0.753	-0.551	202	-0.747	-0.552	195
Mo(O)Tp*Cl	$(CH_2)_2$	Co	-0.342	-0.546	204	-0.345	-0.548	203
Mo(O)Tp*Cl	$(CH_2)_3$	Co	-0.356	-0.551	195	-0.347	-0.549	203
Mo(O)Tp*Cl	$(CH_2)_4$	Co	-0.359	-0.553	194	-0.351	-0.550	199
Mo(O)Tp*Cl	C_6H_4	Co	-0.352	-0.548	196	-0.351	-0.549	198

[1]Reduction potential for the process $Ni^{2+} + e^- \rightarrow Ni^+$

[2]Reduction potential for the process $Co^{2+} + e^- \rightarrow Co^+$

[3]Reduction potential for the process $Mo(O)^{3+} + e^- \rightarrow Mo(O)^{2+}$

[4]Peak potential difference between E^1 and E^3 in mV

[5]Peak potential difference between E^2 and E^3 in mV

Table 16: DPV reduction potentials for *p*-bimetallic complexes in ACN and DCM

			ACN			DCM		
M'	B	M	$E(V)^{1,2}$	$E(V)^{3}$	$\Delta E(mV)^{4,5}$	$E(V)^{1,2}$	$E(V)^{3}$	$\Delta E(mV)^{4,5}$
Mo(O)Tp*Cl	$(CH_2)_2$	Ni	-0.762	-0.552	210	-0.757	-0.543	214
Mo(O)Tp*Cl	$(CH_2)_3$	Ni	-0.763	-0.559	204	-0.759	-0.547	212
Mo(O)Tp*Cl	$(CH_2)_4$	Ni	-0.764	-0.565	199	-0.762	-0.553	209
Mo(O)Tp*Cl	C_6H_4	Ni	-0.755	-0.552	203	-0.754	-0.549	205
Mo(O)Tp*Cl	$(CH_2)_2$	Co	-0.346	-0.546	200	-0.343	-0.565	222
Mo(O)Tp*Cl	$(CH_2)_3$	Co	-0.357	-0.552	195	-0.352	-0.553	201
Mo(O)Tp*Cl	$(CH_2)_4$	Co	-0.359	-0.549	190	-0.355	-0.547	192
Mo(O)Tp*Cl	C_6H_4	Co	-0.356	-0.553	197	-0.353	-0.552	199

[1]Reduction potential for the process $Ni^{2+} + e^- \rightarrow Ni^+$

[2]Reduction potential for the process $Co^{2+} + e^- \rightarrow Co^+$

[3]Reduction potential for the process $Mo(O)^{3+} + e^- \rightarrow Mo(O)^{2+}$

[4]Peak potential difference between E^1 and E^3 in mV

[5]Peak potential difference between E^2 and E^3 in mV

CHAPTER FIVE

CONCLUSION AND RECOMMENDATIONS

5.1 Conclusion

The [Mo^{V}(O)Tp*Cl fragment has proved to be ideal for the study of long-distance electronic interactions across conjugated bridging ligands. The study has shown that electronic interactions between two metal centres are determined by the nature of the bridging ligand, and the results should be of fundamental interest for the design of future multinuclear compounds in the areas of molecular electronics.

The UV/Vis spectra contain a broad absorption in the visible region, which is assigned to a metal-to-ligand charge transfer (M.L.C.T) for two reasons. Firstly, the wide variation in λ_{max} with the nature of the linking group between the two metals suggests the involvement of the ligand in the transitions; it is consistent with the presence of d-d character in the transitions since the ligand field would not be substantially perturbed by remote substituents on the schiff base ligands. Secondly, the spectra also contain a transition near 580.0nm, whose constancy suggests a d-d transition, possibly enhanced by intensity borrowing from adjacent-charge transfer bands.

Cyclic voltammetric studies indicated that the length of the polymethylene carbon chain of the ligand backbone shifted the reduction potential of monometallic complexes of nickel cathodically by 16 to 19mV. For the cobalt monometallic complexes, on the other hand, the reduction potentials increased cathodically as the length of the polymethylene chain increases. Differential Pulse Voltammetry (DPV) confirmed these findings.

Electrochemical studies of bimetallic complexes were found to be solvent dependent with the compounds having molybdenum centre reducing reversibly in dichloromethane and ACN. The reduction was high in ACN than in DCM. $Mo(O)^{3+}$ unit on the redox behaviour of nickel and cobalt centres showed a cathodic shift. The ΔE values ranges from the theoretical value of 59mV to 180mV at a scan rate 500mV/s. Further study of the bimetallic complexes revealed that molybdenum centres reduced more cathodically in nickel bimetallic complexes than in cobalt. This shows that the nature of the central metal of the bimetallic complexes influences the electrochemical properties of $Mo(O)^{3+}$. Changing the substitution pattern from *meta* to *para* also influences the electrochemical properties of bimetallic complexes. For nickel schiff base complexes, the reduction potential shifted more cathodically by a value of 10mV in *meta* substituted complexes than in *para* substituted complexes. For cobalt complexes, the shift in *meta* complexes was higher than in para complexes by a value of 13mV. For the bimetallic complexes, the shift was dependent on both the position of substitution and the solvent. Type B nickel bimetallic complexes in both ACN and DCM experienced a higher shift than for type A but in both cases, the shifts in DCM were lower than those observed in ACN. Type B Cobalt bimetallic complexes in ACN experienced higher shifts of not more than 16mV than in DCM. For *p*-cobalt complexes, the shift was higher in DCM than in ACN by almost 14mV. It was observed that ΔE decreases with;

i. Increasing length of the bridging ligand.
ii. Changing the substitution pattern from para to *meta*.
iii. Changing the solvent from ACN to DCM.

5.2 Recommendations

Further cumulative electrochemical work of similar systems needs to be done with different metals in the central cavity and extended polymethylene carbon chain in the schiff base ligands to confirm these findings.

REFERENCES

Akabori, S., Habata, Y., Sakamoto, Y. and Sato, M. (1985). *Bull. Chem. Soc*., **58**, 783.

Amitava, D., Drane, A. S. and McCleverty, J. A. (1983). Alkoxy, amido and thiolato complexes of tris(3,5-dmethyl pyrazolyl) borato (nitrosyl)–molybdenum fluoride, chloride and bromide. *Polyhedron*, **2**, 53-57.

Amoroso, A. J., argil Thomson, A. M. W., Maher, J.P., Mcleverty, J. A., Ward, M.D. (1995). Di-, tri- and tetranucleating pyridyl which facilitate multi-centre magnetic exchange between paramagnetic molybdenum centres. *Inorg. Chem.*, 34, 4828-4835.

Andrea, D., Dante, G., Claudio, S. and Lorenzo, S. (2004). Quinoid Metal Complexes: Towards Molecular Switches. *Acc. Chem. Res*., **37**.

Balzani, V. and Scandola, F. (1991). *Supramolecular Photochemistry*; Ellis Horwood, **140**.

Barigelleti, F. and Lucia, F. (2000). Photoactive molecular wires based on metal complexes. *Chem. Soc. Rev*., **29**, 1-12.

Briggs, T.N., Jones, C.J., Neaves, B.D., Murr, N.E. and Colquhoun, H. (1985). Electrochemical and chemical properties of diiodonitrosyl {tris (3,5-dimethylpyrazolyl) hydroborate molybdenum, Mo{$HB(Me_2pz)_3$}$(NO)I_2$, and related complexes, *J. Chem. Soc. Dalton Trans*., 1249.

Bushby, R. J. and Pallaud J. L. (1995). Molecular Magnets. In Introduction to Molecular Electronics. Petty M. C., Bryce, M. R., Bloor, D.; Eds.; Edward Arnold: London, 72-91.

Callahan, R.W., Brown, M.G., and Meyer, J.T. (1975). Effects of weak metal-metal interactions in ligands-bridged complexes of ruthenium. Dimeric complexes containing ruthenium ions in different coordination environments. *Inorg. Chem*., **14,** 1443.

Charsely, S.M., Jones, C. J., McCleverty, J. A., Weaves B.D. and Sarah, R. J. (1988). Monometallic, homo- and hetero bimetallic complexes based on redox-active tris (3,5-dimethyl pyrazolyl) borato molybdenum and tungsten nitrosyls. Part 7. Compounds containing strongly interacting redox centres derived from *para*- substituted anilines and phenols. *Journal of Chemical Society*. Dalton Trans. **16**, 283.

Christian, D.G. (1986). Analytical Chemistry, 4th Edition. John Willey and Sons.

Cleland, W.E., Kerry, M., Barnhart, K., Yamanouchi, D.C., Mabbs, F.E., Ortegala, R.B.

and Enemark J. H. (1987). Synthesis, Structures and Spectroscopic properties of Six-coordinate Mononuclear Oxo-Molybdenum (V) Complexes Stabilized by the Hydrotris (3,5-dimethyl-1-pyrazolyl) Borate Ligand, *Coord. Chem. Rev*., **48**, 59-82.

Cotton, F. A. (1972). Advanced Inorganic Chemistry. *Interscience publishers*, 3rd Ed, 801-1055.

Cotton, F. A. (1980). Advanced Inorganic Chemistry. *Interscience publishers*, London, **4**:413.

Cotton, F. A., Geoffrey, W., Carlos, A. M. and Manfred B. (1999). Advanced Inorganic Chemistry, *Interscience Publishers,* 6: 972-974.

Cram, D. J. and Cram J. M. (1994). Container Molecules and Their Guests. *Royal Society of Chemistry*: Monographs in Supramolecular Chemistry.

Cramer, S. P. and Stiefel, E. I. (1985). Molybdenum Enzymes. **8**: 411-441

Creutz, C. (1983). The Synthesis, redox properties and ligand binding of heterobinuclear transition metal macrocyclic ligand complexes, *Progressive Inorganic Chemistry,* **30,** 1.

Cruetz, C. and Taube, H. (1973). Binuclear Complexes of Ruthenium Ammines. *Journal of America Chemical Society*. **95**, 1086-1084.

Culbertson, J.B., Albright, R., Baker, D. and Sweitzer, P. (1935). Steric hindrance as a factor in the hydrolytic stability of aromatic ketimines, *Proc. Iowa Acad. Sci.*, **40**, 113.

Daniel, L. R., Christian, G., Kenneth, K. B., Christine, A. L., Jaydeep, J.S., Lamba, A. L. and Roger, D. S. (2000). Synthesis of Tris(pyrazolyl) methane Ligands and {[tris(pyrazolyl) methane] $Mn(CO)_3$}SO_3CF_3 complexes: Comparison of ligand donor properties. *J. Org. Chem.*, 120-128.

Day, M. C. (1981). *Theoretical Inorganic Chemistry*. 165-166.

Day, P., Bradley, D.C. and Bloor, D. (1990). "Molecular Chemistry for Electronics", *London, Royal Society*.

Dayagi, S. and Degan, Y. (1970). The Chemistry of the Carbon-nitrogen Double bond, *Wiley Interscience*, New York, 81.

Dockal, E.R., Jones, T.E., Sokol, W.F., Engever, R.J., Rorabacher, D.B. and Ochrymowycz, L.A. (1976). Redox Properties of Copper-thioether Complexes. Comparison to Blue Copper Protein Behaviour. *Journal of American Chemical Society*, **98**, 4322.

Elder, R.C., Blubaugh, E.A., Hineman, W.R., Birke, P.J. and McMillin, D.R. (1983). Thin Layer Spectro-electrochemical Studies of Copper and Nickel Unsymmetrical Schiff Base Complexes. *Journal of Inorganic Chemistry*, 2777.

Enemark, J. H. (1986). Synthesis, Structures and Spectroscopic properties of Six-coordinate Mononuclear Oxo-Molybdenum (V) Complexes Stabilized by the Hydrotris (3,5 dimethyl-1-pyrazolyl) borate Ligand, *Coord. Chem. Rev*., **48**, 59-82.

Evans, D., Osborn, J.A. and Wilkinson G. (1968). Hydroformylaation of Alkenes by Use of Rhodium Complex Catalysts. *Journal of Chemical Society*, 3133-3142.

Fabbrizzi, L. and Poggi, A. (1999). Sensors and Switches from Supramolecular Chemistry.**448**, 261.

Fabbrizi, L.; Gatti, F.; Pallavicini, P.; Zambarbieri, E. (1999). Redox Driven Intramolecular Anion Translocation Between Transition Metal Centres. *Chem. Eur. J*. 5, 682-690.

Fujita, J., Tanaka, M., Suemune, H., Koga, N., Matsuda, K. and Lwamura, H. (1996). Antiferromagnetic Exchange Interaction Among the Three Spins Placed in an Isosceles Triangular Configuration in 2,4-Dimethoxy-1,3,5-Benzenetriyltris(N-Tert-Butyl Nitroxide). *Journal of American Chemical Society*, **118**, 9347-9351.

Greenwood, N.N., Michael, Mark, B., Xavier, L. R. F., Kennedy, J.D. and Mark, T. (1988). Preparation, Structure and Nuclear Magnetic Resonance Properties of the Nine-Vertex Nido-rhenaborane[$(PMe_2Ph_3)_3H_2ReB_8H_{11}$] and Some Related Chemistry. *Journal of chemical Society, Dalton Trans*., 1969-1981.

Hammet, L.P. (1940), Physical Organic Chemistry. McGraw-Hill Book Co., Inc., New York, 333.

Hariharan, H. and Urbach, F. (1971). Stereochemistry of Tetradentate Schiff Base Complexes of Cobalt (II), *Journal of Inorganic Chemistry*, **10**, 2667.

Harris, C.M. and Mckenzie, F. (1962). The Preparation and Colour of Tris-2,2'-bipyridyl

and Bis-2,2'2"-terpyridylrhodium (III) Salts, *Elsevier*, **25**, 171-174.

Hawkes, M.J.B., Billing, E. and Gray, H.B. (1966). *Journal of American Chemical Society***.** **88**, 4873.

Holm, R.H. (1960). Studies on Ni (II) Complexes I. Spectra of Tricyclic Schiff base complexes of Ni (II) and Cu(II), *Journal of American Chemical Society*., **82**, 5632.

Holm, R.H., Everret, G.W. and Chakravorty, A. (1966). Metal Complexes of Schiff Bases and β-ketoamines. *Progress in Inorganic Chemistry*.

Jing, J., Gaus, P.L. and Haim, A. (1979). *Journal of American Chem*. **101**, 6193.

Jolly, W.L. (1985). *Modern Inorganic Chemistry*, McGraw-Hill.

Jones, C.J. (1998). Transition Metals as Structural Components in the Construction of Molecular Containers. *Chemical Society Reviews*, **27**, 289.

Jorgensen, K. Chr. (1963). Inorganic Complexes. *Academic press*, London and Newyork.

Kagwanja, S.M., Jones, C.J., Maher, J.P. and McCleverty, J.A. (1994). Formation of Trimetallic Complexes Containing Redox Active Nitrosyl molybdenum Tris(3,5-dimethyl pyrazolyl) Borato Groups, *Polyhedron*, **13,** 2615.

Kagwanja, S.M., McCleverty, J.A. and Jones, C.J. (1994). Reaction of Molybdenum Mononitrosyl Halides with Schiff Bases; Hydrolysis of Azomethine Link Formation of Monometallic Tris(3,5-dimethyl pyrazolyl) Borato Phenolato Complexes. *Polyhedron.***13**, 329.

Kitafima, N. and Tolman, W.B. (1995). *Prog. Inorg. Chem.*, **43**, 419.

Kipkemboi, P. K., Kiprono P. C. and Sanga J. J. (2003). Vibrational Spectra of t-butyl Alcohol, t-butylamine and t-butyl Alcohol + t-butylamine Binary Liquid Mixtures. *Bulletin of Chemical Society of Ethiopia*, **17(2)**, 211-218.

Layer, W.R. (1962). "*Chemistry of Imines"*, 489.

Leussing, D.L. and Stanfield, C.K. (1966). Kinetics of Formation of N-pyruvylidene glycianato zinc(II), *Journal of American Chemical Society*, **88**, 5726.

Lindoy, L. F. (1989). The Chemistry of Macrocyclic Ligand Complexes. Cambridge University Press, 90.

Lippard, S.J. and Sussana, H. (1997). Synthesis, characterization, and magnetic studies of two novel isostructural pentanuclear Iron(II) Complexes**.** *Accounts of Chemical Resources***.** **3**6**,** 50-58.

Liprot, G. F. (1974). Modern Inorganic Chemistry, **2**, ELBS.

Lutta, T.S. (1996). Msc. Thesis Egerton University.

Lutta, T.S. and Kagwanja, S.M. (2000). Synthesis and Electrochemical Studies of Heterobinuclear Complexes Containing Copper and Molybdenum Nitrosyl Groups Linked by Schiff base Ligands, *Transition Metal Chemistry*, **25**, 415-420.

Lutta, T.S. and Kagwanja, S.M. (2001). Synthesis and Electrochemical Studies of Heterobinuclear Zinc and Molybdenum Nitrosyl Complexes Linked by Schiff Bases, *Transition Metal Chemistry*, **26**, 523-527.

Mark, H. W., Partha, B., Tione, B., Bryan, S., Wicks, E., F., Mark W. O., Enemark, J. H. and Martin, L. K. (1997). Photoinduced Electron Transfer in Covalently Linked Oxomolybdenum (V) Porphyrin Systems. *Journal of Inorganic Chemistry*, **36**, 5676-5677.

McCleverty, J.A. (1983). Alkoxy, Amido, Hydrazido and Related Compounds of Molybdenum and Tungsten. *Royal Society of Chemistry*, London.

McCleverty, J.A., Charsley, S. M., Jones, C.J., Neaves, B.D., Reynolds, S.J and Denti, G. (1988). *Journal of Chemical Society*. Dalton Trans., 293.

McQuillan, A. W., Cargill, T., Dante G., McCleverty, J. A., Navas, E. R. and Michael, D. W. (1996). Effects of Systematic Variation in Bridging Ligand Structure on the Electrochemical and Magnetic Properties of a Series of Dinuclear Molybdenum Complexes. *Journal of Inorganic Chemistry*, **35**, 2701-2703.

Meyer, T.J. (1989). Inorganic Compounds with Unusual Properties. *Account of Chemistry Resources*. **22**,164.

Nikles, D.E., Powers, M.J. and Urbach, F.L (1983). Copper (II) Complexes with

Tetradentate Bis(pyridyl)-dioether and Bis(pyridyl)-diamine Ligands. Effect of Thioether Donors on the electronic Absorption, Spectra, Redox Behaviour and EPR Parameters of Copper (II) Complexes, *Journal of Inorganic Chemistry*, **22**, 3210.

Obaidi, N.A., Beer, P., Bright, J.D., Jones, C.J. and McCleverty, J.A. (1986). Monometallic Homo- and Heterobimetallic Complexes Based on Redox Active Tris(3,5-dimethyl Pyrazolyl) Borato Molybdenum and Tungsten Nitrosyl. *Journal of Chemical Society*, **19**,307.

Obaidi, N.A., Charsely, S.M., Hussain, W., Jones, C.J., McCleverty, J.A., Neaves, B.D. and Reynolds, S. (1987). Monometallic, Homo- and Heterobimetallic Complexes Based on Redox-active Tris (3, 5-dimethylpyrazolyl) Borate Molybdenum and Tungsten Nitrosyls. *Part V. P-substituent Effects on the Reduction Potential of Aryl Amide Complexes. Transition Metal Chemistry*, **12**, 143.

Patterson, G.S. and Holm, R.H. (1975). *Bio-Inorganic Chemistry*, 4257.

Pier, G.Z. (2004). Metal-Salen Schiff Base Complexes in Catalysis: Practical Aspects. *Chemistry Society Review*, **33**, 410-421.

Reynolds, S.J., Smith, C.F., Jones, C.J. and McCleverty, J.A. (1985). Dicarbonyl Nitrosyl {tris(3,5-dimethylpyrazolyl) Hydroborate}-molybdenum (III) and Iodo-, Alkoxy- and Alkylamido Molybdenum(III) Derivatives. *Inorganic Synthesis*, **23**, 4.

Riederer, M. and Sawdny, W. (1978). Angrew. Chem. Int. Ed., Engl. 7.

Robin, M.B. and Day, P. (1967). Mixed Valence Chemistry – A *Survey and Classification. Advanced Inorganic Chemistry*, **10**, 247.

Sakaguchi, U. and Addison, A.W. (1979). Spectroscopic and Redox Studies of Some Copper (II) Complexes with Biomimetric Donor Atoms: *Implications for Protein Copper Centres. Journal of Chemical Society, Dalton Trans.*, 600.

Silverstein, T.P., Cheng, L. and Allen, J. F. (1991). "Redox Titration of Multiple Protein Phosphorylations in Pea Chloroplast Thylakoids" *Biochim. Biophys.* Acta , 215-220

Smith, D.W. (1990). Inorganic Substances. *Cambridge University Press*.

Speck, J.C., Rowley, R.T. and Horecker, B.L. (1963). Identity of Synthetic N^6-β-glyceryllysine and the C^{14}-labelled Amino Acid Obtained from Sodium Borohydride

Reduction and Hydrolysis of a Complex from C^{14}-fructose 6-phosphate-transaldose Interaction. *Journal of American Chemical Society*, **85**, 1012.

Sullivan, B.P., Calvert, J.M. and Meyer, T.J. (1980). *Journal of Inorganic Chemistry*, **19**, 1404.

Sulton, J.E. and Taube, H. (1981). Metal-to-Metal Interactions in Weakly Coupled Mixed Valence Complexes Based on Ruthenium Ammines. *Journal of Inorganic Chemistry*, **20**, 3125.

Sullivan, B. P.; Calvert, J. M.; Meyer, T. J. *Journal of Inorganic Chemistry,* **1980**, *19,* 1404.

Syamal, A. and Maurya, M.R. (1989). *Coordination Chemistry Review*, **95**, 185.

Tabassum, S., Singh, N.P. and Arjmond, F. (2001). Synthesis, Characterization and toxicity of heterobinuclear complexes of transition metal ions, **31**, 1803.

Taube, H. A. (1978). "Electron Transfer Reactions of Complex Ions in Solution". *New York Acad. Sci.*, **313**, 481.

Thompson, C. A., Gatteschi, D., McCleverty, J. A., Navas, J.A., Rentschler, E. and Ward, M.D. (1966). Effects of Systematic Variation in Bridging Ligand Structure on the Electrochemical and Magnetic Properties of a Series of Dinuclear Molybdenum Complexes. *Inorganic Chemistry*, **35**, 2701-2703.

Trudy, M. and James R. M. (2003). Biochemistry: *The Molecular Basis of Life*. 3rd Ed.

Trofimenko, S. (1993). The Co-ordination Chemistry of Polypyrazolyl Borate Ligands, *Imperial College Press*, London.

Trofimenko, S. (1999). Scorpionates: The Coordination Chemistry of Polypyrazolytorate Ligands. *Imperial College Press*, London.

Van, A. U., Alexander, M.W., Cargill, T., David, A. B., Dante, G., Jeffery J.C.,
McCleverty, J. A., Federico, T. and Michael, D. W. (1977). Roles of Bridging Ligand Topography and Conformation in Controlling Exchange Interactions between Paramagnetic Molybdenum Fragments in Dinuclear and Trinuclear Complexes. *Inorganic Chem*istry, **36**, 3447-3454.

Wagner, E.C. (1954). A Rationalization of Acid-induced Reaction of Methylene Diamines, Methylene Amines and of Formaldehyde and Amines, *Journal Organic Chemistry*, **19**, 1862.

Wlodarczyk, A., Doyle, G. A., Maher, J. P., McCleverty, J. A., Ward, M. D., Thomas, J. A., and Jones, C. J. (1997). Mixed-Valency by Oxidation and Reduction: Molybdenum-Based Super-Creutz-Taube Ion. *Chemical Communications*, 769-770.